UNIVERSITY
of
GREENWICH

DIFFERENTIALLY FED ACTIVE ANTENNAS

MD. HASANUZZAMAN SAGOR

A thesis submitted in partial fulfilment of the
requirements of the University of Greenwich
for the degree of Doctor of Philosophy

October 2014

DECLARATION

"I certify that this work has not been accepted in substance for any degree, and is not concurrently being submitted for any degree other than that of Doctor of Philosophy being studied at the University of Greenwich. I also declare that this work is the result of my own investigations except where otherwise identified by references and that I have not plagiarised the work of others".

Md. Hasanuzzaman Sagor ……

Supervisor: Dr. Peter Callaghan …….

ACKNOWLEDGEMENTS

First of all, I would like to thank the Almighty for providing me with the strength, health, patience and the drive to accomplish this research work.

Then I would like to express my sincere gratitude to my supervisor Dr. Peter Callaghan. I cannot thank him enough for his guidance and assistance that helped me improve my technical skills and academic knowledge. His relentless support, strong motivation and invaluable advice provided a guiding light at critical junctures in my academic and personal life. I believe that having a supervisor like him is a peerless privilege. I speak very sincerely when I say that whatever I have been able to produce so far would not be possible if I did not have his support by me during every instance ever since the start of my PhD life.

I extend my deepest gratitude to my beloved parents, Md. Nuruzzaman & Shamima Zaman, for their support, love and blessings. Their confidence on my abilities helped me to remain focused and motivated me to give my best. I owe a debt of gratitude to my fiancée Humayra Naosaba, who gave me strength and faith in challenging times of my study. Thanks for being a constant support even while staying hundreds of miles away.

I would like to thank all my colleagues and friends for their care and encouragement. I also would acknowledge the lab technicians of University of Greenwich for their help with PCB fabrications. Finally I would gratefully acknowledge the financial support from the University of Greenwich throughout this research project.

ABSTRACT

The original contribution to knowledge made by this research work is demonstrating the benefits of differentially fed balanced transmit antenna in modern communication system. Extensive experimental studies have established the fact that a true differential amplifier feeding a balanced antenna offers higher linearity and lower distortions compared to the single ended feeding technique, even while using the same amplifier.

With continuing advancements in personal communications in this era of digital economy, the demand for wireless connectivity has grown radically, resulting in stringent performance requirement for RF components. Differential circuits are preferred choice in RFIC design due to its good noise immunity and low distortion characteristics. But it is observed that single ended PAs and LNAs are used for the feeding part because of the antenna industry's tendency to stick to conventional 50Ω interface. Therefore, differentially fed transmit balanced antenna is an area of current research, which has been studied in this thesis.

The study was set out with a review of the state-of-the-art in active integrated antennas. Following that, the ground plane influence on antenna radiation pattern was explored and novel techniques to compensate the effects were presented. It was observed that the current flow in a coaxial cable also affects radiation pattern. Hence, a novel method was proposed to measure wireless devices in the anechoic chamber eradicating the need of any cable attachments. Broadband differential amplifiers were then reviewed with a view to feed balanced and unbalanced antennas for demonstrating the potential of differential feeding technique over the conventional one. The amplifier with differential output interface exhibited higher gain and linearity in both bench test and radiated power test. Further improvement in linearity was reported by lowering the output resistance of the amplifier. Afterwards, a broadband antenna with stable radiation pattern and impedance was designed to carry out radiated harmonic measurements, which illustrated that the fully differential output configuration possesses significantly lower harmonic distortion.

All these measurement results have suggested that balanced antenna fed by differential amplifier can be the best solution for applications demanding higher output power, greater linearity and lower distortion. Therefore it is recommended to re-evaluate the idea of power amplifier and antenna interface in RF front-end designs

CONTENTS

FIGURES

TABLES

ABBREVIATION

ACLR	Adjacent Channel Leakage Ratio
ADS	Advanced Design System
AIA	Active Integrated Antenna
AUT	Antenna Under Test
BJT	Bipolar Junction Transistor
CAD	Computer-Aided Design
CMMR	Common Mode Rejection Ratio
CMOS	Complementary Metal-Oxide Semiconductor
CST	Computer Simulation Technology
DUT	Device Under Test
ERP	Effective Radiated Power
E-UTRA	Evolved Universal Terrestrial Radio Access
FET	Field-Effect Transistor
FSPL	Free Space Path Loss
GPS	Global Positioning System
GSM	Global System for Mobile Communications
HAC	Hearing-Aid Compatibility
HD	Harmonic Distortion
IC	Integrated Circuit
IIP	Input Intercept Point
IMD	Inter Modulation Product
I/P	Input Port
LNA	Low Noise Amplifier
LO	Local Oscillator

LTE	Long Term Evolution
MBT	Modified Bow Tie
MIMO	Multiple Input Multiple Output
NWA	Network Analyzer
OIP	Output Intercept Point
O/P	Output Port
PA	Power Amplifier
PAE	Power-Added Efficiency
PCB	Printed Circuit Board
PCS	Personal Communication Service
PIFA	Planar Inverted-F (type) Antenna
PNA	Performance Network Analyzer
RF	Radio Frequency
RFIC	Radio Frequency Integrated Circuit
RFID	Radio Frequency IDentification
SAR	Specific Absorption Rate
SE	Single Ended
SKA	Square Kilometer Array
SNR	Signal-to-Noise Ratio
USB	Universal Serial Bus
VCO	Voltage Controlled Oscillator
VNA	Vector Network Analyzer
VSWR	Voltage Standing Wave Ratio
WCDMA	Wideband Code Division Multiple Access
WLAN	Wireless Local Area Network

Chapter 1

Introduction

1.1 Background

With the increasing expansion of communication technology, the second-generation cellular networks supporting only voice calls and text messages can no longer satisfy users' demand. Consumers these days want access to high-speed data, online gaming, multimedia streaming and various other options in their compact handheld devices. These contemporary demands have placed a range of design challenges to RF engineers, particularly to the power amplifier and antenna designers. Modern RF circuitry nowadays needs to meet strict performance requirements such as large dynamic range, low noise, reduced sensitivity to human body and higher linearity [1].

The balanced antenna caught attention of the antenna research industry for its numerous benefits [2-4] compared to the unbalanced antenna, especially for mobile communication. Balanced antenna offers stable radiation properties and higher efficiency in proximity of human body [5-6], essential for contemporary mobile communication. The user demand for a compact device can be fulfilled by the integrated antenna approach. An active integrated antenna is capable of reducing the size, weight and cost of a design without any compromise in its performance [7]. From the circuitry perspective, improved linearity with lower noise figure can be realised by using differential amplifier [8]. Therefore it is evident that the use of differentially fed active balanced antennas can be the best possible way of meeting those stringent performance requirements of modern communication industry. Thus, this potential research area needs to be explored.

1.2 Objectives & Motivation

Active antennas have been studied by a number of authors and a comprehensive review of this work was made in 2002 [9]. Focus has been put on using discrete devices usually with a

narrow-band resonant antenna. Asymmetrical planar inverted F antennas (PIFAs) usually are the preferred choice of antenna for handset designers due to their compact size, low profile, good electrical performance and ease of fabrication [10-11]. However, PIFA is an unbalanced design, which uses the ground plane as part of the radiator and provides distorted performance. Despite numerous benefits of balanced antenna, it has been repeatedly noticed that the antenna industry tends to stick to the standard '50Ω' interface. Few recently published articles [12-14] for LTE band confirms that. This is due to the eccentricity of the approach and complex measurement techniques of differential devices. However, RFIC industry prefers differential circuits due to their excellent noise immunity. Power amplifiers are the most power-consuming element in the whole transceiver system. Power consumption is directly related to linearity [15], which should be minimized in order to extend the battery life in mobile devices [16]. Thus, it is important to have a high rejection to digital circuitry noise, and maximized linearity. Differential amplifier possesses these features and for this reason RFIC manufacturers now design their IC module with a differential output. But while feeding to an antenna in RF front end, RFIC also adopts single ended interface to match the impedance of the antenna. In a recent (June 2014) report from CML Microcircuits [17], it can be observed that in a modern RFIC transceiver (CMX991) true differential amplifiers were used in circuitry part but at the feed point to antenna single ended PA and LNA along with a balun were adopted. The question arises here is; do they really need to be always single ended or 50 Ω? An extensive research has been carried out to find the solution of this issue.

Differential amplifiers were constructed with single ended and differential output configurations using same RFIC and discrete components. These designs were used to feed balanced and unbalanced antennas to demonstrate the potential of differential feeding technique over the conventional one. Although the concept looks straight forward, successful implementation of this method is difficult to achieve. AIA design requires knowledge in several areas of microwave engineering, including solid state device, circuits and antennas. For this reason this area has not been explored thoroughly. Some research works have been conducted recently but lack of sufficient amount of research exploration are still persistent, which will be discussed in detail in the next chapter.

1.3 Short Technical Description

RF CMOS uses complimentary pairs of transistors as basic building blocks in the circuit design [18-19]. Ideally such RFICs would interconnect using a differential (or balanced) input and output lines. However antenna and RF sub-system design has evolved into unbalanced design resulting in a mismatch between the RFIC and the antenna. The RF circuitry is usually developed on a PCB using 'microstrip' techniques, whereby one side of the PCB is a ground plane and RF signals are constrained on the PCB using microstrip transmission lines. This is ideal for the design of RF amplifiers and circuit using discrete surface mount devices. Though RF circuit design as an RFIC has become common practice, this has introduced a limitation. The RFIC needs to be connected to an unbalanced transmission line or antenna by a transformer or balun. The necessity to introduce a 'balun' to achieve this initiates losses and bandwidth restrictions. However the RFIC can be placed directly at the antenna feed point, eliminating the need for connecting unbalanced transmission line and allowing the use of a balanced antenna.

1.4 Research Contribution

The research aim was to explore the benefits of differentially fed active balanced antenna and the potential of this approach in future communication system. In doing so, a number of contributions have been added to the state-of-the-art in active balanced antenna. A novel method of compensating ground plane effects of a mobile antenna with finite sized ground plane was proposed. Another novel method of measuring a wireless device inside anechoic chamber was introduced. Using broadband amplifiers, the benefits of true differential feeding have been demonstrated. It has been shown that higher power and greater linearity can be achieved from the same device just by adopting fully differential interface. Then a broadband modified bow tie antenna was designed and used to quantify radiated harmonic distortion of 3 different amplifier configurations. Analysis illustrated that differential amplifier had better harmonic distortion compared to the single ended one, and more importantly, differential with true differential output interface had remarkably lower harmonic distortion compared to the differential with single ended output interface. A radiated harmonic distortion characterization with 3 different active antenna configurations has not been seen in literature.

The work presented in this thesis has resulted in three publications with two further papers currently in preparation:

i. Callaghan, P.; Sagor, M.H.; Batchelor, J.C., "Control of ground plane influence on antenna radiation pattern for mobile handheld devices," Antennas and Propagation Conference (LAPC), 2011 Loughborough , vol., no., pp.1,4, 14-15 Nov. 2011.
ii. Sagor, M.H.; Callaghan, P., "Measurement of antenna radiation pattern using injection locking technique," Antennas and Propagation (EuCAP), 2014 8th European Conference on , vol., no., pp.1066,1069, 6-11 April 2014.
iii. Sagor, M.H.; Callaghan, P., "Benefits of active transmit balanced antenna fed by differential power amplifier," Antennas and Propagation Conference (LAPC), 2014 Loughborough , vol., no., pp.732,735, 10-11 Nov. 2014.
a. "Characterizing Effective Radiated Power and Distortion Form Differentially Fed Narrow Band Antennas" (to be submitted) to the IEEE Transactions on Microwave Theory and Techniques.
b. "Measurement of Radiated Harmonic using Broadband Active Balanced Antenna" to be submitted to the IET Transactions of Microwave, Antenna and Propagation.

1.5 Thesis Outline

The remainder of this thesis is structured as follow:

Chapter 2 analyses the state-of-the-art in the active balanced antenna literature. In particular the benefits of balanced antenna for mobile communication have been reported. The recent advances on measurement technique of balanced antenna have been reviewed and the research gap has been reported.

In Chapter 3, simple balanced and unbalanced antennas have been presented and ground plane effect has been investigated. Power distribution of dipole antennas for different wavelengths and radiation pattern of simple monopole antenna over different sized ground plane was investigated. Following that, a mobile antenna with finite sized ground plane has been reported and the ground plane influence has been investigated. Novel techniques have been proposed to control the ground plane current and reduce degradation.

In Chapter 4, a novel measurement method using injection locking technique has been introduced. The method offers measurement for wireless devices inside the modern anechoic chamber without any cable connected to the device under test.

Chapter 5 deals with the design and analysis of basic forms of single ended and differential amplifiers followed by RF single stage, RF partial differential and RF fully differential amplifiers. The performance of these amplifiers were simulated and measured for analysis. Effects of inductors, RF track line and current mirror were also investigated. The complications arose during the design process at higher frequency exposed the challenging part of designing RF amplifier for higher frequency.

Chapter 6 presents broadband differential amplifier with single ended output interface and another same amplifier with differential output interface. The nonlinear distortion characteristics of the LMH6881 were analysed. Techniques to achieve higher gain and linearity from same device by changing output impedance has been investigated. Following that an experimental proof has been presented confirming that differential feeding configuration can provide higher gain and greater linearity compared to its single ended counterpart. The adjacent channel leakage ratio (ACLR) of both active antennas were presented to compare the distortion characteristics of differential and single ended interface.

In Chapter 7, characterization and measurement of harmonic distortion of the LMH6881 differential amplifier were analysed. The harmonic distortion of a single ended amplifier, a differential amplifier with single ended output and a differential amplifier with fully differential output configurations were measured. Measurement results for both bench tests and radiated harmonic tests were assessed and finally from the outcome the best approach for lower level of harmonic distortions was recommended.

Finally, Chapter 8 summarised the contributions of this thesis and concluded the work with some remarks. This chapter also presented directions for future works to broaden the scope of this research.

References

[1] J. I. Agbinya, M. C. Aguayo-Torres (2013), 4G Wireless Communication Networks, Denmark: River Publishers, Chapter 1.

[2] Morishita, H.; Furuuchi, H.; Fujimoto, K., "Performance of balance-fed antenna system for handsets in the vicinity of a human head or hand," Microwaves, Antennas and Propagation, IEE Proceedings , vol.149, no.2, pp.85,91, Apr 2002.

[3] Abd-Alhameed, R.A., Excell, P.S., Khalil, K., Alias, R., Mustafa, J.: SAR and radiation performance of balanced and unbalanced mobile antennas using a hybrid formulation', IEE Proc., Sci. Meas. Technol. Spec. Issue Comput. Electromagn., 2004, 151, (6), pp. 440–444.

[4] Morishita, H., Hayashida, S., Ito, J., Fujimoto, K.: 'Analysis of built-in antenna for handset using human (head, hand, finger) model', Electron. Commun. Jpn., 2003 Part 1, 86, (9), pp. 35–45.

[5] Arenas, J.J., Anguera, J., Puente, C.: 'Balanced and single-ended handset antennas: free space and human loading comparison', Microw. Opt. Technol. Lett., 2009, 51, (9), pp. 2248–2254.

[6] Collins, B.S., Kingsley, S.P., Ide, J.M., Saario, S.A., Schlub, R.W., O'Keefe, S.G.: 'A multi-band hybrid balanced antenna'. IEEE 2006 Int. Workshop on Antenna Tech: Small Antennas; Novel Metamaterials, White Plains, New York, 6–8 March 2006, pp. 100–103.

[7] Navarro. J. A., Chang. K., "Integrated Active Antennas and Spatial Power Combining", John Wiley & Sons, New York, 1996.

[8] K. Kurokawa, "Design Theory of Balanced Transistor Amplifiers," Bell System Tech. J., vol. 44, pp. 1675-1698, Oct. 196511.

[9] Chang, K., York, R.A., Hall, P.S., Itoh, T.: 'Active integrated antennas', IEEE Trans., Vol. MTT-50, No. 3, March 2002, pp937-943.

[10] Huynh, M.-C. and W. Stutzman, "Ground plane effects on planar inverted-F antenna (PIFA) performance" , IEE Proc.-Microw. Antennas Propag., Vol. 150, 209-213, August 2003.

[11] Janapsatya, J., K. P. Esselle, and T. S. Bird, “A dual-band and wideband planar inverted-F antenna for WLAN applications”, Microwave and Optical Technology Letters, Vol. 50, 138-141,January 2008.

[12] Shao-li Zuo; Zhi-ya Zhang; Jia-Wei Yang, "Planar Meander Monopole Antenna With Parasitic Strips and Sleeve Feed for DVB-H/LTE/GSM850/900 Operation in the Mobile Phone," Antennas and Wireless Propagation Letters, IEEE , vol.12, no., pp.27,30, 2013

[13] Yong-Ling Ban; Cheng-Li Liu; Li, J.L.-W.; Rui Li, "Small-Size Wideband Monopole With Distributed Inductive Strip for Seven-Band WWAN/LTE Mobile Phone," Antennas and Wireless Propagation Letters, IEEE , vol.12, no., pp.7,10, 2013

[14] Ching-Song Chuang; Wu-Tung Hsu; Lin Ming Chun, "A compact dual band tree-type MIMO antenna for mobile wireless access network application," Microwave Conference Proceedings (APMC), 2013 Asia-Pacific , vol., no., pp.1169,1171, 5-8 Nov. 2013

[15]J. Laskar, S. Chakraborty, A. Pham (2009), Advanced Integrated Communication Microsystems, Hobokon: John Wiley & Sons, Inc, Chapter 2.

[16]Tae Wook Kim; Bonkee Kim, "A 13-dB IIP3 improved low-power CMOS RF programmable gain amplifier using differential circuit transconductance linearization for various terrestrial mobile D-TV applications," Solid-State Circuits, IEEE Journal of , vol.41, no.4, pp.945,953, April 2006

[17] CML Microelectronics, “RF Quadrature Transceiver” CMX991 Datasheet, June 2014; Available at: http://www.cmlmicro.com/products/CMX991_RF_Quadrature_Transceiver/ Last accessed: 31st October, 2014.

[18] Hernandez, J.: ‘Basic guidelines to design RF CMOS cells for wireless receivers’, Microwave Eng. Europe, April 2000, pp49-53

[19] Hsu, H.M.: ‘Implementation of 0.18um RFCMOS technology for system-on-a-chip applications’, IEEE Proc.-Microw. Ant. Prop., Vol 153, No. 6, Dec 2006, pp516-522.

Chapter 2

Review of Active Integrated Antenna Technology

2.1 Introduction

In this chapter extensive review has been carried out on the literature surrounding differential active integrated antenna (AIA) technology. An overview of the history of antenna, amplifier and AIA has been presented discussing the major contributions in the field. In the following sections, classifications and applications of AIA technology has been explored. The benefits of balanced antenna for mobile communication are reported in the subsequent section. More specifically, the measurement technique of balanced antenna has been looked over and recent advances reported in literature on this topic have been thoroughly reviewed. This complete review has resulted in finding the research gap and has worked as a motivation in investigating the benefits of differential active antenna approach.

2.2 History of Antenna, Amplifier and AIA

2.2.1 Antenna

Microwave circuits and antennas have become an integral part of modern communication industry. This technology has been developed for last 200 years to reach in its present stage. During 1820s to 1840s, André-Marie Ampère, Michael Faraday, Joseph Henry and Karl Friedrich Gauss have contributed significantly to provide a combined theory of electricity and magnetism [1]. In 1864, James Clark Maxwell elegantly pieced together the work of Lorentz, Faraday, Ampere, and Gauss into a groundbreaking equation of electromagnetic field, known as Maxwell's equations [2]. Maxwell presented the first unified theory of electricity and magnetism and founded the science of electromagnetics. He predicted transverse propagation of waves at a finite speed of light. He postulated that light is an electromagnetic phenomenon of a particular wavelength and predicted that radiation might also occur at another wavelength.

Heinrich Rudolf Hertz validated Maxwell's theory during the late 1880s by using an end-loaded dipole transmitter and a resonant square-loop antenna receiver to demonstrate the generation, propagation, and reception of electromagnetic waves having a wavelength of 4m [3]. His radio system experiments using a cylindrical parabolic reflector at wavelength of 4m and 30cm proved that light is a form of electromagnetic radiation. Hertz is known as the architect of Radio communication as he was the first to conclusively prove the existence of electromagnetic waves [4]. The unit of frequency is named after him to honour his outstanding contribution. This work, however, remained a laboratory curiosity for almost two decades until Gugleilmo Marconi came across with these experiments. Marconi was successful in sending information in the form of electromagnetic waves from one place to another wirelessly [5]. Marconi's contributions granted him the Noble Prize in 1909. In 1927, Shintaro Uda from Tohoku Imperial University of Japan, invented one of the most important antenna designs of that era with the collaboration of Hidetsugu Yagi, a professor at the same university. A Yagi-Uda array, commonly known simply as a Yagi antenna, is a directional antenna consisting of a driven element (typically a dipole or folded dipole) and additional parasitic elements. This design showed a substantial increase in the antenna's directionality and gain compared to a simple dipole [6]. Barrow and Chu reported the electromagnetic theory of horn antenna in 1939 [7], where they provided an adequate explanation of the way in which the electromagnetic horn functions as a radio antenna.

The revolutionary microstrip antenna technology was developed in the early 1970s. A microstrip structure, in other words a conducting strip radiator separated from the ground plane by a dielectric substrate was described by Byron [8]. This half-wavelength wide and several wavelength long radiator strip was fed by coaxial connections at periodic intervals along both radiating edges. In 1973, Dr Martin Cooper and John F. Mitchel of Motorola demonstrated the first handheld mobile phone for private and practical use [9]. After that, there was a substantial surge in the development of antenna technology. These early mobile phones used whip antennas consisting of a straight wire or rod and were bigger in size. Encouraged by the growing demand, researchers have funded efforts to miniaturize electronic components and layouts and as a result the promising Printed Inverted F Antenna (PIFA) was introduced, which first appeared in literature in 1987 [10]. Since then, PIFA antenna structure has emerged as one of the most promising candidate to be used in handheld devices. But

recently research has been focused on the use of balanced antennas for their enormous benefits in portable devices, which will be discussed in Section 2.5.

2.2.2 Amplifier

In the early 1900s, Lee De Forest invented a two-electrode device for detecting electromagnetic waves, which was a variant of the earlier research on the ‘thermionic valve’ by John Ambrose Fleming. In 1906, De Forest added a third element between the cathode (filament) and the anode (plate) of the previously invented vacuum diode, resulting in the creation of first amplifier called the 'triode' [11]. This third electrode was known as ‘the control grid’. The resulting triode or three-electrode vacuum tube could be used as an amplifier of electrical signals, notably for radio reception. The Triode was the fastest electronic switching element of that time, and was later used in early digital electronics including computers. The Triode was vital in the development of transcontinental telephone communications, radio, and radar until the invention of the transistor. In the following years, radio and television provided great stimulation to the tube industry. Production rose from about 1 million tubes in 1922 to about 100 million in 1937 [12]. In the early 1930s, the four element ‘tetrode’ and the five element ‘pentrode’ gained prominence in the electron-tube industry. Rapid advances were made in design and manufacturing techniques for high power and high frequency applications and miniaturization in the years to follow.

On the 23rd December 1947, the electronics industry experienced the advent of a completely new direction of development when Walter H. Brattain and John Bardeen demonstrated the amplifying action of the first transistor at the Bell Telephone Laboratories [13]. The original transistor (a point-contact transistor) was a three terminal transistor. The advantages of this solid-state device over the tube were immediately obvious: it was smaller and lightweight, it had no heater requirement or heater loss and it had a rugged construction. It was more efficient since the device itself absorbed less power. In 1965, the balanced transistor amplifier was proposed by R. S. Engelbrecht of Bell Labs as a way of providing a good input match when an amplifier was tuned for optimum noise performance. Engelbrecht and Kurokawa first reported this approach [14], and a subsequent paper by Kurokawa [15] explored the

theory of the balanced amplifier in more detail. According to Engelbrecht and Kurokawa, the main advantages of the balanced design over more conventional multistage amplifier are:

"1) Improved input and output impedance matching, gain flatness, phase linearity, gain compression, and intermodulation characteristics, 2) Possible designing of the amplifier simultaneously for minimum noise figure and good input match, 3) Relatively little effect to overall amplifier gain and matching by changes in the distribution of transistor impedance characteristics, provided that transistors can be selected in similar pairs, 4) The amplifier gain is easily controlled over a wide range by the dc bias with little degradation of the gain flatness and impedance matches." [15]

In their experiment, a four-stage balanced amplifier was designed and constructed in printed circuit form for L-band operation. The results have shown that the above advantages could be obtained at the expense of an increased number of transistors in the circuit. After this experiment balanced amplifier became a prominent research topic amongst researchers and the technology advanced in a distinct surge. But this early stage research was mostly conducted in lower frequency analog circuitry and digital devices, and much less so in RF and microwave applications.

2.2.3 Active Integrated Antenna (AIA)

An AIA is a microwave circuit in which the output or input port is free space, instead of a conventional 50Ω interface. This approach integrates the traditionally separated sub-circuits into a single compact and efficient unit. When applied in the context of active integrated antennas, the antenna provides circuit functions such as duplexing, filtering and harmonic rejection besides its original role as a radiator. This technology has been developed in order to overcome the fundamental limitations on output power of semiconductor circuits. Suitable transmission lines become very lossy at higher frequencies due to radiation losses, substrate losses and increased skin-effect ohmic losses [16-17]. Integrating active elements directly into the antenna can significantly compensate these losses.

The implementation of the integrated antenna concept may be in its infancy, but the idea is not new. The study of active antennas received profound attention and some pioneering works

were reported in the 1960s and 1970s [18-22], after the advent of high-frequency transistors. Several investigators at Ohio State University demonstrated both diode- and transistor integrated antennas. Amongst them, Copeland and Robertson demonstrated a half-wavelength dipole antenna, together with a transistor amplifier, which they called as an 'Antennafier' [23]. During the IEEE Antennas and Propagation Conference of 1968, Meinke and Landstorfer described the mating of a FET transistor to the terminals of a dipole to serve as a VHF amplifier for reception at 700 MHz [24]. Following this work, Ramsdale and Maclean used BJTs and dipoles for transmitting applications in 1971 [25]. They demonstrated large height reductions by using the active antenna concept in 1974 [26] and later in 1975 [27]. Dawoud and Anderson et. al from University of Sheffield, reported better bandwidth of monopole antennas and reduction in the frequency dependency of antenna arrays fed by microwave transistors [28-31]

Several research works on active antennas for different applications were carried out in late 1970s and early 1980s [32-35]. Then Thomas et al. developed a modern active microstrip antenna in Marconi Space and Defence Systems, UK. This is generally accepted as the first modern active antenna and the work was published in February 1985 [36]. It was a Gunn diode integrated rectangular microstrip patch antenna operating at X-band frequencies. Perkins described an active dual circular patch antenna in the following year [37]. In 1990s, numerous innovative designs on AIA concept were proposed and successfully demonstrated with Tatsou Itoh from University of California, Los Angeles being the forerunner in most of them [38-44]. Along with him, Radisic presented the first AIA concept using power amplifier [45]. They used a class-B GaAs FET power amplifier integrated with a patch antenna, which is shorted in the middle so that the input impedance at the second harmonic becomes zero and the PAE was increased by 7%. In [46] the authors employed a modified circular segment microstrip antenna on a single-ended amplifier, which is capable of reactively terminating both the second and third harmonics. They also proposed harmonic tuning and EMI reduction using active antenna with power amplifier [47-48]. Extensive research works have been carried out in this promising research area of AIA over the last decade. These will be discussed in the next sections along with the measurement techniques of active balanced antenna.

2.3 Classification and Advantages of Conventional AIA

In an AIA, the active device and the antenna are treated as a single entity, which differs from the traditional design methodology where the antenna and RF front-ends are different components connected to standard 50Ω transmission lines. The basic functions of active devices in AIAs are RF signal amplification, RF signal generation or frequency conversion. The active integrated antennas can be classified into the oscillator type, amplifier type and frequency conversion type, depending on the function of the active device [49]. For the amplifier-type AIAs, when the antenna is placed at the input port it acts as source impedance for the active device. In this case the AIA acts as a receiver. In contrast, when the antenna is connected at the output port, it is regarded as load impedance to the active device and the AIA functions as a transmitter. Interest in this type of AIA is growing due to its potential applications in spatial power combining amplifier [50] and in compact high efficiency RF front-end transmitters and receivers [51-55].

AIAs are generally integrated with planar microstrip [56-57] or PIFA [58-59] antennas. However, many other types of antennas employed for the integrated antenna operations have been reported, including dipoles [60-62], printed patch antennas [63], antennas with notch [64-65], slot antennas [66], log periodic antennas [67], yagi antennas [68-69] etc. Active antennas overcome some of the drawbacks traditionally related to conventional antennas such as loss between the RF front-end and the antenna, mutual coupling between array elements and limitation of frequency of operation. AIAs have the potential of reducing the size, weight and cost of a transmitter, receiver and transceiver design without compromising performance by incorporating the circuit component functions at the antenna terminal [70]. AIAs also facilitate systems with desirable features such as minimum power consumption, high degree of multiple functionality and enhanced reliability [17]. As the active device is connected in the immediate vicinity of the antenna, the antenna itself works as a matching network, avoiding the integration of additional matching circuit in the system. By directly integrating active devices into antenna elements feed line losses can be significantly reduced, which is particularly important at higher frequencies [49]. It is believed that to meet the growing demand of portable electronic devices active antenna systems will be extensively used to cover significantly wider bandwidth with smaller physical volumes.

2.4 Applications of AIA

AIAs can be used as an alternative to conventional approaches for many applications. In most cases it provides greater performance compared to the conventional approach. Even if AIAs provide nearly the same performance as that using a conventional approach, the reduction of size and cost would greatly enhance the system's usefulness. For these enormous benefits and advantages AIAs have drawn a great deal of attention in the research community. AIAs have been extensively used in the automotive industry [71-73], GPS [74-76] and location and direction finding services [77-79]. Because of its compactness and low cost, AIAs have versatile applications in the growing area of wireless communications [80-82] and in RF front-end [83]. In a recent publication this year (2014), Montero et al. has adopted active antenna approach to design an antenna system suitable for future 5G mobile communications [84]. Television [85-86], satellite [87-88] and radar [89-90] sectors also have been greatly benefitted by integrated antenna approach. AIA also offers potential advantages for personal communication systems such as RFID tags [91-93], sensors [94], smart cards [95] and wireless identification system [96]. AIAs have also been adopted in weather forecasting radar [97], security alarm system [98] and high precision distance measurement applications [99].

2.5 Different AIA Approaches

It has been discussed that the integrated antenna approach differs from the more conventional approaches for the fact that there is no obvious distinction or boundary between the component and the antenna. The antenna serves as a load for the component and as the radiator and/or receiver for the system. These configurations are made up of at least two components: a solid-state device and an antenna. An integrated system consisting of a balanced antenna fed by differential active components have provided a new paradigm for designing modern microwave systems. This new balanced approach of this promising technology is attractive for practical applications in modern mobile communication and portable devices, which is discussed in the next section. The single ended approach and new balanced approach of AIA is shown in Figure 2.1.

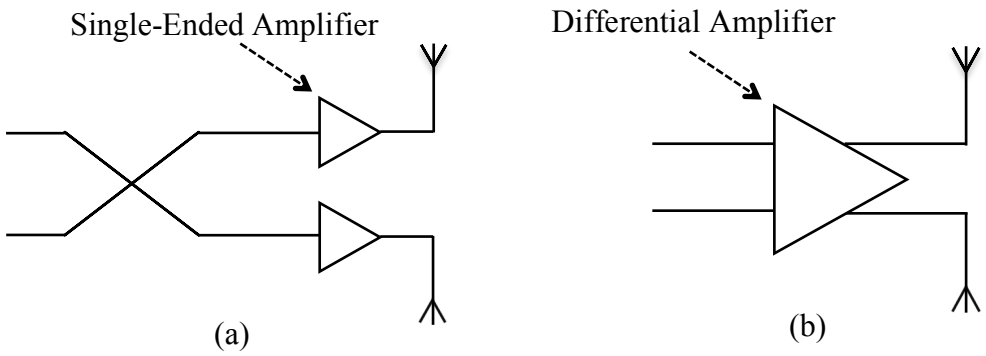

Figure 2.1: (a) Old approach of AIA in RF front end and (b) New balanced approach

2.6 Balanced Antenna for Mobile Communication

The balanced antenna caught attention of the antenna research industry for its numerous benefits compared to unbalanced antennas. By definition, a balanced antenna is a symmetrical antenna fed by signals of equal amplitude and 180 degree out of phase. Dipoles and loops are the most commonly encountered balanced antennas. In addition, balanced antennas may also be realized in meander-line, helix, microstrip forms and so on [100].

With the increasing expansion of wireless technology, the demand for wireless devices has skyrocketed. This increasing number of portable devices creates a need for more power efficient topology, wider impedance bandwidth but maintaining excellent radiation performance. Asymmetrical planar inverted F antennas (PIFAs) usually are preferred choice of antenna for handset designers due to their compact size, low profile, good electrical performance and ease of manufacturing [101-104]. However, the PIFA is a narrowband, unbalanced design, which uses the ground plane as part of the radiator to enable small antennas to achieve sufficient gain and bandwidth. In this kind of unbalanced antennas radiating currents are induced on both the ground plane and the antenna element. As a consequence, the ground plane also becomes a part of the radiating element. As the currents on the ground plane and other metallic structures of the terminal (chassis) couple strongly to the user's body, these antennas exhibit very variable performance when the handset is held in the hand or comes in proximity of the human body. This is mainly because the user holding the mobile device largely takes the place of the ground plane and the unpredictable

characteristics of the human body changes the matching and decreases the radiation efficiency of the antenna. [105].

Plenty of research have been carried out recently in reducing this unintended user effects and all those results have proposed the superiority of balanced antenna. Balanced structure doesn't use the chassis as a ground plane, hence it remains isolated from the handset's chassis and performance degradation can be reduced when users hold the handset adjacent to the human body. In 2002, Morishita et al. analyzed a balanced antenna both theoretically and experimentally and showed that by using balanced structure the current on the handset body can be reduced remarkably and the influence of the human body on antenna performance can be reduced significantly [106]. In [107] authors demonstrated that the SAR (Specific Absorption Rate) value for the balanced antenna is significantly lower with a more consistent radiation pattern compared to its unbalanced counterpart. J. J. Arenas et al. presented a comparison study between single-ended antenna and balanced antenna in two scenarios, one in free space and the other with dielectric (human hand) model, at 2.4 GHz ISM band. In both cases, the balanced antenna showed more stable radiation properties when the human hand interacted with the ground plane [108]. Several other novel mobile antenna designs with balanced technique have confirmed the enhanced stability of their performance in the vicinity of human head and/ or hand [109-111].

A balanced antenna shows more efficiency when used in a mobile handset. In [112] the performance of a balanced antenna was compared with a conventional one, by substituting it into a standard commercial handset. The comparative efficiencies were shown in graphs where balanced one was clearly giving noticeably better performance, both in lower and higher frequency bands. Balanced antennas are also preferred for many applications due to their better isolation between the input and output ends as well as superior matching properties. The feasibility of balanced antenna structures was studied at GSM 900 and 1800 bands in [113]. Also the specific absorption rate (SAR), hearing-aid compatibility (HAC) and the user's effect on matching and radiation efficiency were considered. It was reported that balanced antenna structures provide better performance in all of these aspects at UHF frequencies.

Modern smartphones come with integrated GPS and navigation system within them. In 2007, Collins et.al [114] designed a balanced antenna for receiving GPS signals. The antenna has been field-tested on a GPS USB dongle and compared with a similar dongle using an 18xl8mm ceramic patch antenna. The outcomes suggested that the balanced antenna performs favorably with conventional patch and helix antennas and has a lower manufacturing cost and is smaller and lighter. This makes the size and the complexity of the system become smaller and simpler, which are very important for mobile application. [115] demonstrated that balanced antenna provides better performance over the 2.4GHz and 5GHz WLAN bands in terms of antenna return loss, radiation pattern and power gain.

2.7 Measurement of Balanced Antenna

It has been confirmed in a study by Morishita [106], that in order to achieve these enormous advantages of balanced antenna, it must be fed in a differential or balanced way. Although the concept look straight forward, successful implementation of this active balanced antenna approach has been difficult to achieve. The major problem with using balanced circuits is the fact that most available test equipment is intended for unbalanced devices. The related infrastructures are also unbalanced, which include the objects that are usually used for antenna measurements such as calibration standards, transmission lines and connectors, and even an industry standard reference impedance of 50Ω. These are the reasons why researchers usually tend to avoid balanced circuits.

Accurate measurement of differential devices at microwave and millimeter-wave frequencies is a challenge. The techniques are not as obvious as with the single-ended ones, and they require some specific methods that are suggested in the literature [116-117]. When connecting symmetrical antenna to an asymmetrical measurement setup the currents in the two accesses will not be equal, because a common mode current can circulate on the ground plane. To amplify the differential signals coming from or going into each antenna element a passive balanced-unbalanced (balun) transformer is typically used along with a differential amplifier. The characterization of active differential devices requires an expensive four-port vector network analyser. Thus, it is a common practice to attach baluns to convert between single-ended and differential signals and perform the measurement using a lower cost two-port

vector network analyser (VNA). But the use of a balun introduces loss and efficiency problems and does not come close to a fully integrated solution. Vadim Issakov et al. measured a device directly using a four-port network analyser and compared the result with a measurement using baluns and a two-port network analyser [118]. It has been clearly shown how a balun affects the gain and efficiency of a device in the measurement process. Moreover, matching circuits or baluns are frequency dependent and require extra design efforts to remove their impact [119]. A balun also increases the size and complexity of a device. Avoiding these drawbacks is a challenge for researchers in the field of measurement techniques of active balanced antenna.

2.8 Benefits and Recent Advances in Differentially Fed AIA

Due to the lack of low-loss, small sized passive baluns, it is always desirable to create a measurement setup that allows the characterization of differential antennas without using a balun. An obvious design approach is therefore to use a balanced antenna fed by a differential amplifier. With a differential amplifier, the balun will no longer be necessary as the differential signal can be directly fed into the antenna. Hence a compact RF front-end design with lower losses would be realized. RFIC designers also prefer differential circuits as they offer improved noise, greater impedance match and larger signal handling capability [120].

Linearity is one of the most important factors in future cellular technology and researchers have already reported that differentially fed active circuits can provide greater linearity [121-123]. In mobile telephony, differential feeding is used to significantly reduce the human body effect on the performances of a mobile device [106]. Differential signal can also increase the immunity to the interference between the PCB broad and the IC, which can improve the signal to noise ratio (SNR) of the system. This is important in communications since higher SNR can ensure transmission with less error. Because of these proven benefits, RFIC manufacturers now design their IC module with a differential output [124].

Differentially fed antennas present a major advantage compared to the conventional asymmetrical systems, which is the elimination of the common mode current. It is necessary that common mode (in phase) signals are rejected in certain applications, otherwise the shape

of the radiation pattern will be distorted and consequently the receiver sensitivity will be degraded [125]. A fully differentially fed power amplifier also offers gain doubling, higher harmonics rejection and additional matching improvement at higher frequency [126].

Despite all these reported advantages of differentially fed AIAs, recent published works on mobile antennas [84, 127-128] show that researchers still tend to sidestep balanced circuits and antennas. Although the RFIC industry widely uses balanced amplifiers because of their benefits, but they use single ended PAs and LNAs for the feeding part [129]. The load impedance of a differential interface is not the industry standard 50Ω, and most of the researchers do not want to come out of the conventional thinking of using co-axial cable to feed all kind of devices.

During 1998 to 2007, researchers from University of California, Los Angeles and University of Birmingham, UK proposed numerous innovative designs on differentially fed antenna [130-137]. Those works presented various benefits of differentially fed AIA compared to single ended AIA such as higher gain, harmonic rejection, reduced system noise, better PAE, more stable radiation pattern and tighter integration between the antenna and transceiver system. But they applied those concepts by using push–pull power amplifiers, which is not a true differential feed. Unlike fully differential two-port output configuration push-pull amplifier consists 2 output terminals along with a third ground terminal. Figure 2.2 represents a diagram of push-pull differentially fed AIA technique.

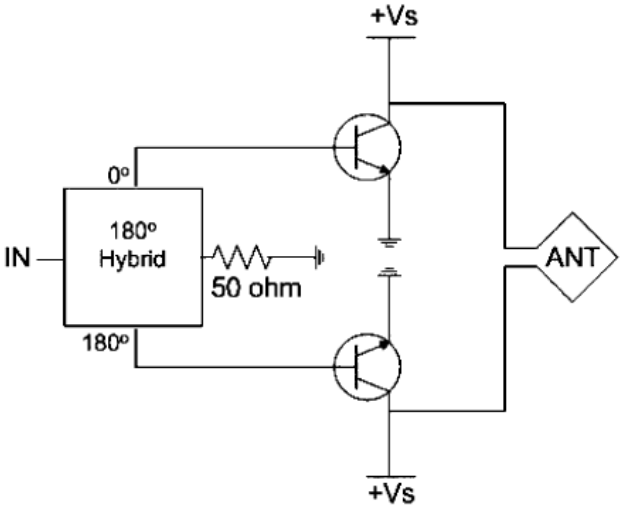

Figure 2.2: Integrated balanced antenna with push-pull concept [138]

In 2007, scientists from a Spanish university proposed that connecting active devices differentially could avoid the use of a balun [139]. They presented that by placing the active device directly to the antenna port delivering the required 180º phase difference at the balanced output, the optimum matching condition can be achieved without any additional matching circuit. This work showed a reduction of total size, complexity and losses of the system, compared to the conventional balun feeding structures. In the same year, two amplifiers working in a 'differential manner' were configured to provide a hybrid feed to a patch antenna but balanced antenna wasn't considered [140]. In 2009 Bourtoutian et al. reported the benefits of measuring differential circuit without balun. It was reported that the elimination of matching circuit or balun reduces the front-end's size, weight, and losses, thus lowering the cost and enhancing the autonomy. They proposed a novel method that allows the measurement of the return loss of a differential antenna using two coaxial ports [141]. Differential antenna was treated like a two port component here. The central cores of two coaxial cables were connected to the two accesses of the differential antenna to form two measurement ports, as indicated in Figure 2.3. They compared the radiation pattern of same antenna using the unbalanced and balanced feed. It was presented that the pattern of the unbalanced feed is non symmetrical because of the coaxial cable's radiation due to the common mode current circulating on its outer conductor. But the radiation pattern of the differentially fed antenna was almost in perfect symmetry. It made researchers think to come out of the conventional approach of using 50Ω load impedance to feed all kinds of devices. Bourtoutian fed the antenna differentially with two co-axial cables, but didn't use an active device or a power amplifier for feeding the balanced antenna.

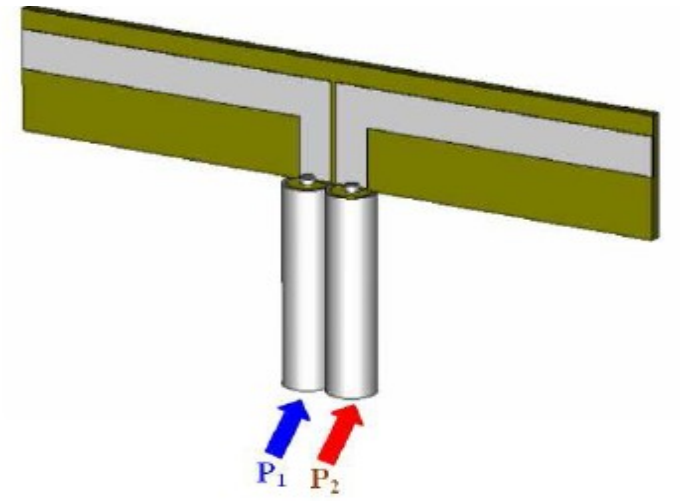

Figure 2.3: Dipole antenna fed by two coaxial cables ensuring balanced functionality [141].

Wadefalk et al. presented a true differential amplifier feeding a balanced antenna in 2010 [125]. They demonstrated a greater CMMR with a low noise figure by using this fully symmetrical differential feeding technique. But they adopted a separate circuit of active balun for the impedance transformation, which we want to avoid in a true differential feeding technique. A study in 2011 suggested that cross-polarization radiation characteristics of dual-port fed microstrip antenna are better than that of single-port fed antenna, and the phase difference of excitation of 180° of the dual-port fed antenna can give the best radiation property [142]. Another study proposed a tunable balanced antenna and demonstrated that balanced antenna delivers greater isolation in MIMO applications [143]. However, they used external matching circuits on each ports and a balun circuit, which would initiate distortion.

The benefits of using a true differential amplifier fed by a balanced antenna as a receiver have been demonstrated in [144], where researchers from Carlos III University, Spain, designed and analysed a fully differential amplifier topology. They focused on the design of broadband differential LNAs to feed differential broadband antenna arrays. This paper also considered a non-50Ω and varying antenna impedance and implemented in microstrip technology with discrete surface mount components. This design was proposed for the ambitious Square Kilometer Array (SKA) project [145]

2.9 Summary & Research Gap

The rapid advances in modern telecommunication have resulted in the development of the 3rd and 4th generation communications technology. These modern technologies seek stringent performance requirements for RF amplifiers such as large dynamic range, low distortion, high sensitivity, high efficiency and particularly high linearity [146]. They also demand wideband antennas to cover the required frequency bands for multiple applications.

It has already been stated in this chapter that several research works have reported benefits of implementing balanced antenna and differential amplifier for future mobile applications. Therefore, integrating differential amplifier feeding a balanced wideband antenna can offer solutions for those tougher requirements of modern communication devices. However this area

appears to be ignored, the reason might be due to the eccentricity of the approach and complex measurement techniques. Some research works have been conducted recently on this topic but most of them were not with a true differential feed. Few studies used fully differential feed but included an additional balun, which introduces distortion and frequency limitations. As mentioned earlier, the benefits of using a true differential amplifier fed by a balanced antenna as a receiver have been demonstrated recently. So it can be established that feeding a balanced transmit antenna with a fully differential power amplifier is an area of current research.

References

[1] A. A. Huurdeman (2003), *The Worldwide History of Telecommunications*, John Wiley & Sons, Hoboken, NJ, Chapter 4.

[2] James Clerk Maxwell, "A Dynamical Theory of the Electromagnetic Fie7ld", *Philosophical Transactions of the Royal Society of London* **155**, 459–512 (1865).

[3] J. D. Kraus, "Antenna Since Hertz and Marconi," IEEE Transactions on Antennas and Propagations, Vol. 33, No. 2, pp. 131 – 137, February 1985.

[4] H. R. Hertz, "Electric Waves: Being Researches on the Propagation of Electric Action with Finite Velocity Through Space", Macmillan, New York, 1893; reprinted Dover, New York, 1962.

[5] Marconi, G., "Wireless telegraphy," *Electrical Engineers, Journal of the Institution of* ,vol.28, no.139, pp.273-290, April 1899.

[6] David B. Davidson (2010), *Computational Electromagnetics for RF and Microwave Engineering*, Cambridge: Cambridge University Press, Chapter 5.

[7] Barrow, W.L.; Chu, L.J.; , "Theory of the Electromagnetic Horn," *Proceedings of the IRE* , vol.27, no.1, pp. 51- 64, Jan. 1939.

[8] E. V. Byron, "A new flush-mounted antenna element for phased array application," in Proc. Phased-Array Antenna Symp.. 1970, pp. 187-192.

[9] Martin Cooper; Richard W. Dronsuth; Albert J. Mikulski; Charles N. Lynk, Jr.; James J. Mikulski; John F. Mitchell; Roy A Richardson; John H. Sangster; "*Patent for the First Cell Phone System (Radio Telephone System)"*; September 16, 1975.

[10] Taga, T.; Tsunekawa, K., "Performance Analysis of a Built-In Planar Inverted F Antenna for 800 MHz Band Portable Radio Units," Selected Areas in Communications, IEEE Journal on , vol.5, no.5, pp.921,929, Jun 1987.

[11] Lee De Forest,; , "The Audion; A New Receiver for Wireless Telegraphy," American Institute of Electrical Engineers, Transactions of the , vol.XXV, no., pp.735-763, Jan. 1906.

[12] Robert L. Boylested (2006), *Electronics Devices and Circuit Theory*, Prentice-Hall, Chapter 2.

[13] December 23, 1947: Invention of the First Transistor, by American Physical Society; available at: http://www.aps.org/publications/apsnews/200011/history.cfm (Accessed: 22nd September, 2014).

[14] S. Engelbrecht and K. Kurokawa, "A Wideband Low Noise L-Band Balanced Transistor Amplifier," Proc.IEEE, vol. 53, no.3, pp. 237-247, March 1965.

[15] K. Kurokawa, "Design Theory of Balanced Transistor Amplifiers," Bell System Tech. J., vol. 44, pp. 1675-1698, Oct. 196511.

[16] Pucel, Robert A, "Design Considerations for Monolithic Microwave Circuits," Microwave Theory and Techniques, IEEE Transactions on , vol.29, no.6, pp.513,534, Jun 1981.

[17] Yongxi Qian; Itoh, T., "Progress in active integrated antennas and their applications," *Microwave Theory and Techniques, IEEE Transactions on* , vol.46, no.11, pp.1891,1900, Nov 1998.

[18] Frost, A, "Parametric amplifier antenna," Antennas and Propagation, IEEE Transactions on , vol.12, no.2, pp.234,235, Mar 1964.

[19] Fujimoto, K., "Active antennas: Tunnel-diode-loaded dipoles," *Proceedings of the IEEE* , vol.53, no.5, pp.556,556, May 1965.

[20] Meinke, H. H., "Tunnel diodes integrated with microwave antenna systems," *Radio and Electronic Engineer* , vol.31, no.2, pp.76,80, February 1966.

[21] Pelletier, M.; Cummins, J.; Sanzgiri, S., "Analysis of active antennas by the method of moments," *Antennas and Propagation Society International Symposium, 1972* , vol.10, no., pp.77,80, Dec 1972.

[22] Rangole, P.K.; Midha, S.S., "Short antenna with active inductance," *Electronics Letters* , vol.10, no.22, pp.462,463, October 31 1974.

[23] Copeland, John R.; Robertson, William J.; Verstraete, Robert G., "Antennafier arrays," *Antennas and Propagation, IEEE Transactions on* , vol.12, no.2, pp.227,233, Mar 1964.

[24] H. Meinke and F. M. Landstorfer, "Noise and Bandwidth Limitations with Transistorized Antennas," IEEE Antennas and Propagataion Symposium, Boston, September 1968.

[25] Ramsdale, P.A; Maclean, T. S M, "Active loop-dipole aerials," *Electrical Engineers, Proceedings of the Institution of* , vol.118, no.12, pp.1698,1710, December 1971.

[26] T. S. M. Maclean and P. A. Ramsdale, "Short Active Aerials for Transmission," International Journal of Electronics, Vol. 36, No. 2, pp. 261-269, February 1974.

[27] Maclean, T. S M; Morris, G., "Short range active transmitting antenna with very large height reduction," *Antennas and Propagation, IEEE Transactions on* , vol.23, no.2, pp.286,287, Mar 1975.

[28] Anderson, A; Davies, W.; Dawoud, M.; Galanakis, D., "Note on transistor-fed active-array antennas," *Antennas and Propagation, IEEE Trans. on* , vol.19, no.4, pp.537,539, 1971.

[29] Dawoud, M.M.; Anderson, AP., "Calculations showing the reduction in the frequency dependence of a two-element array antenna fed by microwave transistors," *Antennas and Propagation, IEEE Transactions on* , vol.20, no.4, pp.497,499, Jul 1972.

[30] Anderson, AP.; Dawoud, M.M., "The performance of transistor fed monopoles in active antennas," *Antennas and Propagation, IEEE Trans. on* , vol.21, no.3, pp.371,374, May 1973.

[31] Dawoud, M.M.; Anderson, AP., "Experimental verification of the reduced frequency dependence of active receiving arrays," *Antennas and Propagation, IEEE Transactions on* , vol.22, no.2, pp.342,344, Mar 1974.

[32] Stark, A, "Some special features of active receiving antennas," *Antennas and Propagation Society International Symposium, 1980* , vol.18, no., pp.387,388.

[33] Nordholt, Ernst H.; Van Willigen, Durk, "A new approach to active antenna design," *Antennas and Propagation, IEEE Trans. on* , vol.28, no.6, pp.904,910, Nov 1980.

[34] Hopf, J.; Lindenmeier, H., "Active loop antennas," *Antennas and Propagation Society International Symposium, 1982* , vol.20, no., pp.560,563, 24-28 May 1982.

[35] Nordholt, Ernst H.; Van Eerden, B., "An integrated amplifier for an active car-radio antenna," *Solid-State Circuits, IEEE Journal of* , vol.17, no.3, pp.591,593, June 1982.

[36] H. J. Thomas, D. L. Fudge, and G. Morris. "Gunn Source Integrated with Microstrip Patch," Microwave and RF (ISSN 0745-2993), Vol. 24, No. 2, pp. 87-91, February 1985.

[37] T. O. Perkins III, “Active Microstrip Circular Patch Antenna” *Microwave journal*, Vol. 30, No. 3, pp. 109-117, March 1987.

[38] Toland, B.; Lin, J.; Houshmand, B.; Itoh, T., "FDTD analysis of an active antenna," *Microwave and Guided Wave Letters, IEEE* , vol.3, no.11, pp.423,425, Nov. 1993.

[39] Kawasaki, S.; Itoh, T., "Optical Interaction of Active Integrated Antennas," *Microwave Conference, 1994. 24th European* , vol.1, no., pp.185,193, 5-9 Sept. 1994.

[40] Jenshan Lin; Itoh, T., "Active integrated antennas," *Microwave Theory and Techniques, IEEE Transactions on* , vol.42, no.12, pp.2186,2194, Dec 1994.

[41] Siou-Teck Chew; Tatsuo Itoh, "An active antenna phased array Doppler radar with tracking capability," *Antennas and Propagation Society International Symposium, 1995. AP-S. Digest* , vol.3, no., pp.1368,1371 vol.3, 18-23 June 1995.

[42] Pobanz, Carl W.; Jenshan Lin; Itoh, T., "Active integrated antennas for microwave wireless systems," *Signals, Systems, and Electronics, 1995. ISSSE '95, Proceedings., 1995 URSI International Symposium on* , vol., no., pp.1,4, 25-27 Oct 1995.

[43] Itoh, T., "Active integrated antennas for wireless applications," *Microwave Conference Proceedings, 1997. APMC, 1997 Asia-Pacific* , vol.1, no., pp.309,312 vol.1, 2-5 Dec 1997.

[44] Qian, Y.; Deal, W.R.; Kaneda, N.; Itoh, T., "Microstrip-fed quasi-Yagi antenna with broadband characteristics," *Electronics Letters* , vol.34, no.23, pp.2194,2196, 12 Nov 1998.

[45] Radisic, V.; Siou-Teck Chew; Yongxi Qian; Itoh, T., "High-efficiency power amplifier integrated with antenna," *Microwave and Guided Wave Letters, IEEE* , vol.7, no.2, pp.39,41, Feb 1997.

[46] V. Radisic, Y. Qian, and T. Itoh, “Class-F power amplifier integrated with circular sector microstrip antenna,” in *IEEE MTT-S Int. Microwave Symp. Dig.,*Denver, CO, June 1997, pp. 687–690.

[47] Radisic, V.; Yongxi Qian; Itoh, T., "Broadband power amplifier integrated with slot antenna and novel harmonic tuning structure," *Microwave Symposium Digest, 1998 IEEE MTT-S International* , vol.3, no., pp.1895,1898 vol.3, 7-12 June 1998.

[48] Radisic, V.; Yongxi Qian; Itoh, T., "Active antenna approach to high efficiency power amplifiers with EMI reduction," *Military Communications Conference, 1998. MILCOM 98. Proceedings., IEEE* , vol.3, no., pp.699,703 vol.3, 18-21 Oct 1998.

[49] R.Garg, P. Bhartia, I. Bahl and A. Ittipiboon, “Microstrip Antenna Design Handbook”, Artech House, Inc. 2001; Chapter 11.

[50] Lunden, O.-P., "Power combining of Ku-band active dipoles in a cylindrical resonant cavity," *Microwave Symposium Digest, 1995., IEEE MTT-S International* , vol., no., pp.701,704 vol.2, 16-20 May 1995.

[51] Younkyu Chung; Hang, Cynthia Y.; Cai, S.; Yongxi Qian; Wen, C.P.; Wang, K.L.; Itoh, T., "AlGaN/GaN HFET power amplifier integrated with microstrip antenna for RF front-end applications,"*Microwave Theory and Techniques, IEEE Transactions on* , vol.51, no.2, pp.653,659, Feb 2003.

[52] Hyungrak Kim; Ick-Jae Yoon; Young Joong Yoon, "A novel fully integrated transmitter front-end with high power-added efficiency," *Microwave Theory and Techniques, IEEE Transactions on* , vol.53, no.10, pp.3206,3214, Oct. 2005.

[53] Hyungrak Kim; Young Joong Yoon, "Wideband Design of the Fully Integrated Transmitter Front-End With High Power-Added Efficiency," *Microwave Theory and Techniques, IEEE Transactions on* , vol.55, no.5, pp.916,924, May 2007.

[54] Moreira, C.P.; Shirakawa, A A; Kerherve, E.; Pham, J-M; Jarry, P.; Belot, D.; Ancey, P., "Design of a Fully-integrated BiCMOS/FBAR Reconfigurable RF Receiver Front-End," *Integrated Circuits and Systems Design, 18th Symposium on* , vol., no., pp.138,143, 4-7 Sept. 2005.

[55] Jun Wu; Peichen Jiang; Dongpo Chen; Jianjun Zhou, "A Dual-Band GNSS RF Front End With a Pseudo-Differential LNA," *Circuits and Systems II: Express Briefs, IEEE Transactions on* , vol.58, no.3, pp.134,138, March 2011.

[56] Labadie, N.R.; Sharma, S.K.; Rebeiz, G.M., "A Circularly Polarized Multiple Radiating Mode Microstrip Antenna for Satellite Receive Applications," *Antennas and Propagation, IEEE Transactions on* , vol.62, no.7, pp.3490,3500, July 2014.

[57] Karnfelt, C.; Hallbjorner, P.; Zirath, H.; Alping, A, "High gain active microstrip antenna for 60-GHz WLAN/WPAN applications," *Microwave Theory and Techniques, IEEE Transactions on* , vol.54, no.6, pp.2593,2603, June 2006.

[58] Ellis, G.A; Liw, S., "Active planar inverted-F antennas for wireless applications," *Antennas and Propagation, IEEE Transactions on* , vol.51, no.10, pp.2899,2906, Oct. 2003.

[59] Sanchez-Montero, R.; Rigelsford, J.M.; Lopez-Espi, P.L.; Alpuente Hermosilla, J., "An active multiband antenna for future wireless communications," *Antennas and Propagation (EuCAP), 2014 8th European Conference on* , vol., no., pp.2989,2991, 6-11 April 2014.

[60] Cheng, S.; Hallbjorner, P.; Rydberg, A; Vanotterdijk, D.; van Engen, P., "T-matched dipole antenna integrated in electrically small body-worn wireless sensor node," *Microwaves, Antennas & Propagation, IET* , vol.3, no.5, pp.774,781, August 2009.

[61] Alvarez-Folgueiras, M.; Rodriguez-Gonzalez, J.A; Ares-Pena, F., "Low-Sidelobe Patterns From Small, Low-Loss Uniformly Fed Linear Arrays Illuminating Parasitic Dipoles," *Antennas and Propagation, IEEE Transactions on* , vol.57, no.5, pp.1584,1586, May 2009.

[62] Jun-Ho Choi; Joon-ho So; Cheol-Sun Park; Seung-Sub Oh, "Active composite dipole antenna for direction finding array antenna applications," *Antennas and Propagation Society International Symposium 2006, IEEE* , vol., no., pp.1153,1156, 9-14 July 2006.

[63] Xiaoyu Cheng; Jun Shi; Jungkwun Kim; Cheolbok Kim; Senior, D.E.; Yong-Kyu Yoon, "Compact self-packaged active folded patch antenna with omni-directional radiation pattern," *Electronic Components and Technology Conference (ECTC), 2011 IEEE 61st* , vol., no., pp.1041,1046, May 31 2011-June 3 2011.

[64] Loizeau, S.; Sibille, A, "Reconfigurable ultra-wide band monopole antenna with a continuously tunable band notch," *Microwaves, Antennas & Propagation, IET* , vol.8, no.5, pp.346,350, April 8 2014.

[65] W.K. Leverich, X.-D. Wu and K. Chang, “New FET active notch antenna”, Electronics Letters, vol. 28, no. 24, pp. 2239-2240, November 1992.

[66] H.P. Moyer and R.A. York, “Active cavity-backed slot antenna”, IEEE microwave and guided wave letters, vol. 3, no. 4, pp. 95-97, April 1993.

[67] Rahim, M. K A; Gardner, P., "Active microstrip log periodic antenna," *RF and Microwave Conference, 2004. RFM 2004. Proceedings* , vol., no., pp.136,139, 5-6 Oct. 2004.

[68] Yong Cai; Guo, Y.J.; Bird, T.S., "A Frequency Reconfigurable Printed Yagi-Uda Dipole Antenna for Cognitive Radio Applications," *Antennas and Propagation, IEEE Transactions on* , vol.60, no.6, pp.2905,2912, June 2012

[69] Cai Run-nan; Lin Shu; Huang Guan-long; Zhang Xue-ying; Zhang Xing-qi; Zhang Wen-bin; Wang Jin-xiang, "Research on a novel Yagi-Uda antenna fed by balanced microstrip line," *Microwave Conference Proceedings (CJMW), 2011 China-Japan Joint* , vol., no., pp.1,4, 20-22 April 2011

[70] Navarro. J. A., Chang. K., "Integrated Active Antennas and Spatial Power Combining", John Wiley & Sons, New York, 1996.

[71] Kaleja, M.; Biebl, E., "Active integrated antennas for automotive applications," *Antennas for Automotives (Ref. No. 2000/002), IEE Colloquium on* , vol., no., pp.2/1,2/5, 2000.

[72] Xue, Q.; Wong, H.; Shum, K.M.; Luk, K.M.; Chan, C.H., "Active receiving antennas for automotive applications," *Antennas and Propagation Society International Symposium, 2004. IEEE* , vol.2, no., pp.1443,1446 Vol.2, 20-25 June 2004.

[73] Reiter, Leopold; Boge, Alexander; Negut, Alexandru; Lindenmeier, Stefan, "A new low-cost active rod antenna for automotive reception of all terrestrial audio broadcast services," *Antennas and Propagation (EuCAP), 2014 8th European Conference on* , vol., no., pp.2981,2984, 6-11 April 2014.

[74] Yegin, K., "AMPS/PCS/GPS Active Antenna for Emergency Call Systems," *Antennas and Wireless Propagation Letters, IEEE* , vol.6, no., pp.255,258, 2007.

[75] Jahagirdar, D. R., "A GPS+GLONOSS active antenna for extremely high temperature aerospace applications," *Antennas and Propagation Society International Symposium (APSURSI), 2012 IEEE*, vol., no., pp.1,2, 8-14 July 2012.

[76] Dierck, A; Rogier, H.; Declercq, F., "A Wearable Active Antenna for Global Positioning System and Satellite Phone," *Antennas and Propagation, IEEE Transactions on* , vol.61, no.2, pp.532,538, Feb. 2013.

[77] Jun-Ho Choi; Joon-ho So; Cheol-Sun Park; Seung-Sub Oh, "Active composite dipole antenna for direction finding array antenna applications," *Antennas and Propagation Society International Symposium 2006, IEEE* , vol., no., pp.1153,1156, 9-14 July 2006.

[78] Ong, L.T.; Tan, P.K., "Active receiving antennas for direction finding," *Antennas and Propagation in Wireless Communications (APWC), 2013 IEEE-APS Topical Conference on* , vol., no., pp.192,195, 9-13 Sept. 2013.

[79] Zhang, D.; Yang, L.T.; Chen, M.; Zhao, S.; Guo, M.; Zhang, Y., "Real-Time Locating Systems Using Active RFID for Internet of Things," *Systems Journal, IEEE* , 2014, vol.PP, no.99, pp.1,10.

[80] Itoh, T., "Active integrated antennas for wireless applications," *Microwave Conference Proceedings, 1997. APMC, 1997 Asia-Pacific* , vol.1, no., pp.309,312 vol.1, 2-5 Dec 1997.

[81] Ellis, G.A; Liw, S., "Active planar inverted-F antennas for wireless applications," *Antennas and Propagation, IEEE Transactions on* , vol.51, no.10, pp.2899,2906, Oct. 2003.

[82] Shi Zhao Fan; Eng Leong Tan, "A low cost omnidirectional high gain active integrated antenna for WLAN applications," *Antennas and Propagation (APCAP), 2012 IEEE Asia-Pacific Conference on* , vol., no., pp.124,125, 27-29 Aug. 2012.

[83] Yin Qin; Gao, S.; Sambell, A, "Broadband high-efficiency circularly polarized active antenna and array for RF front-end application," *Microwave Theory and Techniques, IEEE Transactions on* , vol.54, no.7, pp.2910,2916, July 2006.

[84] Sanchez-Montero, R.; Rigelsford, J.M.; Lopez-Espi, P.L.; Alpuente-Hermosilla, J., "An active multiband antenna for future wireless communications," *Antennas and Propagation (EuCAP), 2014 8th European Conference on* , vol., no., pp.2989,2991, 6-11 April 2014.

[85] Taguchi, M.; Wakimoto, Y.; Komine, I; Tanaka, K., "Active dipole antenna for television receiver," *Antennas and Propagation Society International Symposium, 1994. AP-S. Digest* , vol.1, no., pp.636,639 vol.1, 20-24 June 1994.

[86] Anashkinm, AA, "Evaluation of Traveling-Way Tubes Availability in Active Phased Array Antennas for Digital Television," *Actual Problems of Electron Devices Engineering, International Conference on* , vol., no., pp.12,16, 20-21 Sept. 2006.

[87] Codispoti, G.; Lisi, M.; Santachiara, V., "X-band SAR active antenna design for small satellite applications," *Antennas and Propagation Society International Symposium, 1995. AP-S. Digest* , vol.1, no., pp.666,669 vol.1, 18-23 June 1995.

[88] Labadie, N.R.; Sharma, S.K.; Rebeiz, G.M., "A Circularly Polarized Multiple Radiating Mode Microstrip Antenna for Satellite Receive Applications," *Antennas and Propagation, IEEE Transactions on* , vol.62, no.7, pp.3490,3500, July 2014.

[89] Siou Teck Chew; Tong, D. T K; Wu, M.C.; Itoh, T., "Active antenna array with optical interaction for application in radar system," *Microwave Systems Conference, 1995. Conference Proceedings., IEEE NTC '95* , vol., no., pp.185,188, 17-19 May 1995.

[90] Lin, S.; Qian, Y.; Itoh, T., "A low noise active integrated antenna receiver for monopulse radar applications," *Microwave Symposium Digest, 2001 IEEE MTT-S International* , vol.2, no., pp.1395,1398 vol.2, 20-24 May 2001.

[91] Hudec, P.; Svanda, M.; Polivka, Milan, "Active UHF antennas for demanding RFID applications," *Microwave Conference (EuMC), 2010 European* , vol., no., pp.1098,1101, 28-30 Sept. 2010.

[92] Omar, M.Q.; Widad, I; Mokhtar, M.; Inzarulfaisham, AR.; Miskam, M.A, "Embedded active RFID with WSN for machine condition monitoring," *Wireless Sensor (ICWISE), 2013 IEEE Conference on* , vol., no., pp.42,46, 2-4 Dec. 2013.

[93] Tuset-Peiro, P.; Alonso, L.; Vezquez-Gallego, F.; Alonso-Zarate, J.; Vilajosana-Guillen, X., "Demonstrating Low-Power Distributed Queuing for active RFID communications at 433 MHz,"*Computer Communications Workshops, 2014 IEEE Conference on* , vol., no., pp.157,158, April 27 2014-May 2 2014.

[94] Lazaro, A; Ramos, A; Villarino, R.; Girbau, D., "Active UWB Reflector for RFID and Wireless Sensor Networks," *Antennas and Propagation, IEEE Transactions on* , vol.61, no.9, pp.4767,4774, Sept. 2013.

[95] Hawkes, R., Davies, I., and Price, W. (1990), *Integrated Circuit Cards, Tags and Tokens: New Technology and Applications,* Oxford : BPS Professional Books, Chapter 2.

[96] Georgiadis, A; Collado, A; Kim, Sangkil; Hoseon Lee; Tentzeris, M.M., "UHF solar powered active oscillator antenna on low cost flexible substrate for wireless identification applications,"*Microwave Symposium Digest (MTT), 2012 IEEE MTT-S International* , vol., no., pp.1,3, 17-22 June 2012.

[97] Razban, T.; Robert, B., "Weather Forecasting Radar Antenna: An Application of Active Microstrip Antennas," *Microwave Conference, 1992. 22nd European* , vol.2, no., pp.888,893, 5-9 Sept. 1992.

[98] S. Battiboia, A. Caliumi, S. Catena, E. Marazzi, and L. Masini, "Low-Power X-Band Radar for Indoor Burglar Alarms," IEEE Trans. Microwave Theory and Tech., vol. MTT-43, pp. 1710-1714, July 1995.

[99] Nalezinski, M.; Vossiek, M.; Heide, P., "Novel 24 GHz FMCW front-end with 2.45 GHz SAW reference path for high-precision distance measurements," *Microwave Symposium Digest, 1997., IEEE MTT-S International* , vol.1, no., pp.185,188 vol.1, 8-13 June 1997.

[100] Zhou, D.; Abd-Alhameed, R.A; Excell, P.S., "Wideband Balanced Folded Dipole Antenna for Mobile Handsets," *Antennas and Propagation, 2007. EuCAP 2007. The Second European Conference on* , vol., no., pp.1,5, 11-16 Nov. 2007.

[101] Li, Z. and Y. Rahmat-Samii, "Optimization of PIFA-IFA combination in handset antenna designs " , IEEE Trans. on Antennas and Propagation, Vol. 53, No. 5, 1770-1778, May 2005.

[102] Wang, Y.-S., M.-C. Lee, and S.-J. Chung, "Two PIFA-related miniaturized dual-band antennas" , IEEE Trans. on Antennas and Propagation, Vol. 55, No. 3, 805{811, March 2007.

[103] Huynh, M.-C. and W. Stutzman, "Ground plane effects on planar inverted-F antenna (PIFA) performance" , IEE Proc.-Microw. Antennas Propag., Vol. 150, 209-213, August 2003.

[104] Janapsatya, J., K. P. Esselle, and T. S. Bird, "A dual-band and wideband planar inverted-F antenna for WLAN applications", Microwave and Optical Technology Letters, Vol. 50, 138-141,January 2008.

[105] Ogawa, K.; Iwai, H.; Koyanagi, Y., "A balance-fed planar built-in antenna," *Antennas, Propagation and EM Theory, 2000. Proceedings. ISAPE 2000. 5th International Symposium on* , vol., no., pp.680,683, 15-18 Aug. 2000.

[106] Morishita, H.; Furuuchi, H.; Fujimoto, K., "Performance of balance-fed antenna system for handsets in the vicinity of a human head or hand," *Microwaves, Antennas and Propagation, IEE Proceedings* , vol.149, no.2, pp.85,91, Apr 2002.

[107] Abd-Alhameed, R.A., Excell, P.S., Khalil, K., Alias, R., Mustafa, J.: SAR and radiation performance of balanced and unbalanced mobile antennas using a hybrid formulation', IEE Proc., Sci. Meas. Technol. Spec. Issue Comput. Electromagn., 2004, 151, (6), pp. 440–444.

[108] Arenas, J.J., Anguera, J., Puente, C.: 'Balanced and single-ended handset antennas: free space and human loading comparison', Microw. Opt. Technol. Lett., 2009, 51, (9), pp. 2248–2254.

[109] Morishita, H., Hayashida, S., Ito, J., Fujimoto, K.: 'Analysis of built-in antenna for handset using human (head, hand, finger) model', Electron. Commun. Jpn., 2003 Part 1, 86, (9), pp. 35–45.

[110] Navsariwala, U., Svigelj, J.: 'A reduced sized balanced antenna for 2.4 GHz WLAN'. IEEE Int. Symp. on Antennas and Propagation, June 2003, vol. 2, pp. 6–9] .

[111] Alhaddad, A G.; Ramli, K. N.; Abd-Alhameed, R.A; Zhou, D., "Interaction between electromagnetic field and human body for dual band balanced antenna using hybrid computational method,"*Antennas and Propagation Conference (LAPC), 2010 Loughborough* , vol., no., pp.449,452, 8-9 Nov. 2010.

[112] Collins, B.S., Kingsley, S.P., Ide, J.M., Saario, S.A., Schlub, R.W., O'Keefe, S.G.: 'A multi-band hybrid balanced antenna'. IEEE 2006 Int. Workshop on Antenna Tech: Small Antennas; Novel Metamaterials, White Plains, New York, 6–8 March 2006, pp. 100–103.

[113] Ilvonen, J.; Holopainen, J.; Kivekas, O.; Valkonen, R.; Icheln, C.; Vainikainen, P.; , "Balanced antenna structures of mobile terminals," *Antennas and Propagation (EuCAP), 2010 Proceedings of the Fourth European Conference on* , vol., no., pp.1-5, 12-16 Apr 2010.

[114] Collins, B.S.; Iellici, D.; Kingsley, S.P.; Raffaelli, S.; , "Balanced Antennas for GPS and Galileo Receivers," *Antennas and Propagation Conference, 2007. LAPC 2007. Loughborough* , vol., no., pp.321-324, 2-3 April 2007.

[115] Alhaddad, AG.; Abd-Alhameed, R.A; Zhou, D.; See, C.H.; Elfergani, IT.E.; Excell, P.S., "Low profile dual-band-balanced handset antenna with dual-arm structure for WLAN application,"*Microwaves, Antennas & Propagation, IET* , vol.5, no.9, pp.1045,1053, 2011.

[116] D. E. Bockelman and W. R. Eisenstadt, "Combined differential and common-mode scattering parameters: Theory and simulation," *IEEE Trans. Microw. Theory Tech.*, vol. 43, no. 7, pp. 1530–1539, Jul. 1995.

[117] L. Belostotski and J. W. Haslett, “A technique for differential noise figure measurement of differential LNAs,” *IEEE Trans. Instrum. Meas.*, vol. 57, no. 7, pp. 1298–1303, Jul. 2008.

[118] Issakov, V.; Wojnowski, M.; Thiede, A.; Winkler, V.; Tiebout, M.; Simburger, W.; , "Considerations on the measurement of active differential devices using baluns," *Microwaves, Communications, Antennas and Electronics Systems, 2009. COMCAS 2009. IEEE International Conference on* , vol., no., pp.1-7, 9-11 Nov. 2009

[119] Ning Yang; Caloz, C.; Ke Wu, "Measurement of balanced antennas using mixed-mode network parameters," *General Assembly and Scientific Symposium, 2011 URSI* , vol., no., pp.1,4, 13-20 Aug. 2011.

[120] Richard C. Li (2012), *RF Circuit Design (Information and Communication Technology Series,)*. 2nd ed. Blackwell: Wiley & Sons Inc. Chapter 13.

[121] Yoon, J.; Park, C., "A CMOS LNA Using a Harmonic Rejection Technique to Enhance Its Linearity," *Microwave and Wireless Components Letters, IEEE* , vol.24, no.9, pp.605,607, Sept. 2014.

[122] Pan, H.-Y.M.; Larson, L.E., "An Improved Broadband High Linearity SiGe HBT Differential Amplifier," *Circuits and Systems I: Regular Papers, IEEE Transactions on* , vol.58, no.8, pp.1685,1694, Aug. 2011.

[123] Wu, R.; Lidgey, F.J.; Hayatleh, K.; Hart, B. L., "Design of Differential Amplifier with Negative Impedance Compensation," *Circuits and Systems for Communications, 2008. ICCSC 2008. 4th IEEE International Conference on* , vol., no., pp.589,593, 26-28 May 2008.

[124] Siu Yee Mok; Ka Tsun Mok; Wing Shing Chan, "Active broadband integrated antenna for differential application," *Microwave Conference, 2006. APMC 2006. Asia-Pacific* , vol., no., pp.235,238, 12-15 Dec. 2006.

[125] Wadefalk, N.; Kildal, P. -S; Zirath, H., "A Low Noise Integrated 0.3-16 GHz Differential Amplifier for Balanced Ultra Wideband Antennas," *Compound Semiconductor Integrated Circuit Symposium (CSICS), 2010 IEEE* , vol., no., pp.1,4, 3-6 Oct. 2010.

[126] Hang, Cynthia Y.; Deal, W.R.; Yongxi Qian; Itoh, T., "High-efficiency push-pull power amplifier integrated with quasi-Yagi antenna," *Microwave Theory and Techniques, IEEE Transactions on* , vol.49, no.6, pp.1155,1161, Jun 2001.

[127] Jui-Han Lu; Jia-Ling Guo, "Small-Size Octaband Monopole Antenna in an LTE/WWAN Mobile Phone," Antennas and Wireless Propagation Letters, IEEE , vol.13, no., pp.548,551, 2014.

[128] Shao-li Zuo; Zhi-ya Zhang; Jia-Wei Yang, "Planar Meander Monopole Antenna With Parasitic Strips and Sleeve Feed for DVBH/ LTE/GSM850/900 Operation in the Mobile Phone," Antennas and Wireless Propagation Letters, IEEE , vol.12, no., pp.27,30, 2013.

[129] D. Pilgrim: 'Reconfigurable CMOS RF Front End', Microwv Journal, June'14, p 22-40.

[130] Deal, W.R.; Radisic, V.; Yongxi Qian; Itoh, T., "Novel push-pull integrated antenna transmitter front-end," *Microwave and Guided Wave Lett, IEEE* ,vol.8, no.11, pp.405,407, Nov 1998.

[131] Deal, W.R.; Radisic, V.; Yongxi Qian; Itoh, T., "Integrated-antenna push-pull power amplifiers," *Microwave Theory and Techniques, IEEE Transactions on* , vol.47, no.8, pp.1418,1425, Aug 1999.

[132] Hang,.Y.; Deal, W.R.; Yongxi Qian; Itoh, T.,"Push-pull power amplifier integrated with microstrip leaky-wave antenna,"*Electronics Letters* ,vol.35,no.22, pp.1891,1893,28 1999.

[133] Hang, C.Y.; Deal, W.R.; Qian, Y.; Itoh, T., "Push-pull power amplifier integrated with quasi-Yagi antenna for power combining and harmonic tuning," *Microwave Symposium Digest. 2000 IEEE MTT-S International* , vol.1, no., pp.533,536 vol.1, 11-16 June 2000.

[134] Gao, S.C.; Gardner, P., "Novel integrated antenna for LINC power amplifiers," *Antennas and Propagation Society International Symposium, 2002. IEEE* , vol.2, no., pp.508,511 vol.2, 2002.

[135] Chan, K.M.; Lee, E.; Gardner, P., "Differential Feeding Technique for Active Integrated Antennas," *Wireless Technology, 2006. The 9th European Conference on* , vol., no., pp.1,3, 10-12 Sept. 2006.

[136] Chan, K.M.; Lee, E.; Gardner, P., "Compact push-pull active integrated transmitting antenna," *Microwave Conference, 2005 European* , vol.3, no., pp.4 pp.,, 4-6 Oct. 2005.

[137] Chan, K.M.; Lee, E.; Gardner, P.; Hall, P.S., "A differentially fed electrically small antenna," *Antennas and Propagation Society International Symposium, 2007 IEEE* , vol., no., pp.2447,2450, 9-15 June 2007.

[138] Lee, E.; Chan, K.M.; Gardner, P.; Dodgson, T.E., "Active Integrated Antenna Design Using a Contact-Less, Proximity Coupled, Differentially Fed Technique," *Antennas and Propagation, IEEE Transactions on* , vol.55, no.2, pp.267,276, Feb. 2007.

[139] Serrano, R.; Aguasca, A; Romeu, J.; Blanch, S.; Jofre, L.; Cabedo, M.; Antonino, E.; Valero, A; Ferrando, M., "Active balanced feeding for compact wideband antennas," *Antennas and Propagation Society International Symposium, 2007 IEEE* , vol., no., pp.2829,2832, 9-15 June 2007.

[140] Zubir, F.; Gardner, P., "Differentially fed multilayer antennas with harmonic filtering for push-pull Class B Power Amplifier integration," Microwave Conference (EuMC), 2013 European , vol., no., pp.96,99, 6-10 Oct. 2013 .

[141] Bourtoutian, R.; Delaveaud, C.; Toutain, S.; , "Differential antenna design and characterization," *Antennas and Propagation, 2009. EuCAP 2009. 3rd European Conference on* , vol., no., pp.2398-2402, 23-27 March 2009.

[142] Weiwei Xu; Junhong Wang; Zhan Zhang; Meie Chen, "Radiation and scattering properties of the dual-port fed differential microstrip antennas," *Microwave, Antenna, Propagation, and EMC Technologies for Wireless Communications (MAPE), 2011 IEEE 4th International Symposium on* , vol., no., pp.124,127, 1-3 Nov. 2011.

[143] Zhen Hua Hu; Hall, P.S.; Gardner, P.; Nechayev, Y., "Wide tunable balanced antenna for mobile terminals and its potential for MIMO applications," *Antennas and Propagation Conference (LAPC), 2011 Loughborough* , vol., no., pp.1,4, 14-15 Nov. 2011.

[144] García-Pérez, O.; Segovia-Vargas, D.; García-Muñoz, L.E.; Jiménez-Martín, J.L.; González-Posadas, V.; , "Broadband Differential Low-Noise Amplifier for Active Differential Arrays," *Microwave Theory and Techniques, IEEE Transactions on* , vol.59, no.1, pp.108-115, Jan. 2011.

[145] Mittra, R., "Square Kilometer Array-A unique instrument for exploring the mysteries of the universe using the Square Kilometer Array," *Applied Electromagnetics Conference (AEMC), 2009* , vol., no., pp.1,6, 14-16 Dec. 2009.

[146] J. I. Agbinya, M. C. Aguayo-Torres (2013), *4G Wireless Communication Networks*, Denmark: River Publishers, Chapter 1.

Chapter 3

Balanced Antenna for Mobile Communication

3.1 Introduction

The significant development in wireless communication requires designing differentially fed antennas using a differential amplifier to achieve higher power and greater linearity. Performing this whole process is a challenge, as one has to be experienced in antenna design as well as in RF/microwave circuit design. In this chapter, balanced and unbalanced antennas are introduced and the ground plane effect is investigated. Initially balanced and unbalanced antennas and transmission lines have been discussed, followed by current distribution in coaxial cable, mechanism of balun circuit and impedance of balanced and unbalanced antennas. Subsequent sections describe the power distribution of dipole antennas for different wavelengths and radiation pattern of simple monopole antenna over ground plane of different sizes. Following that, an antenna for mobile handheld device is reported and the ground plane influence is investigated. Techniques have been examined to control the ground plane current and reduce degradation by using choke-slot on the solid ground plane of a mobile antenna.

3.2 Unbalanced Transmission Lines and Antennas

An unbalanced transmission line's conductors have unequal impedances with respect to ground contrasting to a balanced line. In an unbalanced transmission line, the electromagnetic fields around the conductors are not the same and do not cancel out, so radiation from the transmission line occurs. In the case of coaxial cable, the current flowing on the *inside* of the shield is equal to the current on the center conductor, thereby maintaining a balance inside the cable, as shown in Figure 3.1. The current on the cable's center conductor flows into the left side of the dipole. And the equal and opposite current on the inside of the shield flows partly along the outside of the shield and partly into the right half of the dipole [1]. As a result, the desired power is effectively divided into an unwanted and harmful power caused by unwanted current and voltage in undesired place. The extraneous current flowing along the outer surface of the shield will not be balanced against anything and will lead to an unbalanced condition with radiation from the feed line occurring as a consequence. Such radiation and unequal

current will consume power from the energy transferred between the antenna and the receiver or transmitter system and therefore will decrease efficiency and performance of the entire system.

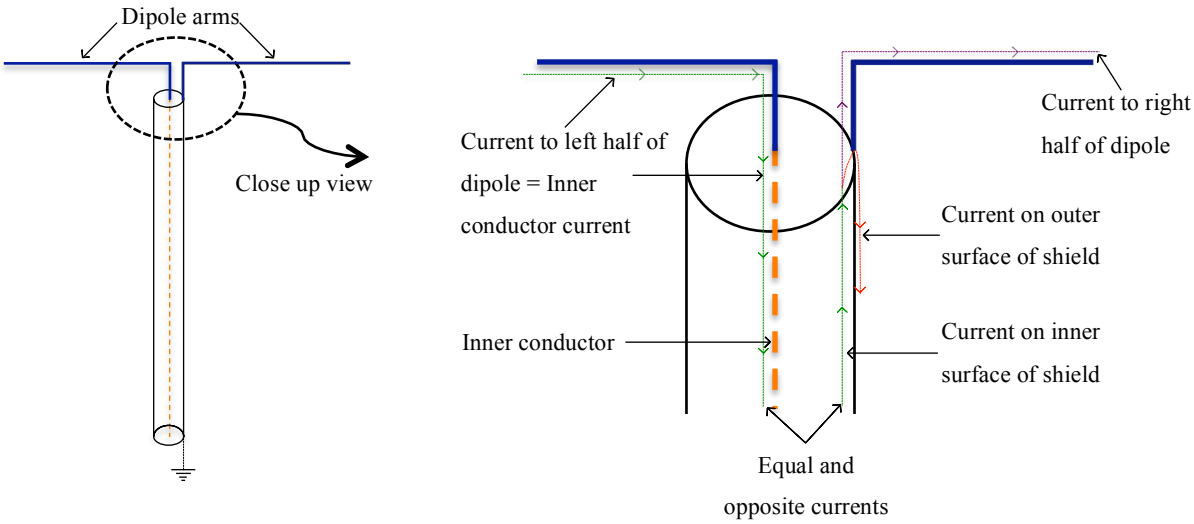

Figure 3.1: Coaxial cable current distribution feeding a dipole antenna [2]

In addition, usually the coax shield is connected to the ground part of a monopole antenna. Since the voltage at ground should be constant, the full voltage differential occurs between the centre conductor and ground. As a result the transmission line acts as a part of the antenna. Therefore, it can be said that the antenna accounts for only half the radiation mechanism, and the ground plane is the other half [3]. For these reasons, coaxial cable is referred to as an unbalanced transmission line. Also, if an antenna is fed off-center where the feed is placed away from the center of the antenna, there may be a natural tendency for more current to flow into one side of the feed point than the other, resulting in an unbalanced condition [4].

Many handset designs utilize antennas with unbalanced terminals fed by these unbalanced lines, usually for size considerations. In this type of antenna, the radiation currents are induced on the conducting surfaces of the handset chassis, as well as on the radiating element itself [5]. The most commonly used example of this type of antenna is the PIFA. They are in widespread use due to their size advantages, low profile, and relative low costs in high volume manufacturing compared to the conventional radiators [6-8]. The generic PIFA structure comprises a ground plane, top patch, shorting post and is fed by an unbalanced

transmission line, which gives rise to λ/4-resonator [9-10]. It should be noted that the height and shorting post impose practical limits on the antenna size [11]. However, in this kind of unbalanced antenna, the ground plane plays a significant role in antenna radiation characteristics due to the loss induced by hand or head. When a user holds a device designed with such antennas, coupling will take place between the user's hand and the ground plane and this can significantly perturb antenna performance, which has been discussed in the previous chapter. The best solution to this problem is to isolate or reduce the current flow from the antenna to the ground plane. Several means to reduce this unwanted degradation have been tried so far. The most effective way is to construct an antenna with a balanced structure and feed the antenna with a balanced line.

3.3 Balanced Antennas

The recent upsurge in the demand for portable wireless communication products has caused much research interest in balanced antenna technology due to their stable and improved performance compared to their unbalanced counterpart. A balanced antenna is a symmetrical antenna fed by two signals of equal amplitude and opposite in phase. While an unbalanced antenna has only a single terminal and is driven against the local ground plane, a balanced antenna is one with two terminals exhibiting equal impedances with respect to the ground plane. These two terminals are excited with equal voltages with a phase difference of 180°. Figure 3.2 illustrates the balanced and unbalanced antenna arrangements, where 3.2 (a) is the simplest example of a balanced dipole antenna, 3.2 (b) represents a monopole having a single radiating element by using one arm of the antenna as ground plane and 3.2 (c) demonstrates an integrated balanced antenna/amplifier structure, eliminating the need for connecting unbalanced transmission line to the antenna.

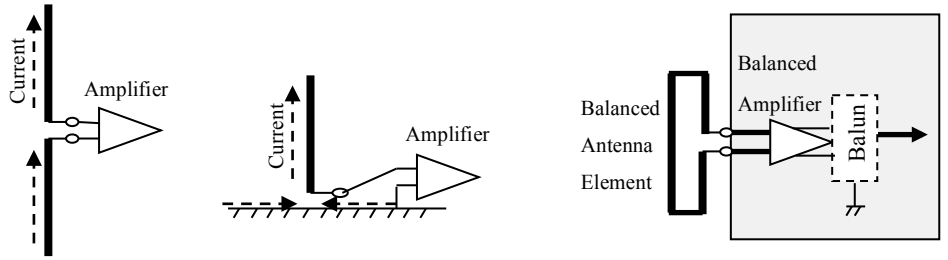

(a) Ideal Dipole *(b) Ideal Monopole* *(c) Balanced Antenna / Amplifier*

Figure 3.2: Balanced and unbalanced antenna arrangements

Centre fed dipole with symmetric arms and loops are the most commonly used balanced antennas. Balanced antennas possess various benefits over their unbalanced counterparts, especially in mobile handheld devices. A balanced antenna with balanced feed keeps the ground plane almost free of induced current [12], hence any degradation of the antenna performance due to the influence of the human body can be largely eliminated. The maximum SAR values have been shown to be substantially reduced using balanced antennas when placed next to the human head, compared with conventional unbalanced antennas [13]. There is almost no influence on balanced antenna impedance when it comes near to a big lossy medium such as human body. The dimensions of the device have nearly no effect on antenna performance and a balanced antenna does not need to be sited at any particular place of a handheld device because its operation is independent of any ground plane excitation [14].

3.4 Unbalanced – Balanced Operation Using Balun Circuit

A balanced antenna must be fed in a balanced way in order to attain its advantages. Balanced antenna fed by unbalanced transmission line (such as a coaxial cable) can produce common mode currents, which can radiate and distort the radiation pattern. To prevent this, dipoles fed by coaxial cables have a balun between the cable and the antenna, to eliminate the unwanted portion of the transmission line current and to provide a balanced state at the input terminals of the antenna [15]. A balun is an unbalanced to balanced transformer used to connect two different types of transmission lines. By using balun, most of the imperfections introduced by the unbalanced feeding can be eliminated. A schematic diagram of a two-terminal balanced antenna fed by a balun is shown in Figure 3.3. The balance is characterized by nearly zero current on the outer surface of the coaxial cable ($I_s = 0$), equal impedances looking into each terminal ($Z_{ag} = Z_{bg}$), the equal driving voltages that are in opposite direction ($V_a = -V_b$) and equal terminal currents ($I_b = -I_a$) that are opposite in phase.

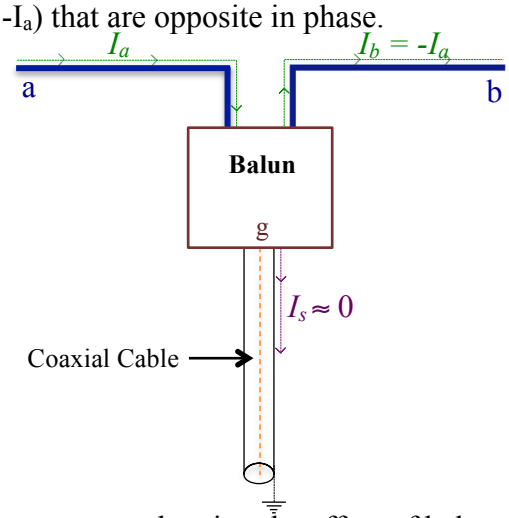

Figure 3.3: Dipole antenna system showing the effect of balun (Reproduced from [16])

Many circuits benefit from balanced inputs and outputs in order to reduce noise and harmonic distortions as well as improve the dynamic range of the circuits. Thus, it is a common practice to assign balanced-unbalanced transformer to convert between single-ended and differential signals and perform the measurement in a balanced way. However, there are some drawbacks of attaching a balun in a circuit. Researchers have already reported and proved that balun affects the gain and efficiency of a device in the measurement process, which has been discussed in the previous chapter. It also increases the size of the device and limits impedance bandwidth. Avoiding this loss is a challenge for researchers in the field of measurement techniques of active balanced antenna.

3.5 Impedance of Basic Unbalanced and Balanced (Dipole) Antenna

The dipole antenna is one of the most important and commonly used types of RF antenna. As the name suggests the dipole antenna consists of two terminals into which radio frequency current flows. This current and the associated voltage cause an electromagnetic signal to be radiated. A dipole is a balanced antenna, meaning that the two poles are symmetrical and the currents on both arms are equal in magnitude and opposite in phase [17]. The most common form of dipole has an electrical length of half a wavelength. As the total length of the dipole is a half wavelength, this makes each similar section of the dipole a quarter wavelength long. The input impedance of an infinitely thin dipole of exactly one half wavelength is $Z_{dipole} = 73 + j42.5\Omega$. The length of a dipole is the principal determining factor for the operation frequency of the dipole antenna. Although ideally the antenna may be an electrical half wavelength, or multiple of half wavelengths, it is not exactly the same length as theoretically calculated for a signal travelling in free space. A dipole antenna will be slightly shorter than the length calculated for a wave travelling in free space [18].

A monopole antenna is a class of radio antenna consisting of a straight rod-shaped conductor, often mounted perpendicularly over some type of planar conductive surface, called as ground plane. The electrical properties of such antennas are dependent upon the geometry of both the monopole elements and ground plane. The typical feed of a monopole antenna is an unbalanced coaxial cable and the monopole antenna is an example of unbalanced antenna. Monopole antennas are half the size of their dipole counterparts, and hence are attractive when a smaller

antenna is needed. So, when placed over a conducting ground plane, a quarter-wave monopole antenna excited by a source at its base exhibits the same radiation pattern in the region above the ground as a half-wave dipole in free space. The phenomenon is explained by image theory [17], where the conducting plane can be replaced with the image of a λ/4 monopole, as shown in Figure 3.4. However, the monopole can only radiate above the ground plane.

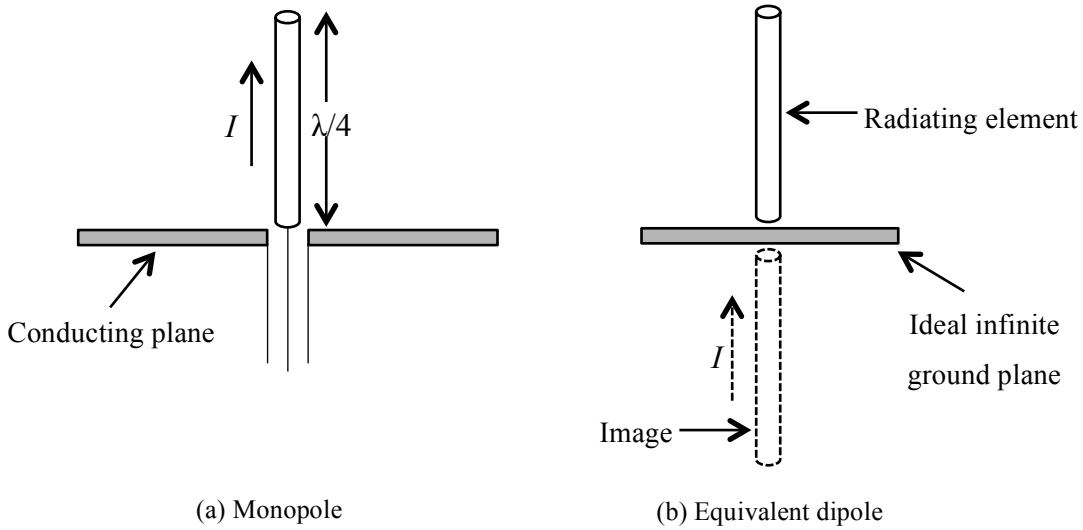

Figure 3.4: (a) Quarter-wave monopole fed against a large solid ground plane, (b) Equivalent half-wave dipole model

The currents and charges on a monopole are the same as on the upper half of its dipole counterpart, but the terminal voltage is only half that of the dipole. Therefore, the relation between the input impedance of a monopole and a dipole can be realized as,

$$Z_{A,mono} = \frac{V_{A,mono}}{I_{A.mono}} = \frac{\frac{1}{2}V_{A,dipole}}{I_{A,dipole}} = \frac{1}{2}Z_{A,dipole} \quad (3.1)$$

So, the input impedance of a monopole is half that of its dipole counterpart [17], which means $Z_{mono} = 36.5 + j21.25\Omega$.

3.6 Investigation of Simple Wire Antennas using CAD Simulation

Wire antennas are one of the simplest antennas and the most versatile for many applications. The practical analysis of antennas was set out by considering these most basic configurations. A half-wavelength wire dipole was designed in Computer Simulation Technology (CST) Microwave Studio software for 1.9 GHz. The return loss and radiation patterns were analyzed which agreed to the theory of basic antenna design. Although half wavelength dipole is the most common of its kind, the length can be multiple of half wavelength for different applications. If the length of the dipole antenna is changed from a half wavelength then the radiation pattern is altered. Simulations were carried out to analyze the difference of radiation pattern of dipole antennas of different wavelengths. The 3D radiation patterns are shown in Figure 3.5, where it can be seen that changing the length of the antenna creates few side lobes in the pattern along with the main lobes. The main lobes move progressively towards the axis of the antenna as the length increases. l is indicating the length of both arms of the dipole.

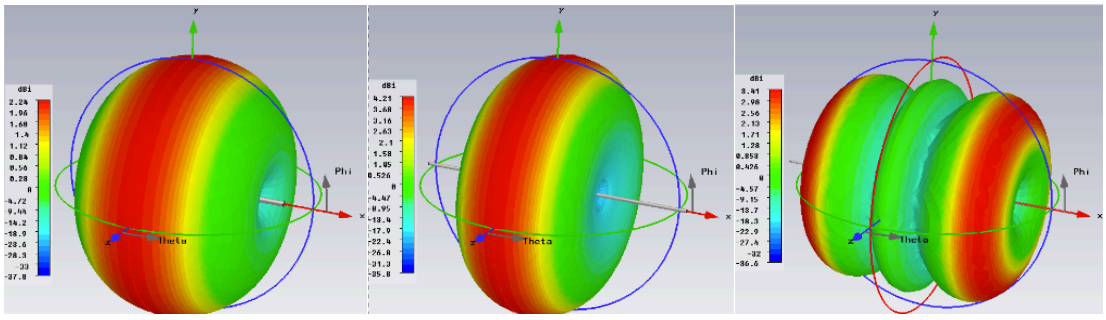

(a) $l = \lambda/2$ (b) $l = \lambda$ (c) $l = 3\lambda/2$

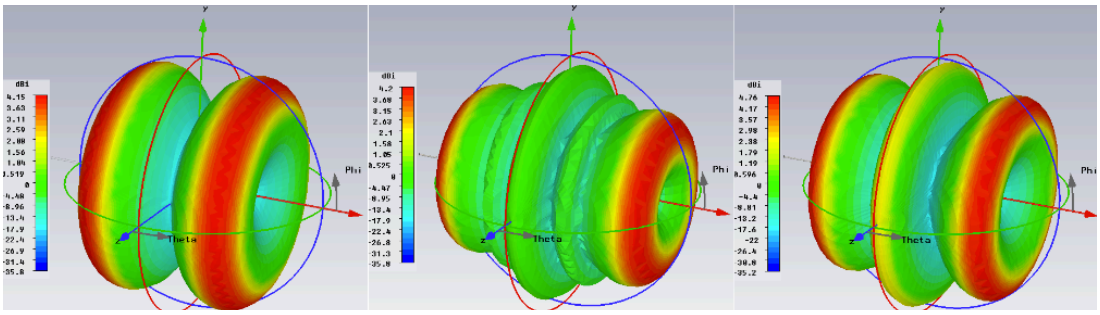

(d) $l = 2\lambda$ (e) $l = 5\lambda/2$ (f) $l = 3\lambda$

Figure 3.5: Radiation pattern of dipole antenna for different wavelengths.

Following that, a quarter wavelength monopole was designed in CST and the performance was analyzed. Theoretically, if a quarter wavelength monopole antenna is placed on an infinite ground plane, the total antenna length can be regarded as half wavelength due to the

image current induced on the ground plane. However, because an infinite ground plane does not exist in reality, the antenna must be installed on a finite sized ground plane. The impedance and radiation pattern are influenced by the size of the antenna [19]. The effect of a large ground plane for monopole antenna has been examined in CST as a basic investigation. The size of the ground plane was varied to see the change of radiation patterns accordingly. The radiation patterns of a quarter wavelength monopole antenna (~38mm) working at the frequency of 1.9 GHz for different size of ground plane are shown in Figure 3.6, where *r* is representing the radius of the circular ground plane or dimension of a square shaped one.

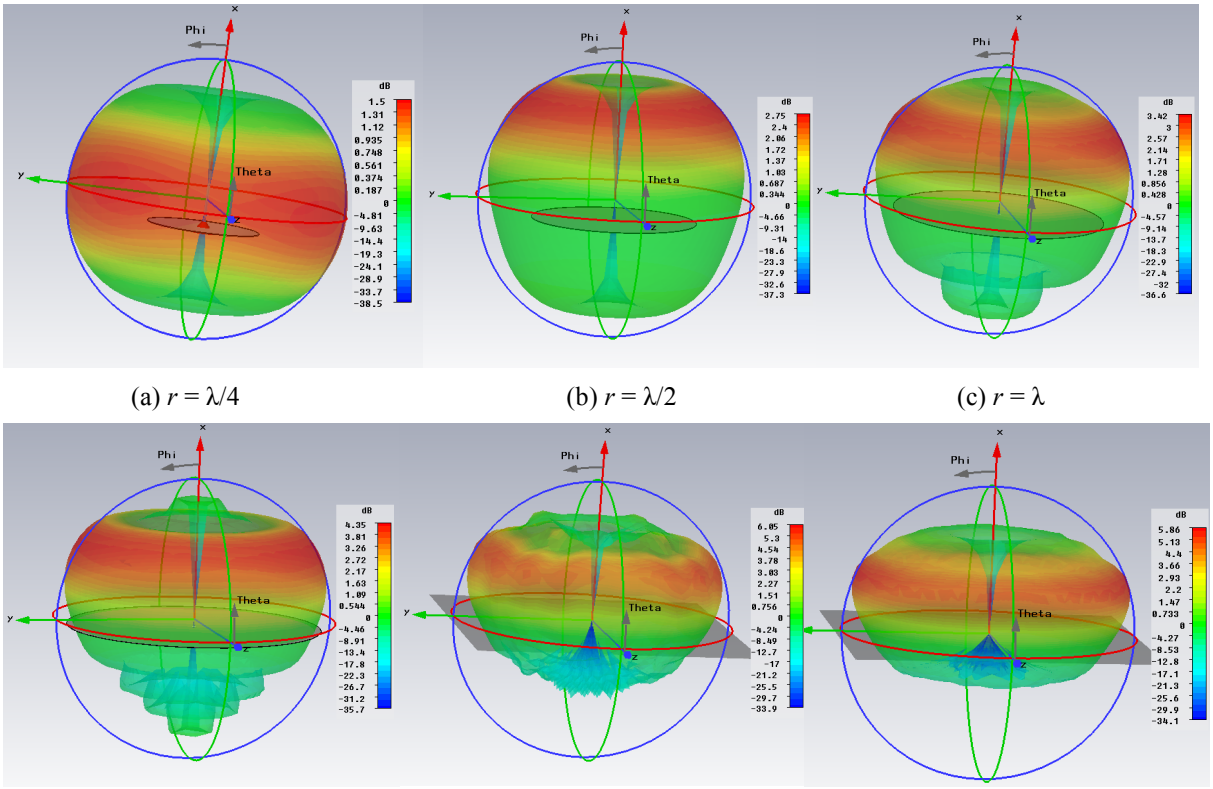

(a) $r = \lambda/4$ (b) $r = \lambda/2$ (c) $r = \lambda$

(d) $r = 2\lambda$ (e) $r = 3\lambda$ (f) $r = 6\lambda$

Figure 3.6: Radiation pattern of monopole for different sizes of ground plane

It can be seen from this figure that for a larger ground plane, the resulting power radiates in a 'skewed' direction, away from the horizontal plane. The radiation pattern for this monopole antenna is still almost omnidirectional for all the cases for azimuth plane. However, the peak radiation direction has changed from the x-y plane to an angle elevated from that plane. As the radiation starts shifting towards one direction, the gain increases as all power starts radiating in one direction. The antenna radiates maximum in the x-y plane when the ground plane approaches infinite size, as in Figure 3.6 (f).

3.7 Characterization of Simple Printed Dipole and Monopole

Printed circuits have drawn the maximum attention of the antenna community in recent years with the development of high frequency semiconductor devices. It has become the primary choice on many applications because of its various attractive features like light weight, low cost, ease of fabrication and so on. In an AIA, antennas are typically implemented on the same PCB as the circuitry. To comply with, balanced and unbalanced antennas on FR4 substrate was designed. It is well known that the wavelength of a radiator in air is set by $\lambda = c/f$ where c is the speed of light and f is the resonant frequency. But adding a substrate has the effect of lowering the impedance and the wavelength since the wavelength is a function of media and air [20]. The wavelength slows down when waves travel through a media rather than air only, so setting the antenna parameters on PCB involves determining the corrections for the new media. The length of the dipole arms on printed board for 900MHz was determined by using CST simulations. A monopole counterpart was also designed with a 1m X 1m metal ground plane. These practical antennas will be used in measurement with the amplifiers later in this study. Figure 3.7 shows both dipole and monopole antennas.

(a) Printed dipole antenna

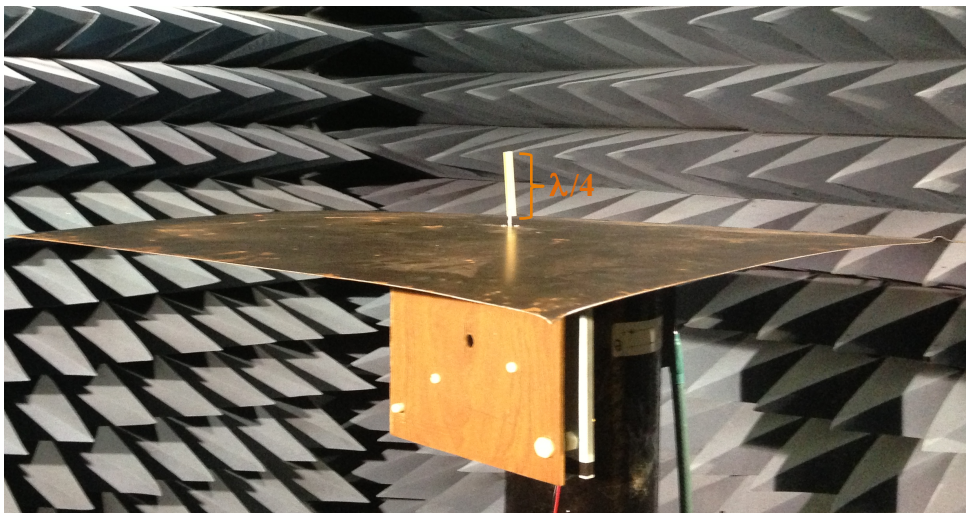

(b) Monopole with ground plane

Figure 3.7: Fabricated balanced antenna (a) and its unbalanced counterpart (b)

Slight extended width of the substrate was left on the dipole design considering the effect of an antenna designed on a same substrate along with active circuitry. The simulated and measured return loss (S_{11}) for both antennas are shown in Figure 3.8 and the radiation patterns in both azimuth (horizontal) and elevation (vertical) planes are shown in Figure 3.9.

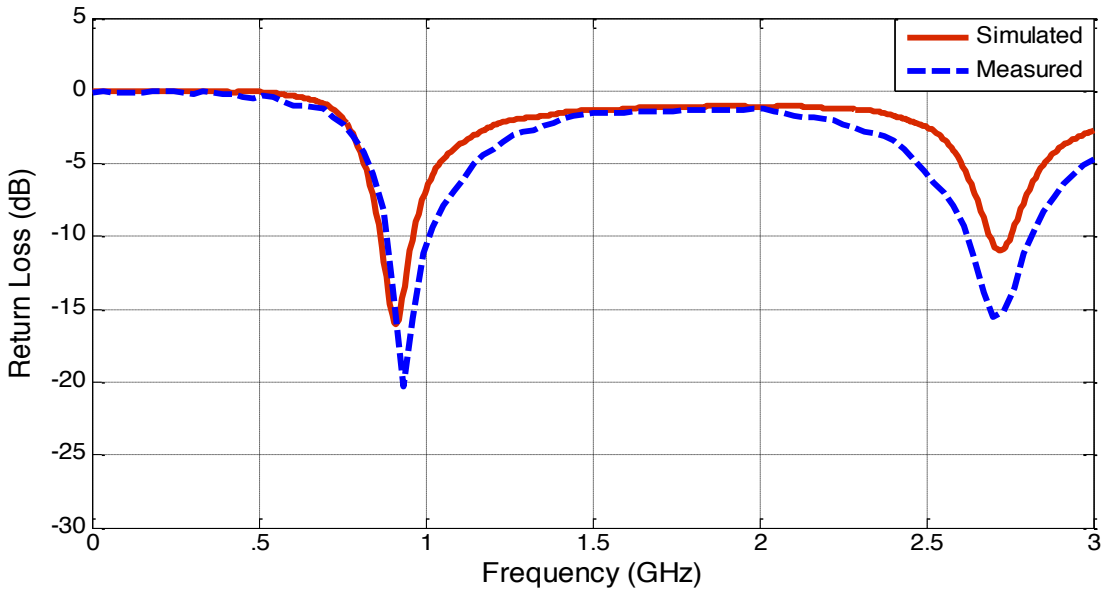

(a) Balanced Antenna

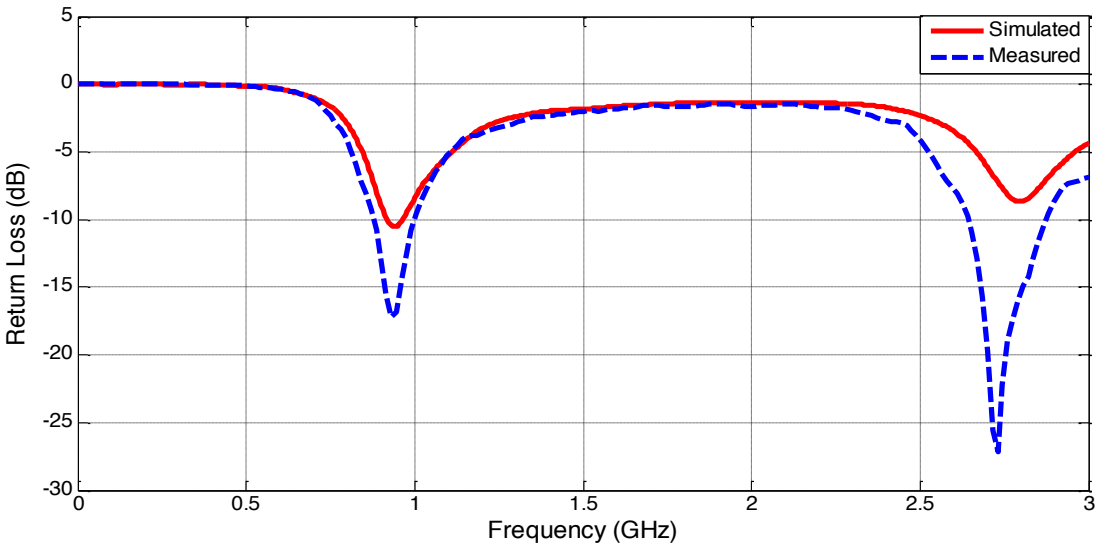

(b) Unbalanced Antenna

Figure 3.8: Simulated and measured return loss for balanced and unbalanced antennas

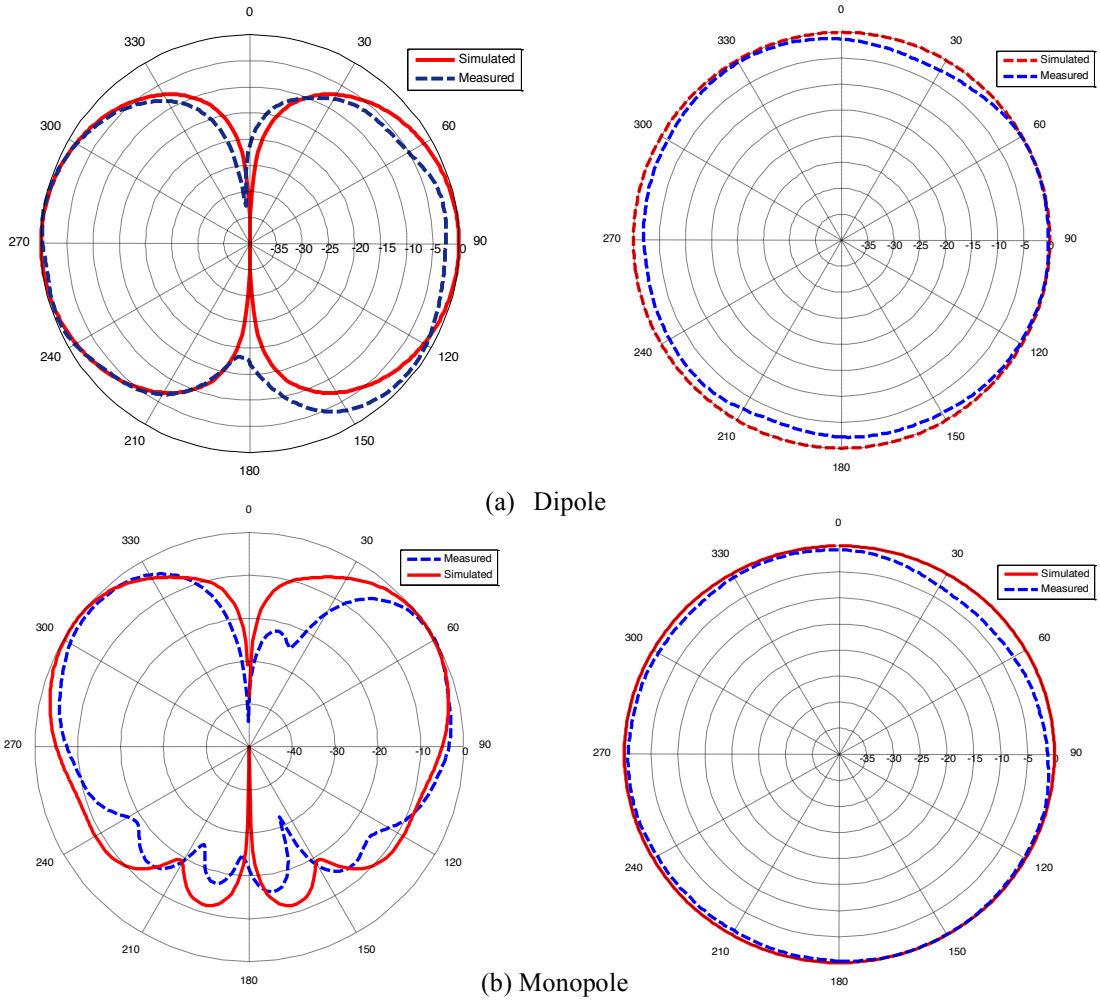

(a) Dipole

(b) Monopole

Figure 3.9: Simulated (solid line) and measured (dashed) radiation pattern for the balanced (a) and unbalanced (b) antenna in azimuth (left) and elevation (right) plane.

It can be observed that both antennas possess a good return loss at 900 MHz. The antennas have a stable omnidirectional radiation pattern in its azimuth plane as expected from simple monopole and dipole antennas. The simulated and measured results are showing good agreement between them. A slight discrepancy in dipole antenna measurements can be realized as the balanced antenna was fed by unbalanced coaxial cable in these measurements. These simple antennas will be used in measurements to compare conventionally and differentially fed active antenna performances.

3.8 Investigation into Reducing Radiation from Ground Plane Currents

After investigating the initial exercise of the ground plane effects on monopole antenna radiation pattern, a challenge was taken to introduce a way of controlling ground plane current on a mobile handheld device. In order to achieve this, the effects of a choke-slot on solid ground plane of a mobile antenna fabricated on FR4 substrate has been investigated. Techniques have been discussed to control the ground plane current and reduce any degradation. The simulations and measurements show that introducing a slot on a conventional solid ground plane can significantly improve the radiation pattern of an antenna. Good performance at the Personal Communication Service (PCS 1900) band promises the use of this antenna on personal mobility, advance cellular phone services and wireless communication services. Achieving the maximum gain towards the expected direction for mobile phone application with the help of a choke-slot on the antenna's ground plane demonstrates the effectiveness of this technique.

3.8.1 Background

The boom in consumer wireless devices has driven designers to seek smaller and more compact antennas. The solutions are generally successful but can suffer a pitfall to the unwary designer. The usual design approach places emphasis on tuning the 'element' for VSWR and makes the assumption that the other half of the antenna is realised by image currents in the ground plane. Once the ground plane becomes finite, this may cause severe distortion to the radiation pattern. Studies on the effects of ground plane on antenna performance had been discussed in open literature back in late 1960s [21-23]. Most of these works focused on the characteristics of a monopole antenna mounted on a finite circular ground plane, as investigated in Figure 3.6. Later, the effects of the ground plane on other antenna types including microstrip antennas were also studied [24-25]. Current applications require antennas to be mounted on small ground planes as found in handheld communication devices. The most popular model for a ground plane assumes to be perfectly conducting, planar, and infinite in extent. But real ground planes are finite in size and can be in the plane of the element rather than orthogonal as in those literatures. The finite extent is responsible for results that deviate from those for a perfect ground plane. Thus, models for antennas on a ground plane of infinite extent are not sufficiently accurate for most of these applications.

Generally, when the ground plane is comparable to a wavelength, electrical performance can be different from that of an infinite ground plane [26]. In this experiment, the effects of finite ground plane current have been studied for handheld applications. Simulated and measurement results show that the antenna radiation pattern possesses significant distortion due to ground plane effects. Techniques to compensate for the finite ground plane effect for maintaining good electrical performance are investigated.

3.8.2 Measuring Ground Plane Effects

An early example of the reduced size antenna element for mobile phones is the pinpatch antenna proposed in [27]. Even though this design offered significant reduction in antenna size at that time, careful examination of the polar diagram shows a significant problem. In principle the pin-patch element operates like a reduced size monopole if placed above an infinite ground plane, with maximum radiation uniformly radiated in the azimuth plane. In the example of [27] the radiation pattern actually exhibits a significant 10 dB null in this plane, with major lobes at oblique angles. For a mobile phone application this is far from ideal as this would be in the principal direction towards a base station. The finite sized ground plane causes the problem. In the example, the ground plane is in fact $3\lambda/4$ at the operating frequency; hence the entire structure is operating like a 1λ dipole, hence the nulls on azimuth. While the antenna is essentially defined by the antenna element, the ground plane structure must be included as this is very much part of the antenna. It is seen that while the antenna element appears to provide the desired bandwidth and impedance, the ground plane currents can dominate the radiation pattern. To compound the problem, the size and shape of the ground plane is often outside the remit of the antenna designer (i.e. overall structure). However, it is proposed here that the antenna designer can apply techniques to control the ground plane current and limit any degradation.

An antenna with finite ground plane similar to [27] was considered for this experiment. Instead of using a metallic case, a planar form of that antenna had been introduced with similar dimensions. The ‘Tee’ antenna was fabricated on FR4 substrate with relative permittivity of 4.3 and a thickness of 1.6 mm. The antenna element line width is 1.5 mm. Because of the trend for smaller handheld devices a second design was considered with a

smaller ground plane. Here, the overall length of the structure has been reduced from 137mm to 88.5mm, which would easily fit in contemporary mobile devices.

To illustrate the effects of ground plane current, the radiation properties for the design assembly was computed using CST MWS. The radiation patterns of fabricated antennas were also explored in azimuth plane inside the anechoic chamber at the frequency of 1.9 GHz. In the simulation an ideal source was used at the feed point but for measurement a physical cable was attached. This is indicated in Figure 3.10(a), although in experiments the cable extends along the x-axis and a balun arrangement was used to reduce currents on the outer braid of the cable.

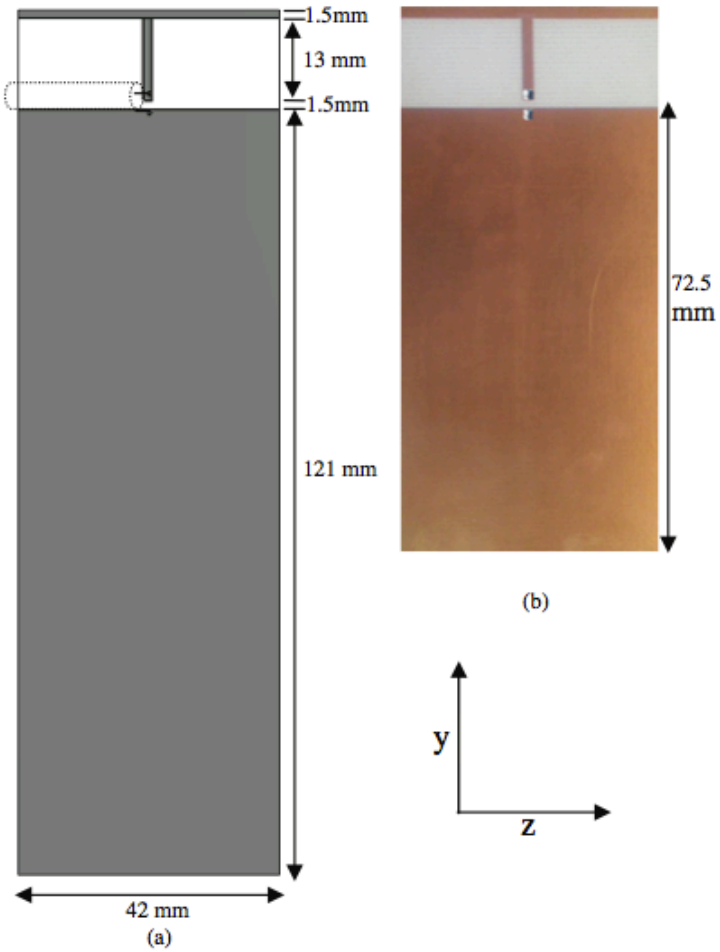

Figure 3.10: (a) Planar antenna with solid ground plane, similar dimensions to [27], (b) Similar antenna printed on PCB with smaller ground plane.

Patterns were taken for E_y polarization in the YZ plane, such that any cable radiation effects are minimized. The results of the antennas with solid ground planes of different lengths are plotted in Figure 3.11.

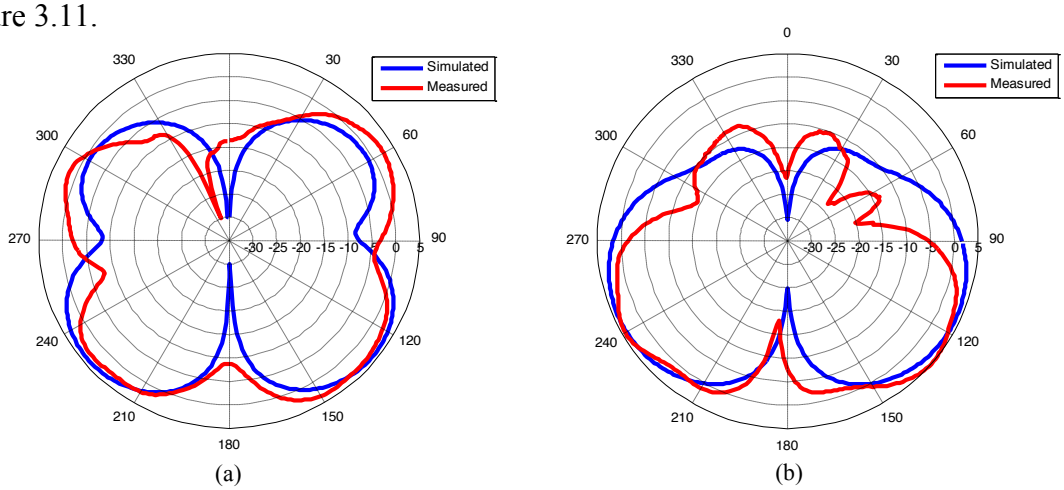

Figure 3.11: Radiation pattern for Ey polarization in the YZ plane (a) antenna of Figure 3.10 (a) and (b) antenna of Figure 3.10 (b) (reduced size)

Results show that the test antenna with bigger solid ground plane suffers from a 10dB null along the z-axis, similar to [27]. But this is the direction we would expect maximum gain if the Tee element were acting as a reduced height monopole. The radiation pattern of a second design with smaller ground plane was examined and it was found that the power distribution was even worse if it is to be used as a communication device antenna. This is due to the radiation pattern being dominated by the ground plane current. The unwanted influence of ground plane currents is not a new problem and solutions that have been applied by antenna designers to other antenna installation problems can be adopted here. A coaxial cable 'choke' balun can be used to feed the antenna in order to reduce the effects of currents flowing on the external surface of the feeding cable. Similarly choke–slot technique can be applied to the ground plane surrounding an antenna such as in [28].

3.8.3 Compensation Techniques

The presence of the ground plane, necessary for RF circuits, suggests the antenna must always be unbalanced; however it is possible to modify the ground structure to limit the regions where antenna currents flow. A few methods have been investigated as discussed in this section.

(i) λ/4 truncated ground plane:

One possible solution is introducing a transverse slot cut at a distance of λ/4 on the ground plane. The dimensions of the upper part Tee antenna and the overall size of the antenna are same as the smaller solid ground plane antenna. The width of the slot is 1.5mm, which is a simple line across the X axis. The feeding cable is along the X-axis such that any currents on this cable have minimal effect on the YZ pattern. The overall design has been shown in Figure 3.12 (a). This approach gives an approximating 'doughnut' shaped radiation pattern, shown in Figure 3.12 (c) but the maximum radiation is not exactly on the direction it should be for a good mobile communication antenna. The return loss graph (Figure 3.12 (b)) is showing a better matching at around 1.1 GHz, which is not near our desired frequency of 1.9 GHz.

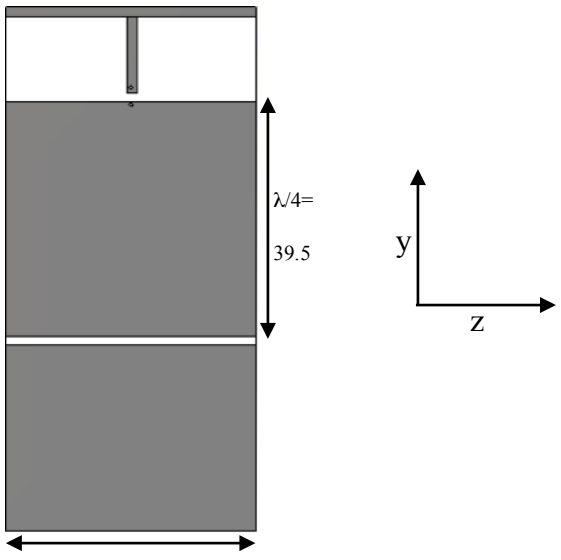

(a) Antenna with truncated ground plane

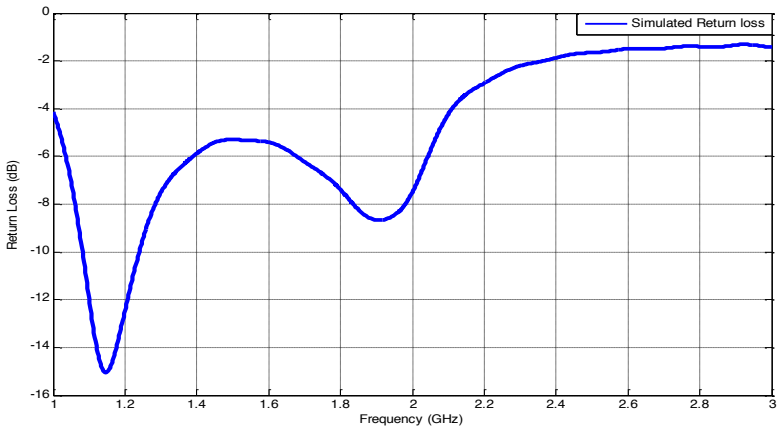

(b)

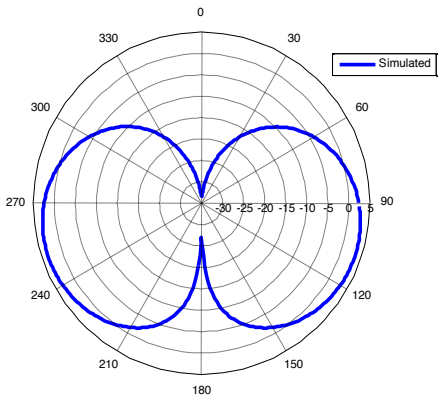

(c)

Figure 3.12: (a) Structure of antenna with truncated ground plane, (b) Return loss and (c) radiation pattern of the antenna with truncated ground plane

(ii) Fragmented ground plane

Another solution is shown in figure 3.13. The ground plane is split into three parts. Part A forms one half of the antenna, while 'B' and'C' create a λ/4 slot-line that 'chokes' off the ground plane current, limiting this to the top area. Section A can be the unbalanced ground plane for the RF circuitry, which compensates for the ground plane effect on the radiation as illustrated in figure 3.14(b). Although it compensates the ground plane effects, the impedance matching remains a concern as it is not matched to our desired frequency band. Figure 3.14(a) shows the return loss of this modified design.

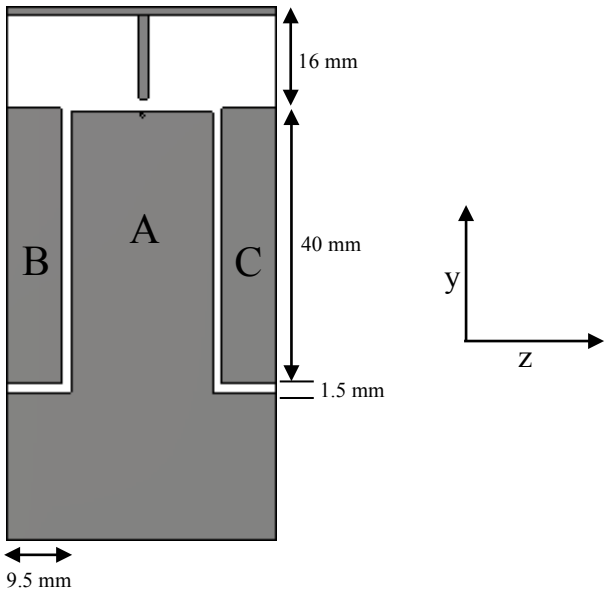

Figure 3.13: Modified ground plane to compensate radiation effects.

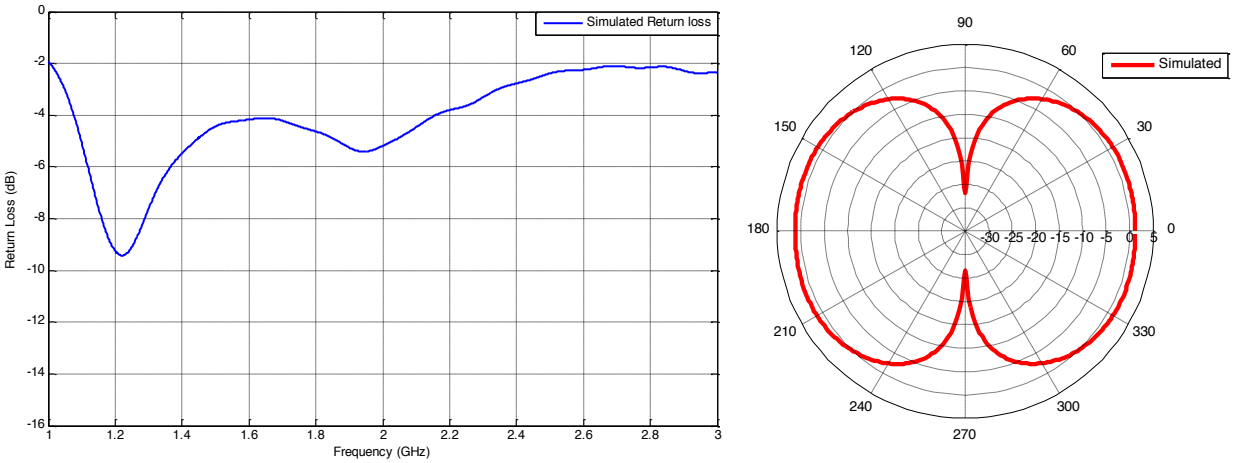

Figure 3.14: (a) Return loss and (b) radiation pattern of the modified ground plane antenna

(iii) λ/4 Choke-Slot Configuration

Another alternative solution using a 'choke-slot' was considered on the same design. Here a slot is cut in the ground plane to create a longitudinal slot line that can be used to create a λ/4 transformer. The width of the slot cut is kept 1.5mm. The antenna 'ground' currents then flow on the outer section of this slot line but the inner section, connected to the lower portion of ground plane is then isolated. The design configuration is illustrated in Figure 3.15(a) below:

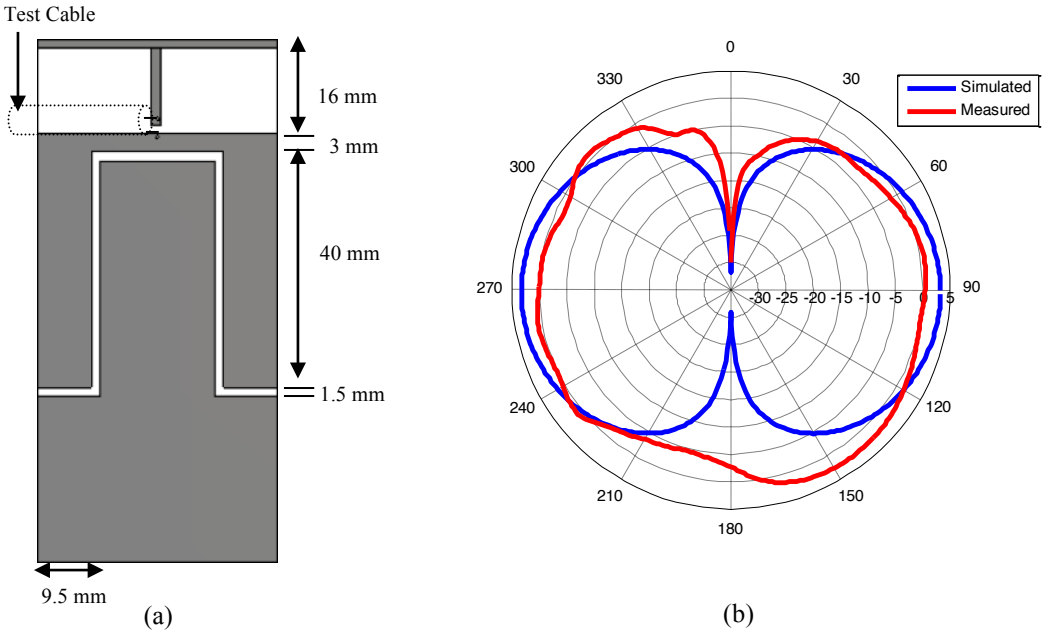

Figure 3.15: (a) Structure of the ground plane compensated antenna with λ/4 choke-slot
(b) Simulated and measured radiation pattern of the antenna

To demonstrate the effect of a λ /4 choke slot the radiation pattern of the antennas with slot cut was simulated using CST MSW. The power distribution of the fabricated approach has been measured with the same experimental setup as solid ground plane antennas. Again E_y polarization in the YZ plane has been considered. The results are presented in Figure 3.15 (b). From the figure it is clear that after introducing the choke-slot the null and degradation is completely eliminated and the radiation characteristic has appeared as an ideal doughnut shaped pattern. One of the reasons of this might be the fact that on the antenna without any slot, the electric currents are mainly concentrated around the feeding strip. Thus, the ground plane significantly affects the impedance and radiation performance of the antenna. As a result, the performance of the slotted ground plane antenna has the advantage of the suppressed ground plane effects over the conventional designs without choke-slot.

Computed and experimental results show good agreement between them. The slight discrepancies are due to the interaction of the essentially 'balanced' antenna being fed by an unbalanced co-axial connection cable. Thus, the experiments results evaluate that there is a significant effect on the antenna's radiation performance due to the change in ground plane structure.

3.8.4 Current Distribution on Antenna Surface for Different Configuration

The current distribution for different configurations is shown in Figure 3.16. It can be seen that more currents are flown on the balanced structure, where the part isolated from the ground plane is working as one part of a dipole antenna. Currents on the isolated ground plane are very low, which will not affect the antenna radiation pattern.

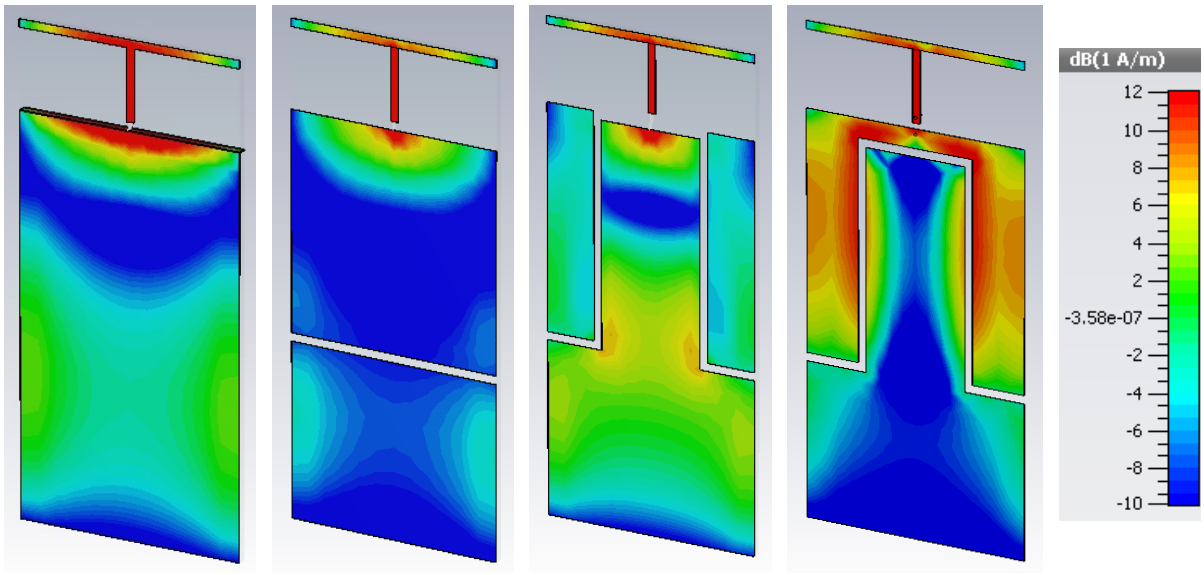

(a) (b) (c) (d)

Figure 3.16: Current distribution at 1.9 GHz on the surface of antenna with (a) solid ground plane, (b) λ/4 truncated ground plane, (c) Fragmented ground plane and (d) λ/4 choke-slot configuration

3.8.5 Return Loss Comparison

The return loss of the solid ground plane antenna (Figure 3.10(b)) and the choke-slot ground plane antenna (Figure 3.15(a)) were simulated in CST Microwave Studio Suite. The impedance performance of the slotted ground plane antenna shows its efficiency at PCS band as we can see a resonance at 1.9GHz from Figure 3.16. While the 'Tee' antenna with solid ground plane is tuned to 1.7GHz. Though there is no significant impact of ground plane size and pattern on the resonance frequency, still we can observe noticeable change in the impedance performance after the slot has been put on the antenna. The return loss of the fabricated antenna was also measured by using an Agilent Vector Network Analyser. The simulated and measured return loss of both the antennas is demonstrated in Figure 3.17. Reasonable agreement is observed between simulated and measured results. There are a number of ripples in the measured return loss plots due to the inefficiencies of the Balun used on the connecting cable at higher frequencies. The antenna structures are essentially 'balanced' antennas whilst the connecting coaxial cable and related measurement system is unbalanced. The return loss is in effect the sum of reflection from the antenna and from the Balun. Closer agreement would be obtained using an improved Balun.

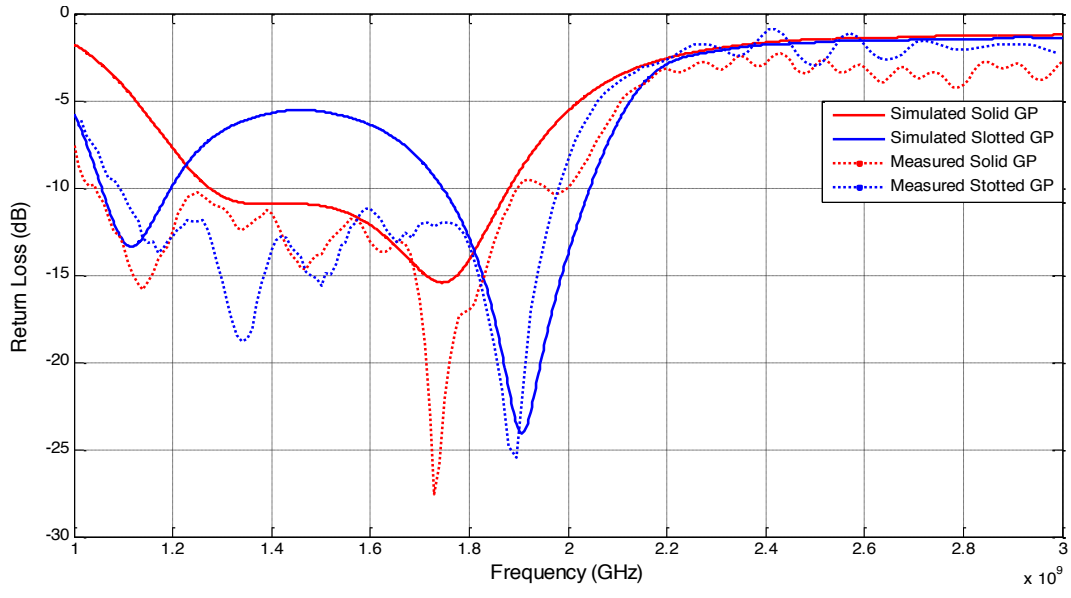

Figure 3.17: Return loss of antenna presented on Figure 3.10 (a) and Figure 3.15 (b)

3.9 Summary

In this chapter, the balanced and unbalanced antenna arrangements have been discussed. Simple printed dipole and monopole antennas have been constructed and analysed, to be used later on for experimental works. The ground plane effect on a planar, reduced height monopole antenna has been studied using simulations from CST MWS and measurements of the prototypes. It has been seen that the finite ground plane can cause significant distortion in the radiation pattern, creating unwanted nulls. It was then demonstrated that these effects can be compensated by introducing 'choke-slots' to limit the flow of current on the ground plane, resulting in more desirable dipole like radiation patterns. Introducing the choke-slot also affected the impedance, causing a small shift in the resonant frequency. This provides more evidence that design of antennas for small portable devices needs to encompass the whole structure – and cannot simply introduce a 'radiating' element – whilst also providing a solution.

References

[1] W. Alan Davis (2001), *Radio Frequency Circuit Design*, USA: John Wiley & Sons Inc., Chapter 4.

[2] Roy. W. Lewallen; " Baluns: What They Do And How They Do It", The ARRL Antenna Compendium, Volume 1, American Radio Relay League, Newington, 1985.

[3] K. Fujimoto, J. R. James (2001), *Mobile Antenna Systems Handbook*, 2nd ed.: Artech House Publishers. Chapter 5.

[4] Azlan, A A; Ali, M.T.; Salleh, M. K M, "A design of off centered feed array (OCFA) antenna for ISM band," *Wireless Technology and Applications (ISWTA), 2012 IEEE Symposium on* , vol., no., pp.233,238, 23-26 Sept. 2012.

[5] Kin-Lu Wong (2003), *Planar Antennas for Wireless Communications*, Hoboken, NJ: John Wiley & Sons, Inc., Chapter 1.

[6] K. R. Boyle and L. P. Ligthart, "Radiating and Balanced Mode Analysis of PIFA Antennas," IEEE Transactions on Antennas and Propagation, , vol. 54 pp. 231- 237, 2006.

[7] Do-Gu Kang; Sung, Y., "Compact Hexaband PIFA Antenna for Mobile Handset Applications," *Antennas and Wireless Propagation Letters, IEEE* , vol.9, no., pp.1127,1130, 2010.

[8] Sanchez-Montero, R.; Rigelsford, J.M.; Lopez-Espi, P.L.; Alpuente-Hermosilla, J., "An active multiband antenna for future wireless communications," *Antennas and Propagation (EuCAP), 2014 8th European Conference on* , vol., no., pp.2989,2991, 6-11 April 2014

[9] W.-I. Kwak, S.-O. Park, and J.-S. Kim, "A Folded Planar Inverted-F Antenna for GSM/DCS/Bluetooth Triple-Band Application," IEEE Antennas and Wireless Propagation Letters,, vol. 5, pp. 18-21, 2006.

[10] B.-N. Kim, S.-O. Park, Y.-S. Yoon, J.-K. Oh, K.-J. Lee, and G.-Y. Koo, "Hexaband Planar Inverted-F Antenna With Novel Feed Structure for Wireless Terminals," IEEE Antennas and Wireless Propagation Letters, vol. 6, pp. 66-69, 2007.

[11] G.A. Ellis and S. Liw, "Active Planar Inverted-F Antennas for WirelessApplications," IEEE Transactions on Antennas and Propagation vol. 51, pp. 2899-2906, 2003.].

[12] Morishita, H.; Furuuchi, H.; Fujimoto, K., "Performance of balance-fed antenna system for handsets in the vicinity of a human head or hand," *Microwaves, Antennas and Propagation, IEE Proceedings* , vol.149, no.2, pp.85,91, Apr 2002

[13] Abd-Alhameed, R.A., Excell, P.S., Khalil, K., Alias, R., Mustafa, J.: SAR and radiation performance of balanced and unbalanced mobile antennas using a hybrid formulation', IEE Proc., Sci. Meas. Technol. Spec. Issue Comput. Electromagn., 2004, 151, (6), pp. 440–444.

[14] Zhi Ning Chen (2007), *Antennas for Portable Devices*, John Wiley & Sons Inc., Chapter 2.

[15] Meys, R. Janssens, F.,"Measuring the impedance of balanced antennas by an S-parameter method," *Antennas and Propagation Magazine, IEEE* , vol.40, no.6, pp.62-65, Dec 1998.

[16] Godara, L. C., 2001. *Handbook of Antennas in Wireless Communications*. Florida: CRC Press, Chapter 5.

[17] Stutzman, Warren L., Thiele, Gary A., 2012. *Antenna Theory and Design*. 3rd ed. USA: John Wiley & Sons, Inc, Chapter 3.

[18] Poisel, R., 2012. *Antenna Systems and Electronic Warfare Applications*. 1st ed. Boston: Artech House.

[19] Arai, Hiroyuki, 2013, *Measurement of Mobile Antenna Systems*, 2nd ed. USA: Artech House, Chapter 3.

[20] Tammy E. Couture (1996), Printed circuit dipole antenna, Motorola, Inc.,US Patent 5495260.

[21] Meier, A.S., and Summers, W.P.: 'Measured impedance of vertical antennas and effects of finite ground planes', Proc. IEEE, 1969, 37, pp. 609–616.

[22] Thiele, G.A., and Newhouse, T.H.: 'A hybrid technique for combining moment methods with the geometrical theory of diffraction', IEEE Transaction on Antennas and Propagation, 1975, 23, (6), pp. 62–69.

[23] Awadalla, K.H., and Maclean, T.S.M.: 'Input impedance of a monopole antenna at the center of a finite ground plane', IEEE Trans. Antennas Propag., 1978, 26, pp. 244–248.

[24] Huang, J.: 'The finite ground plane effect on the microstrip antenna radiation patterns', IEEE Transaction on Antennas and Propagation, 1983, 31, (4) pp. 649–655.

[25] Bhattacharyya, A.K.: 'Effects of ground plane and dielectric truncations on the efficiency of a printed structure', IEEE Transactionon Antennas and Propag.1991, 39, (3), pp. 303–308.

[26] M.-C. Huynh and W. Stutzman; Ground plane effects on planar inverted-F antenna (PIFA) performance; IEE Proc.-Microw. Antennas Propag., Vol. 150, No. 4, August,2003.

[27] Ch. Delaveaud, Ph. Leveque & B. Jecko; 'Small-sized low-profile antenna to replace monople antennas', Elec. Lett., 16th April 1998, Vol. 34, No. 8, pp716-7.

[28] K.D. Swineford; 'Choke-slot ground plane and antenna system', U.S. Patent no 5,132,698, 21 Jul 1992.

Chapter 4

Novel Method to Measure Wireless Devices Using Injection Locking Technique

4.1 Introduction

A major number of applications of radio, and hence antennas, are for portable devices. However, modern antenna test methods require a cable to be attached to the antenna. Often this cable can distort the antenna characteristics. In Chapter 3, it has been shown that the ground plane current and the cable effect can be a significant parameter contributing to the radiation pattern. So to avoid these unwanted effects, the antenna should be measured in a 'wireless' condition. This chapter presents measurement method with practical results enabling antenna measurements to be made in a modern anechoic chamber, overcoming the need to connect a cable to the device under test. Injection locking technique has been used to synchronize the local oscillator on a wireless device.

4.2 Background

The usual approach to measure the radiation pattern of an antenna is to use an anechoic chamber. Early systems used a microwave source connected to the antenna with a detector to measure the radiated field via a suitable receive antenna. To provide a generalized measurement system the detector used was usually a broadband device. This resulted in a high noise floor so early measurement systems were often limited to 20-30 dB of dynamic range. Modern systems use a Vector Network Analyzer (VNA) such that the received signal is synchronized to the transmitted signal [1], allowing narrowband reception and achieving significantly higher dynamic range. Using a VNA has the limitation that the antenna is connected by cable to the VNA. Whilst this is not a problem for large antennas, attaching a cable to a small device containing an integrated antenna can lead to erroneous results. The

cable can change the flow of current on the 'ground plane'. Indeed it has been already reported [2] that the ground plane current can be an important factor while measuring radiation pattern and for correct characterization the complete device should be measured with no cables attached. One solution is by using optical fibre connection to the antenna as reported in [3]. Another solution is to use a local oscillator (LO) on the device under test (DUT) to provide the radiating signal, such that no cables need to be attached. However, this LO must be synchronized to the VNA signal for measurements. Oscillators are well known for their coupling, locking and synchronizing capability and have been extensively used in the literature [4-6]. It has been proposed to use injection-locking technique to accomplish this wireless measurement and initial results have been presented demonstrating the feasibility of this method.

4.3 Measurement Method using Injection Locking

When two oscillators with different but close frequencies are weakly coupled, they synchronize each other such that in the steady state they both oscillate at the same frequency. This incident is known as injection locking [7-9]. Since injection locking can synchronize the frequency of an oscillator to that of its locking signal of small amplitude, it has been widely used as a power efficient means for clock recovery and phase locking In RF circuits [10].

An outline of our proposed measurement technique using this phenomenon is presented in Figure 4.1. Usually a signal from port 1 of the VNA is attached directly to the test antenna and the radiated signal is received by a second receive (RX) antenna and fed back to port 2 of the VNA. The VNA calculates the required scattering parameter that can be passed to a pattern controller, providing both amplitude and phase of the radiated pattern. It is proposed that the antenna being tested is integrated into the wireless device under test (DUT) such that the signal radiated is from an internal LO. To synchronize this LO to the VNA, a locking signal from port 2 is fed to a second 'transmit' (TX) antenna inside the chamber that couples the locking signal to the LO via radiation. In principle, this method should be straightforward, but there are some potential problems that are investigated here. As the locking signal is radiated, it can also be received by the RX antenna – forming an interfering signal that will distort the measurement. Secondly for pattern measurement the DUT is rotated in the

chamber, presenting a practical problem of ensuring there is sufficient coupling between the DUT and the TX antenna to confirm the LO remains locked.

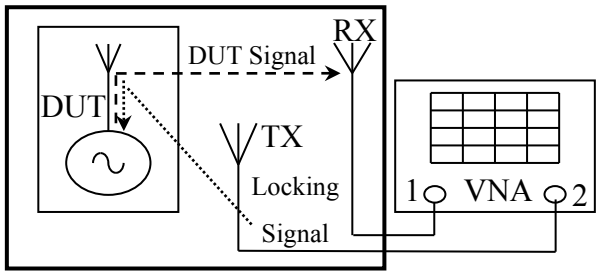

Figure 4.1: Proposed injection locking measurement system

To evaluate the proposed method, measurement of a simple 2.4 GHz dipole antenna of 62mm length was undertaken. For injection locking, a commercially available 2.4 GHz oscillator (Z-communications SMV2490L) was used for the LO. A short cable fed the antenna from the locking oscillator as shown in Figure 4.2. This feed cable included a simple twin-wire λ/4 balun. With this arrangement the co-polar radiation pattern of the antenna (Ey) around the x-axis could be measured either with the LO or independently attaching a cable directly to antenna, with no expected significant distortion of the radiation pattern.

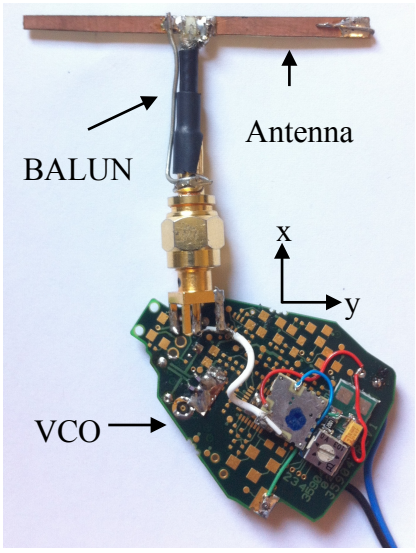

Figure 4.2: 2.4 GHz voltage controlled oscillator and dipole antenna

The setup of the experiment inside the anechoic chamber is shown in Figure 4.3. To provide a locking signal from the VNA, a directive horn antenna was placed facing towards the DUT. The horn antenna was mounted on the rotating platform of the anechoic chamber so that it rotates with the DUT during pattern measurement. The horn radiates a linearly polarized

signal and the arrangement in Figure 4.3 ensures a maximum coupling. A horn was chosen as it has a directive pattern such that direct radiation to the received antenna is minimized.

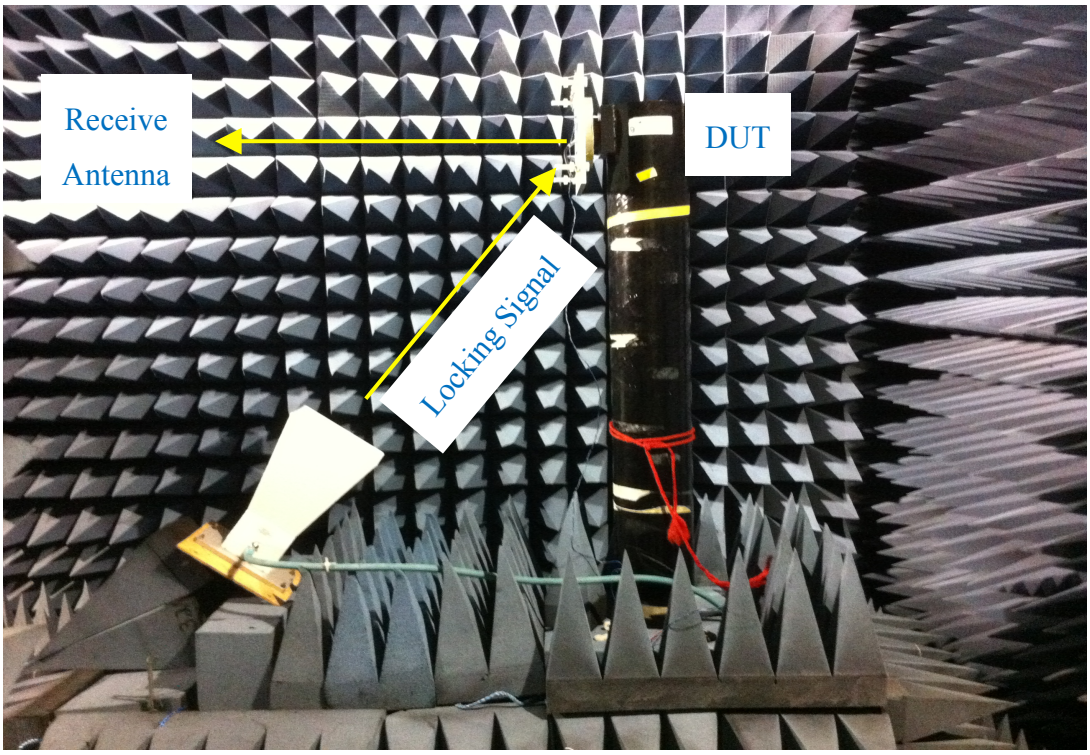

Figure 4.3: Experiment setup inside the anechoic chamber

4.4 Locking Bandwidth and Measurement Results

The locking bandwidth or lock range of an injection-locked oscillator is the difference between the frequency of the local signal at which the oscillator is locked and the natural frequency of the oscillator under injection. Clearly, the larger the locking bandwidth, the more reliable the operation of injection locked oscillators. The lock range of an injection-locked oscillator is therefore a measure of the ability of the oscillator to adjust its oscillation frequency to that of an external locking signal [11]. The injected reference frequency has to be in the locking range of the oscillator to be injection locked, as illustrated in Figure 4.4. Otherwise, the frequency of the local oscillator will only be disturbed by the injection and no injection locking will take place [10]. It can be observed that when injection locked within the locking range, the signal has stable amplitude with respect to time. In the figure, ω_{inj} is the frequency of the local oscillator and ω_n is representing the frequency of the injected signal. If the frequency moves behind or beyond this locking bandwidth, the oscillator loses lock with the injected signal [12].

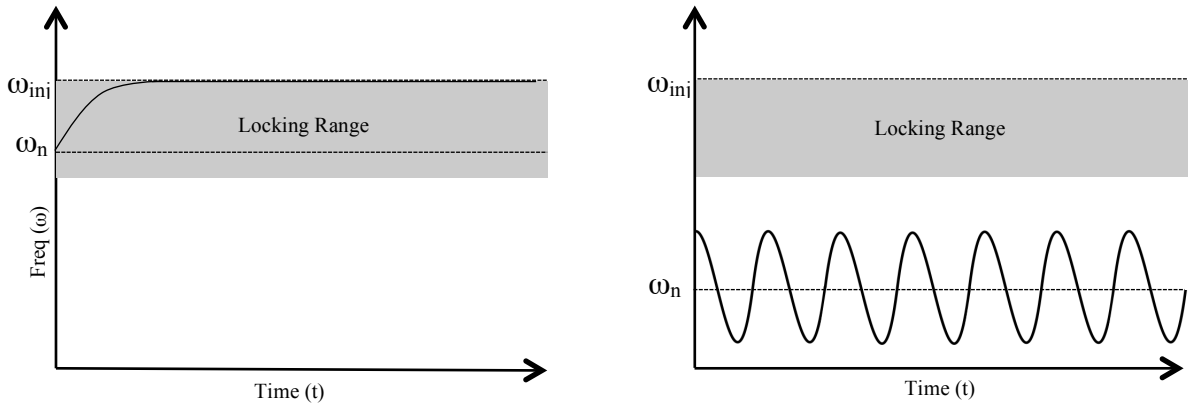

Figure 4.4: Variation of frequency when the injection locked oscillator is within the locking range (left) is outside the locking range (right) of the injected signal [10].

So, it is important that the signal remains locked throughout the whole radiation pattern measurement. To confirm the LO was injection locked to the VNA signal, the received signal was also connected, via a splitter, to a Spectrum Analyzer and was under observation throughout the process. If it loses lock for any period of the measurement the signal will be attenuated by the VNA filtering, distorting the radiation measurement. Typical spectra are shown in Figure 4.5, illustrating locked and unlocked signals. The spectra are centred on 2.407GHz with 10dB/div and 20 kHz/div scale (a narrow frequency span). There are three traces shown on each plot. This is for the same condition, but with the spectra recorded 10 seconds apart. This clearly shows the free-running LO drifts (and this in a 'stationary' position) such that the VNA bandwidth would need to be greater than 100 kHz in order to track the signal. When injection locked the spectrum in Figure 4.5(b) exhibits a stable sharply defined peak (tracking the phase noise of the VNA) such that the VNA could use IF bandwidths below 1 kHz, gaining full benefit from the VNA system.

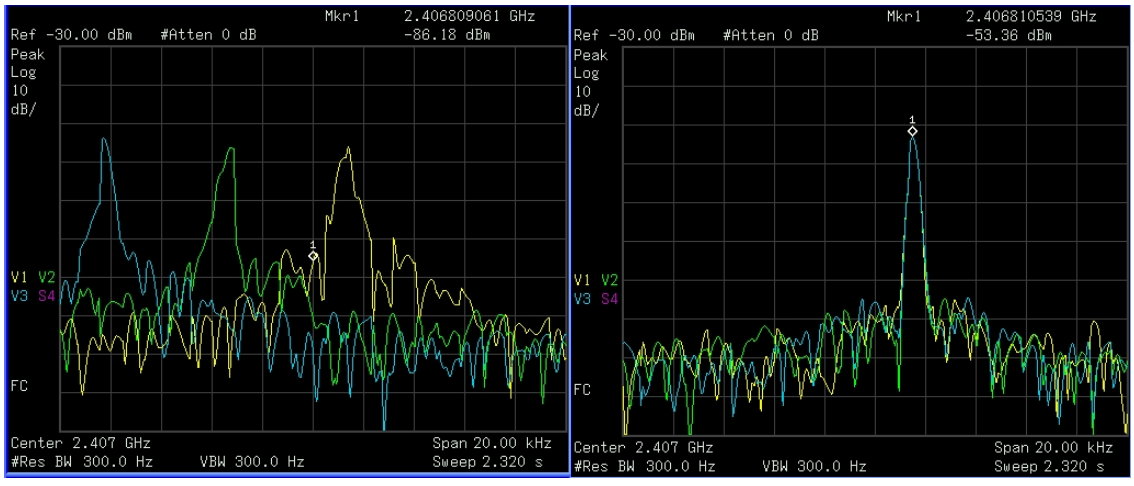

(a) Unlocked (b) Locked

Figure 4.5: Spectrum of received signal confirming injection locking

The locking bandwidth mostly depends on the power of the injected signal. In 1966, Hakki et al. [13], Shaw and Stover [14] and Midford et al. [15] showed experimentally that the locking range of oscillator is proportional to the square root of the injection power. In other words, the frequency locking range is expected to fall off approximately one decade per 20 dB in the power ratio. The square-root relation is held by a wide variety of circuits as long as the injection power is kept sufficiently low [7]. Figure 4.6 below shows the relation between the VNA power level and locking bandwidth achieved in this set-up. It can be observed that the results are maintaining the trend of approximately one decade change in locking frequency range per 20dB change in input power. In this experiment, a minimum of -20 dBm is required to achieve injection locking, although due to the narrow locking bandwidth the LO could easily lose lock (i.e. with frequency drifts caused by vibration and temperature). In practice for this set-up a minimum signal of -10 dBm was determined. A higher level could be used, but this could potentially introduce an interfering signal in the chamber. The LO power level was +13 dBm, hence VNA levels of +10 dBm are comparable to the LO level.

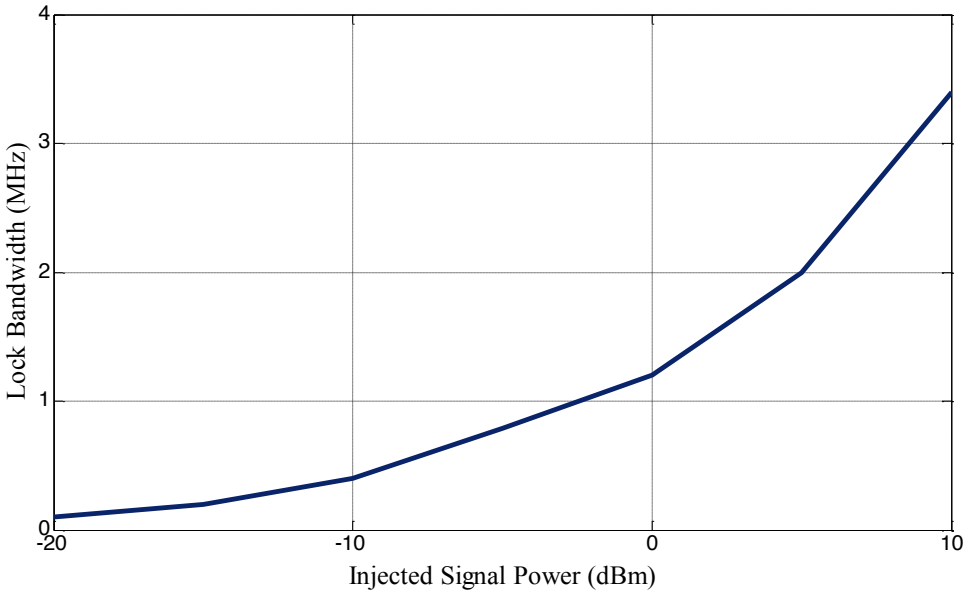

Figure 4.6: Injected power vs locking bandwidth

4.5 Radiation Pattern Measurement

The radiation pattern of a 2.4 GHz dipole antenna was measured conventionally by attaching a cable and then by using the proposed injection locking technique. The measurement was carried out for different power levels of injected signal, ranging from the minimum of -10dbm

to +10dbm. The measured patterns are presented in Figure 4.7. It can be observed from this normalized polar plot that there are discrepancies between the measurement data when the injection locking signal is at +10dbm. At this level the leakage signal from the horn antenna to the receive antenna is about -10dB below the radiated signal from the DUT, causing interference. This is particularly apparent at 330^{o} in Figure 4.7(a) – as the test platform rotates the horn antenna is facing towards the receive antenna (in Figure 4.3 it is shown at 180^{o}, pointing directly away from the receive antenna). This clearly demonstrates a potential problem with the proposed method. However, reducing the locking signal power to -10dbm reduces the interference. The -10 dBm measurement is seen to be close to the 'conventional' measurement in Figure 4.7(b). Indeed the injection locked measurement is closer to the ideal 'doughnut' shape suggesting that the attaching cable for the conventional approach is causing some minor issues.

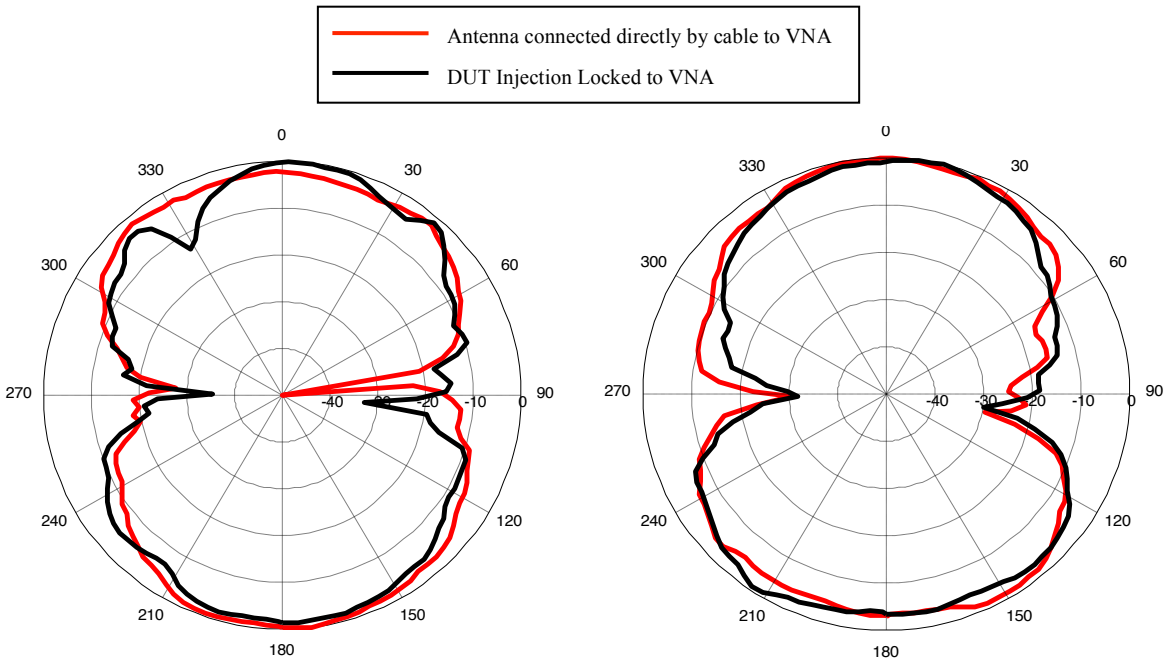

(a) Injecting signal Power 10dbm

(b) Injecting signal Power -10dBm

Figure 4.7: Measured radiation patterns using injection-locking technique

As said earlier that if the signal loses lock during the measurement, it will cause distortion in the radiation pattern. To examine, the injected frequency was set at the edge of the locking bandwidth so that it loses its lock few times during the radiation pattern measurement. Figure 4.8 shows the radiation pattern where there are clear evidence of distortion especially at around 150-180 degree and 260-300 degree of the polar graph.

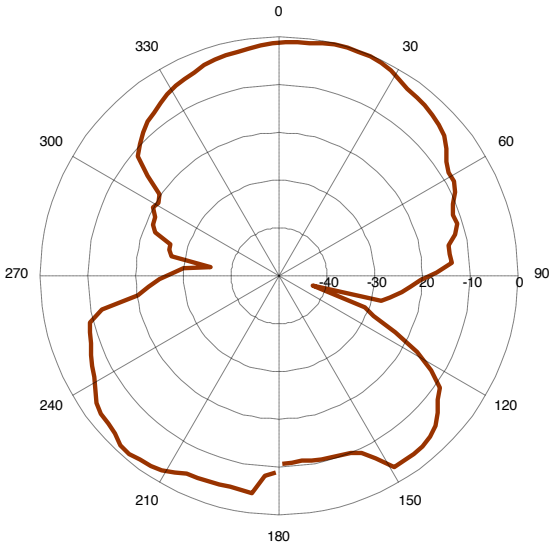

Figure 4.8: Distorted radiation pattern due to the oscillator losing its lock

4.6 Summary

A new method of measuring antenna radiation patterns of wireless devices has been proposed. A small dipole antenna, along with a voltage-controlled oscillator has been used as an example to demonstrate the usefulness of this method. The measured result has validated that this technique gives similar or even better radiation pattern avoiding a cable attached to the DUT. Hence, the difficulty to measure a battery operated wireless device by conventional method in anechoic chamber can be performed by using this alternative method for antenna radiation pattern measurement.

References

[1] Agilent Technologies' Inc : 'Network Analyzer Basics', 2004, [Accessed 1st October 2014]: http://cp.literature.agilent.com/litweb/pdf/5965-7917E.pdf

[2] Callaghan, P.; Sagor, M.H.; Batchelor, J.C., "Control of ground plane influence on antenna radiation pattern for mobile handheld devices," Antennas and Propagation Conference (LAPC), 2011 Loughborough , vol., no., pp.1,4, 14-15 Nov. 2011.

[3] Alexander, M.; Tian Hong Loh; López Betancort, A., "Measurement of electrically small antennas via optical fibre," Antennas & Propagation Conference, 2009. LAPC 2009. Loughborough , vol., no., pp.653,656, 16-17 Nov. 2009.

[4] D. G. Tucker, "Forced oscillations in oscillator circuits, and the synchronization of oscillators," Journal of the Institution of Electrical Engineers - Part I: General, Volume 93, issue 61, 1946 , p. 57 – 58.

[5] Poole, C. R., "Subharmonic injection locking phenomena in synchronous oscillators," *Electronics Letters* , vol.26, no.21, pp.1748,1750, 11 Oct. 1990.

[6] Wen Sun; Jinhu Lü; Shihua Chen; Xinghuo Yu, "Synchronisation of directed coupled harmonic oscillators with sampled-data," *Control Theory & Applications, IET* , vol.8, no.11, pp.937,947, July 17 2014.

[7] R. Adler, "A study of locking phenomena in oscillators," Proc. IEEE, vol. 61, pp. 1380–1385, Oct. 1973.

[8] K. Kurokawa, "Injection locking of microwave solid-state oscillators," Proc. IEEE, vol. 61, pp. 1336–1410, Oct. 1973.

[9] Razavi, B., "A study of injection locking and pulling in oscillators," *Solid-State Circuits, IEEE Journal of* , vol.39, no.9,pp.1415,1424,Sept.2004.

[10] Iniewski, K., (2011), *Integrated Microsystems: Electronics, Photonics, and Biotechnology*, New York: CRC Press, Chapter 12.

[11] Yushi Zhou; Fei Yuan, "A comparative study of lock range of injection-locked active-inductor oscillators," Circuits and Systems (MWSCAS), 2010 53rd IEEE International Midwest Symposium on, vol., no., pp.973,976, 1-4 Aug. 2010.

[12] W. Alan Davis (2001), *Radio Frequency Circuit Design*, USA: John Wiley & Sons Inc.,

Chapter 10.

[13] Hakki, B.W.; Beccone, J.P.; Plauski, S.E., "Phase-locked GaAs CW microwave oscillators," Electron Devices, IEEE Transactions on , vol.ED-13, no.1, pp.197,199, Jan. 1966.

[14] Shaw, R.C.; Stover, H.L., "Phase-locked avalanche diode oscillators," Proceedings of the IEEE , vol.54, no.4, pp.710,711, April 1966.

[15] Midford, T.A; Wanuga, S., "Phase locking of a silicon avalanche transit time oscillator," Proceedings of the IEEE , vol.54, no.7, pp.993,994, July 1966.

Chapter 5

Differential Amplifier Design and Characterization

5.1 Introduction

Amplification is an essential and prevalent microwave circuit function in modern RF and microwave systems. This function is performed in a RF system by using amplifiers. Amplifiers are one of the fundamental components in wireless communications, broadcasting service, and in audio equipment of all kinds. They can be primarily categorized as low noise amplifiers, high gain amplifiers and medium to high power amplifiers. Due to the drastic improvements and innovations in solid-state technology, the industry seeks very high efficient RF power amplifiers to fulfill the demand of modern communication system. Therefore, RF power amplifiers must satisfy a broad set of applications requirements including but not limited to power, linearity, gain, efficiency, thermal management, reliability, ruggedness and cost effectiveness. These requirements create opportunities for further refinements in the RF power transistors to extract peak performance from the architecture [1].

A differential power amplifier with symmetrical transmission to a balanced antenna offers promising performance compared to traditional single-ended concept. This idea will be investigated by using the same amplifier in single-ended and differential form and by analysing their performances. The balanced and unbalanced antenna forms have already been studied as reported in the previous chapter. This chapter focuses on designing and characterizing amplifiers starting with a single ended conventional design followed by a differential, RF single stage, RF partial differential and RF fully differential amplifiers. These RF amplifiers were designed and simulated using AWR Microwave Office simulation software and were fabricated on PCB using microstrip technology and surface mount components. Effects of inductors, RF track line and current mirror were also investigated. It is a real challenge to design a RF fully differential amplifier and plenty of complications arise during the design process at higher frequency. These complications have been reported and

finally a differential RF amplifier with both differential and single ended output configurations was investigated and their performances were analyzed. This analysis has demonstrated that the differential one provides better performance in almost every aspect.

5.2 Single Ended vs Differential Amplifier and Its Benefits:

A single ended signal, unbalanced by definition, is measured by the difference between the node of interest and a constant reference node, which is normally known as ground. Single-ended signals are more prone to noise and electromagnetic coupled interference. Any error source or signal variation introduced in a single-ended configuration will be difficult to remove without using overly complex cancellation techniques [2]. In contrast, differential signals are made up of pairs of balanced signals moving at equal but opposite amplitudes around a reference point. The difference between the positive and negative balanced signals corresponds to the composite differential signal as presented in Figure 5.1. The symmetrical configuration of differential amplifier cancels common-mode noise voltages, voltages that tend to appear on each of the signal lines as equal voltages to ground. By maintaining symmetry on the circuit construction it can be assured that the majority of undesired noise pickup will be common-mode noise and will be attenuated by the differential amplifier [3].

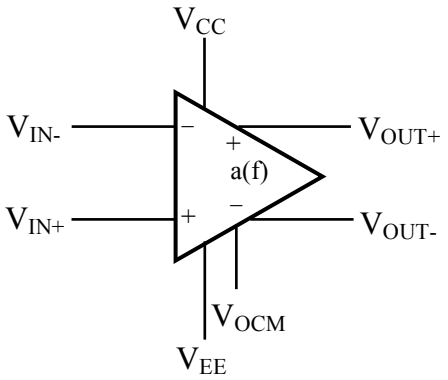

Input Voltage: $(V_{IN+}) - (V_{IN-})$

Output Voltage: $(V_{OUT+}) - (V_{OUT-})$

Input Common Mode Voltage: $\frac{(V_{IN+}) + (V_{IN-})}{2}$

Output Common Mode Voltage: $\frac{(V_{OUT+}) + (V_{OUT-})}{2}$

Figure 5.1: Fully differential amplifier voltage definitions.

In a differentail amplifier two outputs flow in the opposite directions in reference to the ground, thus the difference of them will be two-fold in comparison to that of its single ended output counterpart as shown in Figure 5.2. This increased output swing leads to increased signal-to-noise ratio and also lowers distortion. So it is possible to get doubled output voltage from differential amplifier by using the same component and power source. Alternatively a

lower supply voltage can be used to provide the same signal swing, lowering power dissipation [4]. This makes them ideal for low voltage applications as well.

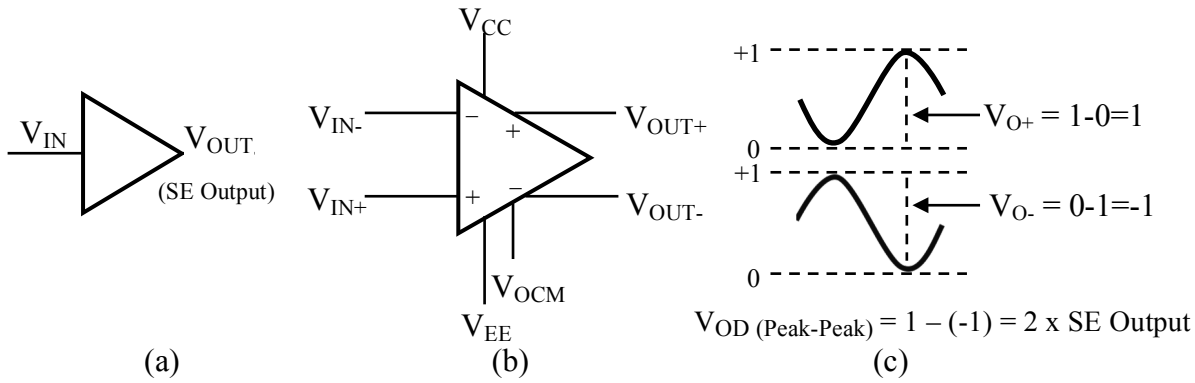

Figure 5.2: (a) Single Ended and (b) Differential topology; (c) Differential Output [5].

A differential topology ideally cancels even-order harmonics and thus improves linearity performance [6]. By taking Taylor Series expansion for both outputs of a nonlinear differential device with respect to its inputs, we get:

$$V_{out+} = a_1 V_{in+} + a_2 V_{in+}^2 + a_3 V_{in+}^3 + \ldots\ldots\ldots \quad (5.1)$$

$$V_{out-} = a_1(-V_{in-}) + a_2(-V_{in-})^2 + a_3(-V_{in-})^3 + \ldots \quad (5.2)$$

In a fully differential amplifier, the odd-order terms retain their polarity, while the even-order terms are always positive. The input-output relationship is an odd function of the input difference voltage V_{id} and thus only odd terms appears in the Taylor series expansion of V_{od} in terms of V_{id} [4]. Taking the differential output ($V_{od} = V_{out+} - V_{out-}$) we get,

$$V_{od} = a_1 V_{id} + a_3 V_{id}^3 + \ldots\ldots\ldots\ldots\ldots \quad (5.3)$$

where a_1, a_2 and a_3 are constants. This harmonic termination at the common source shows a significant improvement on linearity without degrading output power and PAE and the excellent linearity is maintained across a broad frequency range.

Differential amplifiers also feature improved linearity, better common mode rejection ratio (CMMR) and higher immunity to electromagnetic coupling [7]. Moreover, if an error is introduced to a differential system path, it will be added to each of the two balanced signals equally. Because the return path is not a constant reference point, the error will be canceled in the differential signal. Consequently, differential signal chains are less susceptible to noise and interference. Scientists and researchers have been intrigued by diverse and

multifunctional benefits of using the differential amplifier and this is why it has been the center of research attention since the beginning of its invention. Differential approach is the preferred standard in modern RFIC design to utilize the advantages of it, but the antenna industry still has not embraced this potential approach. Using a differential amplifier to feed a balanced antenna is one of the major implications of a differential amplifier, which has many research opportunities.

5.3 Small Signal Single Ended Amplifiers

Initially single ended conventional common-emitter amplifier for lower frequency range was designed. A NPN 2N2222A Bipolar Junction Transistor model was used in ISIS circuit simulation software. The amplifier was biased with basic electronics components by using appropriate biasing formulas. The goal of biasing a transistor is to establish a known Q-point in order to work efficiently and produce an undistorted output signal [8]. Correct biasing of the transistor also establishes its initial AC operating region with practical biasing circuits using either a two or four-resistor bias network.

The transistor is said to be "Cut off" where $V_{CE} = V_{CC}$ and I_C is almost zero and the cut-off point almost touches the lower end of the load line. The point with the maximum value of I_C (where $I_C = V_{CC}/R_L$) and $V_{CC} = 0$, is called "Saturation point" as no further increase in collector current will occur. The collector-emitter voltage drops to approximately zero in this point. The saturation point tells us the maximum possible collector current for the circuit [9]. To bias the transistor, first the value of V_{CE}, I_C and h_{fe} was found from the datasheet of transistor 2N2222A [10]. I_B was calculated by using the relation $h_{fe} = I_C/I_B$. For a silicon transistor, V_{BE} is fixed as 0.7V and the voltage drop across the emitter resistor is 1v. Emitter current I_E is the sum of I_B and I_C and the value of R_4 was achieved by using Ohm's law. Resistors R_1 and R_2 values are found from the potential divider network. Using the supply voltage V_{CC} and base voltage V_B values [11]. The single ended amplifier was then designed in ISIS by using these calculated values. DC blocking capacitors C_2 and C_3 were used to pass only AC signal. Also a bypass capacitor C_1 was included in the emitter leg circuit to prevent any AC appearing on the emitter without changing any of the DC condition. Figure 5.3 illustrates the circuit diagram and Figure 5.4 shows the simulation results.

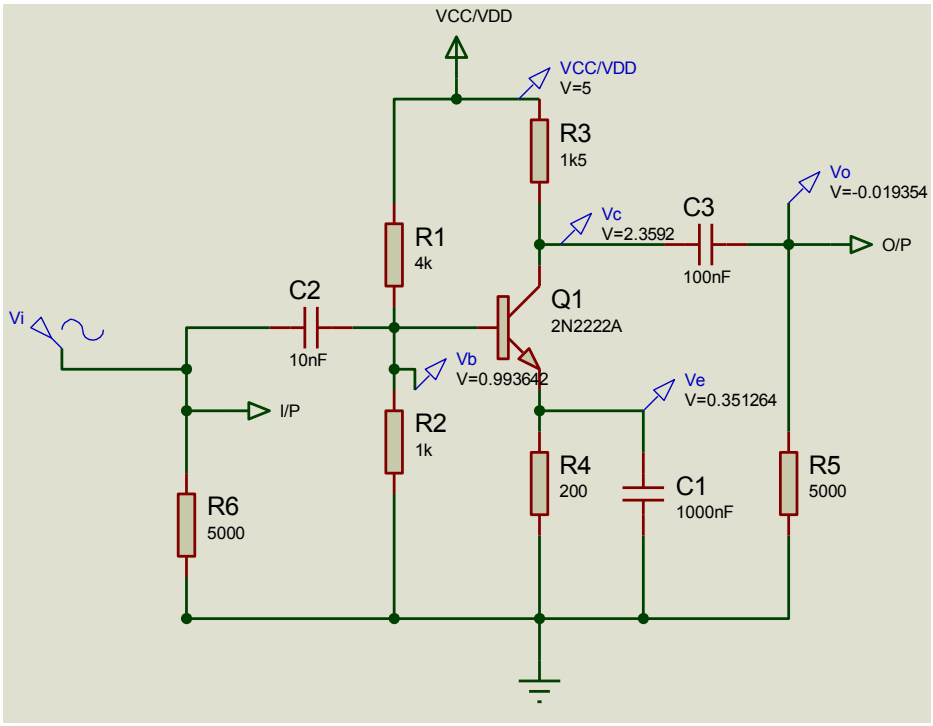

Figure 5.3: Circuit diagram of the single stage amplifier for small signal analysis.

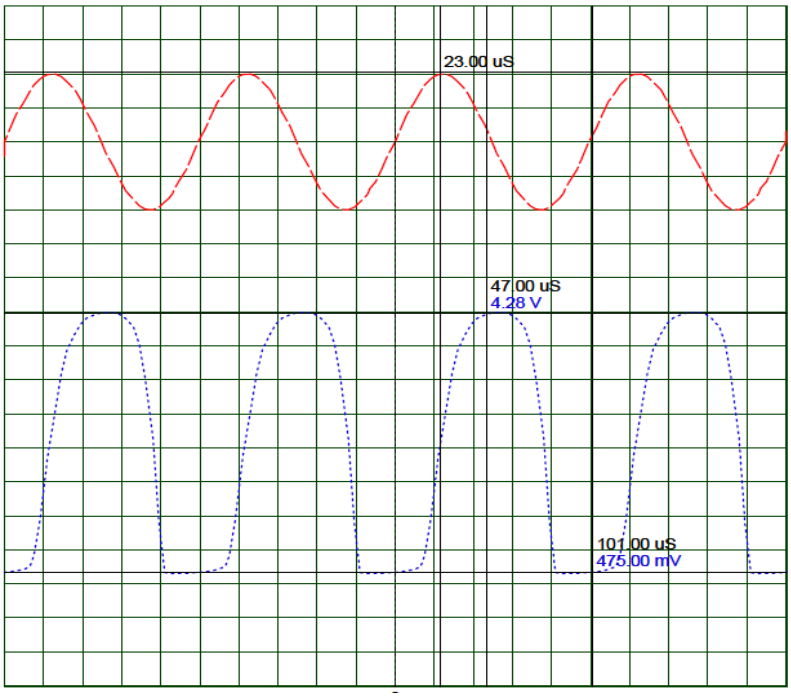

Vo =4.28-0.48 = 3.8Vpp

Figure 5.4: Simulation result of the single stage amplifier for small signal analysis.

It can be observed that the peak to peak voltage for this single ended amplifier is about 3.8V for an input sinusoid signal of 200mv. This implies that there is a good amplification at low frequency with this transistor.

5.4 RF Single Ended Amplifiers

It was relatively easier task to design and simulate amplifier at lower frequency but the complexity comes into play towards the higher frequency RF circuitry design. AWR Microwave Office circuit modelling software was used to design and analyse RF amplifiers. To meet the RF criteria of higher frequency applications, an amplifier was designed using BFP520 transistor. This transistor is suitable for higher gain with lower noise at 1.8 GHz and has a high transition frequency of 45GHz [12]. The transistor was biased with resistors and capacitors using proper biasing methods. The value of V_{CE}, I_C and h_{fe} was found from its datasheet. I_B was calculated by using the relation $h_{fe} = I_C/I_B$ and I_E was found from the formula $I_E = I_C + I_B$. Then the values of resistors were calculated using KCL and voltage divider formula. The RF Single Stage amplifier was then fabricated on 0.8mm FR4 substrate using surface mount devices. Microwave signals are very sensitive to noise and reflections and must be treated with great care. That is why conductors' width, thickness, spacing, turn shapes and routing was carefully designed according to the PCB design rules [13-14]. The tracks have been designed in a manner so that the RF signal propagates through the tracks with less noise and distortions. High frequency components were placed first to minimize length of each RF route. A minimum distance was maintained between RF lines to prevent unintended coupling. It is reported that two parallel conductors should be separated by at least 0.015mm and the length of conductors should be the shortest possible in RF circuits [14]. The trace corners were curved avoiding any sharp angle to comply with the design rule. Figure 5.5 shows the circuit diagram and the fabricated amplifier.

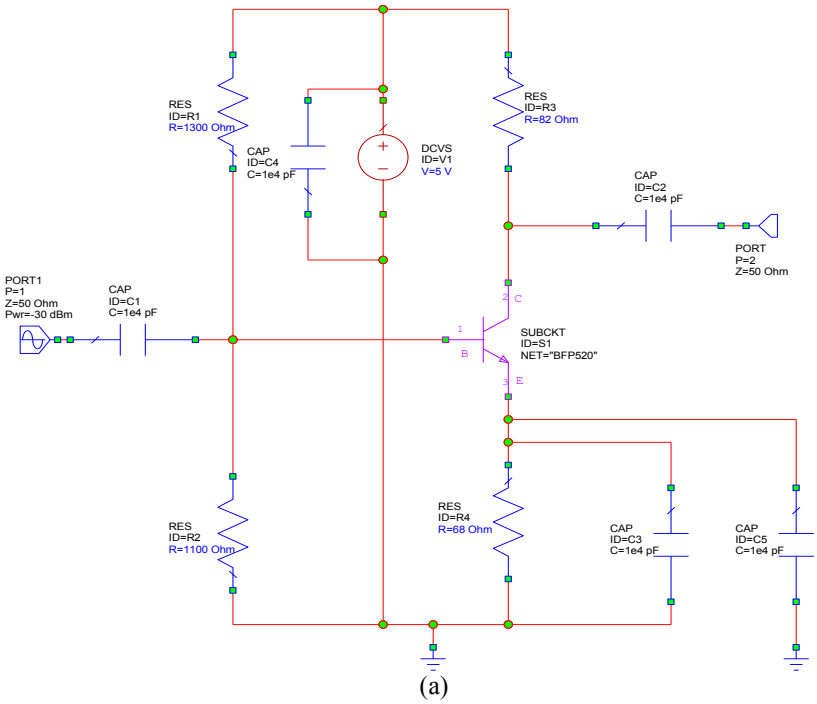

(a)

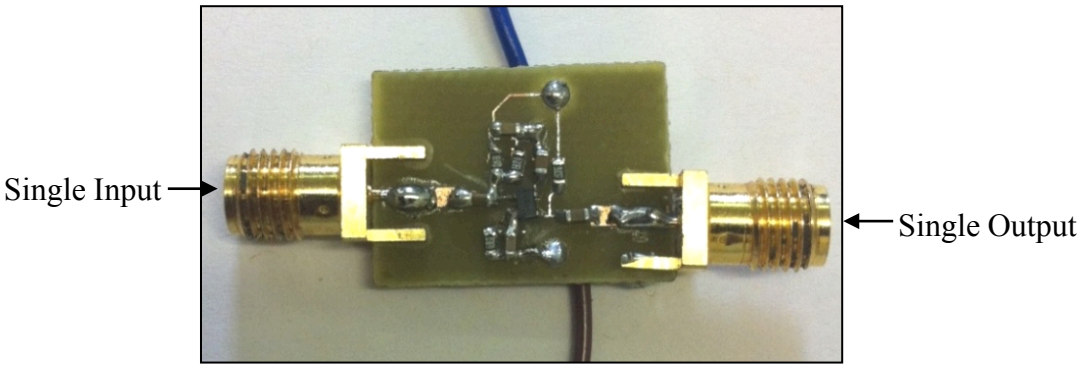

(b)

Figure 5.5: (a) Circuit diagram and (b) fabricated layout of RF single stage amplifier.

The S-parameter was simulated in Microwave Office Software and was measured using a network analyzer. The measured gain is bit lower as the track lines generate some inductance to ground in emitter circuit design. It can be realized that the amplifier is showing good gain and return loss from lower frequency till 2.5 GHz. It can also be noticed that, performance degrades as frequency increases. The simulated and the measured results are plotted in Figure 5.6.

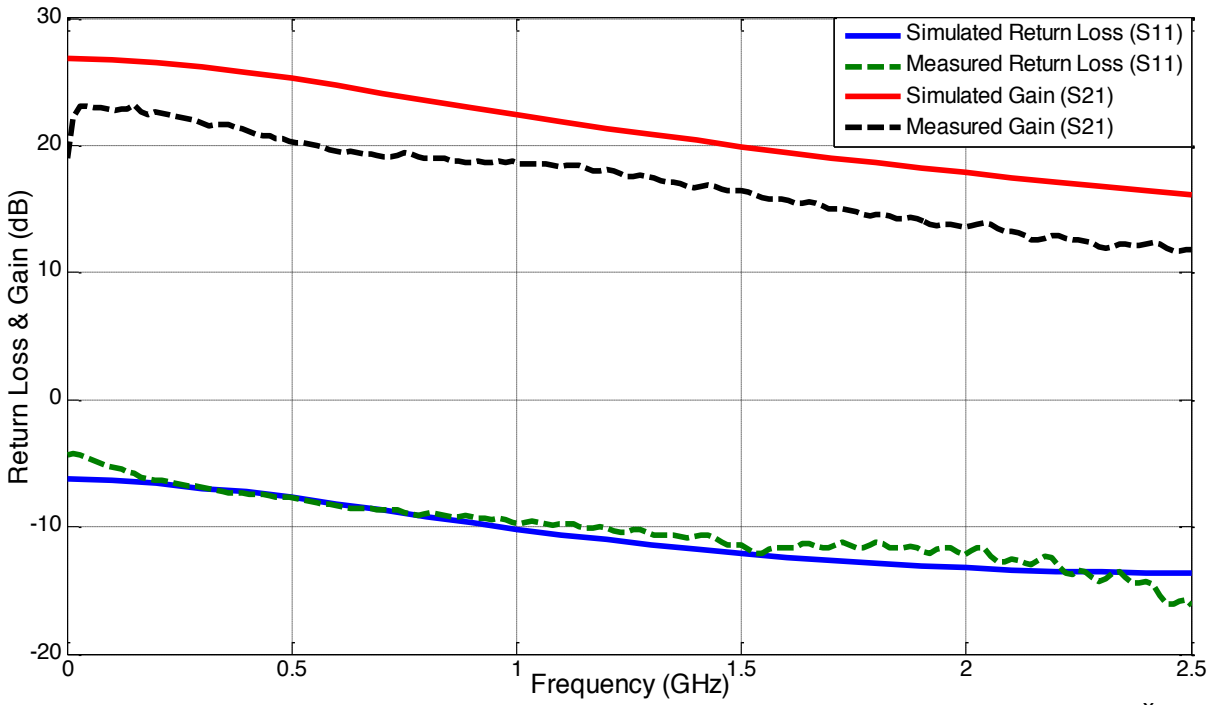

Figure 5.6: Simulation and measurement results of RF single stage amplifier.

5.5 Current Mirror Technique:

A current mirror is a circuit block which functions to generate current in one active device by replicating the current in a second active device. Hence, we can consider that the collector current at one transistor is the mirror image of that at the other transistor. This technique is often used to provide bias currents and active loads in amplifier stages [15]. They simplify the circuit design and offer a considerable flexibility in designing circuits, especially for differential amplifier. Figure 5.7 shows a basic BJT current mirror, where Q_1 and Q_2 are realised as two identical transistors. Here Q_1 together with R determine the reference current I_{REF}. The reference current is passed through the diode-connected transistors Q_1 and establishes a corresponding voltage V_{BE}. This voltage is applied between base and emitter of Q_2. Now, if Q_2 is matched to Q_1, then the collector current of Q_2 will be a mirror image to that of Q_1; that is $I_O = I_{REF}$ [15].

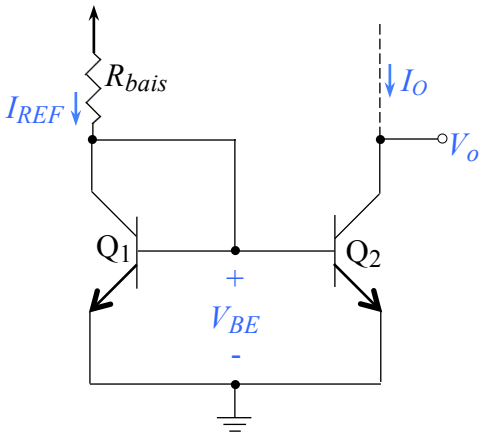

Figure 5.7: A Basic BJT Current Mirror [15].

This phenomenon is known as current mirror. The main function is to regulate current through the load resistor by conveniently adjusting the value of R_{bias}. There are few conditions, which need to be considered to make the current mirror work appropriately. The ratio of the collector current to the base current (β) has to be sufficiently high so that the base current becomes negligible. This is because the finite β or the nonzero base current of the BJT causes error on the current transfer ratio of the bipolar mirror. And the transistor must be operating in the active mode, which in turn is achieved as long as the collector voltage V_O is 0.3V or higher than that of the emitter [15].

This is an example of simplest current mirror. The reduced dependence on B can be achieved by introducing another transistor Q_3, as illustrated in Figure 5.8. Here the emitter of Q_3 supplies the base current of Q_1 and Q_2. The sum of the base currents is then divided by (β_3 +

1), resulting in a much smaller error current that has to be supplied by I_{REF}. It is based on the assumption that Q_1 and Q_2 are matched and thus have equal collector currents, Ic. This extra transistor offers tremendous improvement in reducing the error caused by finite β [15].

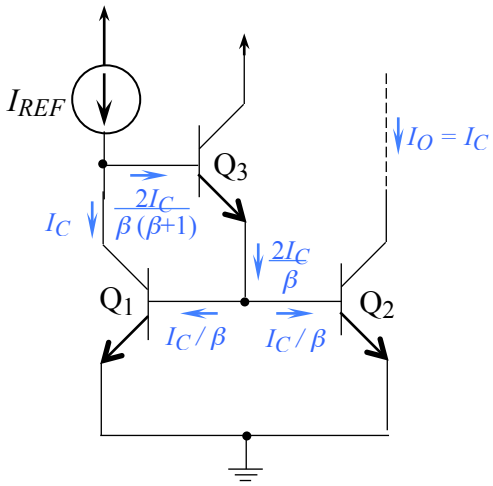

Figure 5.8: A current mirror with base current compensation [15]

5.6 Differential Amplifier Design Using Transistor Array and Current Mirror

A differential amplifier needs to be designed with completely identical pairs of transistors. In this research work several differential amplifiers were designed using two similar transistors have been discussed but their properties are not completely identical. Using a transistor array in differential amplifier design can fulfill this demand. Transistor arrays are a combination of multiple transistors in a single package, which are often used in log amplifiers, differential amplifiers and current mirrors. A HFA3046B ultra high frequency transistor array was used to design a differential amplifier with an implementation of current mirror technique. Each array of HFA3046B consists five dielectrically isolated NPN transistors on a common substrate [16]. Two transistors were used for differential output and one for current mirror. One transistor was used for a completely isolated single ended amplifier design using the identical transistor of the same package. Another similar array for low frequency applications, LM3046M, was also used for a similar low frequency amplifier design. Both amplifiers were fabricated and tested and once again acceptable result was obtained from the lower frequency design but not from RF differential amplifier using HFA3046B. Again it is proved that a differential amplifier design for higher frequency range is not as easy as single ended ones. Figure 5.9 presents the fabricated amplifier with transistor array.

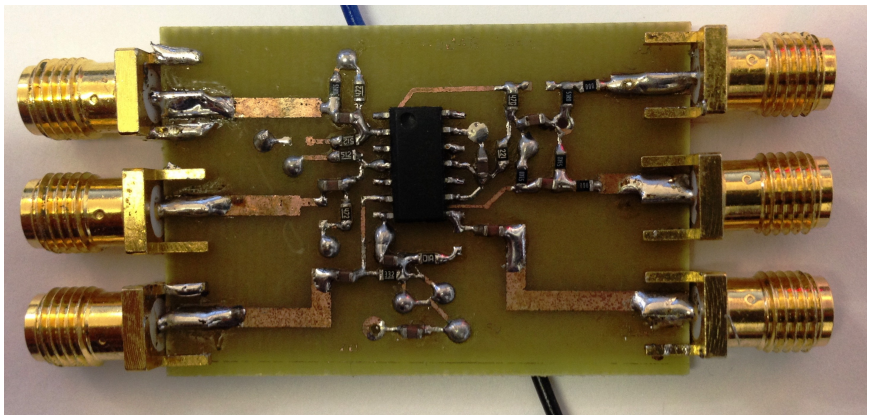

Figure 5.9: Fabricated model of the amplifiers using transistor array and current mirror technique.

5.7 Broadband and Highly Linear Differential Amplifier Design

The impedance of a differential amplifier plays a significant role in its performance. As discussed earlier, the differential impedance is not an industry standard 50Ω, rather the total differential impedance is 100Ω. To measure a differential amplifier either it should be measured differentially with a 4-port network analyzer or the output impedance should be matched with the standard 50Ω interface. It is a common practice to use 'balun' as a converting feeding mechanism between a differential circuit and an unbalanced circuit structure. But use of a balun introduces losses and bandwidth restrictions. To demonstrate the performance of a fully differential amplifier the LMH6881 RFIC from Texas Instruments [17] was chosen as it provides a high power and gain up to 2.5GHz, which is essential to measure the second and third order harmonic distortions for a fundamental frequency of 900 MHz. A broadband highly linear differential amplifier was then designed using the LMH6881 RFIC with single ended output interface with a balun and as well as one with fully differential output interfaces. These designs will be used to examine the benefits of differential amplifier and a true differential interface.

The LMH6881 has 100Ω input impedance and a very low (0.4Ω) output impedance. Benefit of such low-impedance output is that they are less likely to be influenced by the pad capacitance or trace inductance [17]. Also matching load impedance for proper termination is as easy as inserting the proper value of resistor between the load and the amplifier. Therefore,

two 51Ω (nearest available to 50Ω) load-matching resistors were deployed to match the output impedance to 100Ω. These resistors were placed close to the output pins in order to ensure output stability. DC-blocking capacitors were placed on both the input and output signal traces. To match with the 50Ω single ended test equipment, two 2:1 impedance ratio RF transformers from mini-circuits [18] were added adjacent to the input and output ports. Another differential amplifier was also prototyped with fully differential output configuration. Here the expected load impedance is no longer the usual 50Ω to 'ground', but a true balanced 100Ω. A block diagram presented in Figure 5.10 represents the configuration of both these amplifiers.

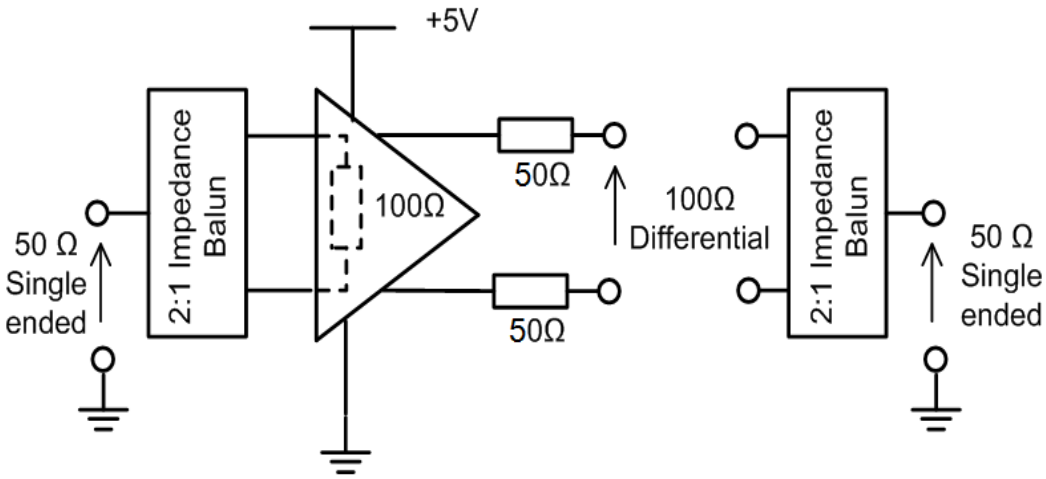

Figure 5.10: Proposed amplifiers configuration.

Figure 5.11 demonstrates the schematic diagram of the amplifier with associated biasing and decoupling components. The differential form was designed by simply removing the balun from the output to provide two 50Ω ports for circuit testing, which are balanced with respect to ground.

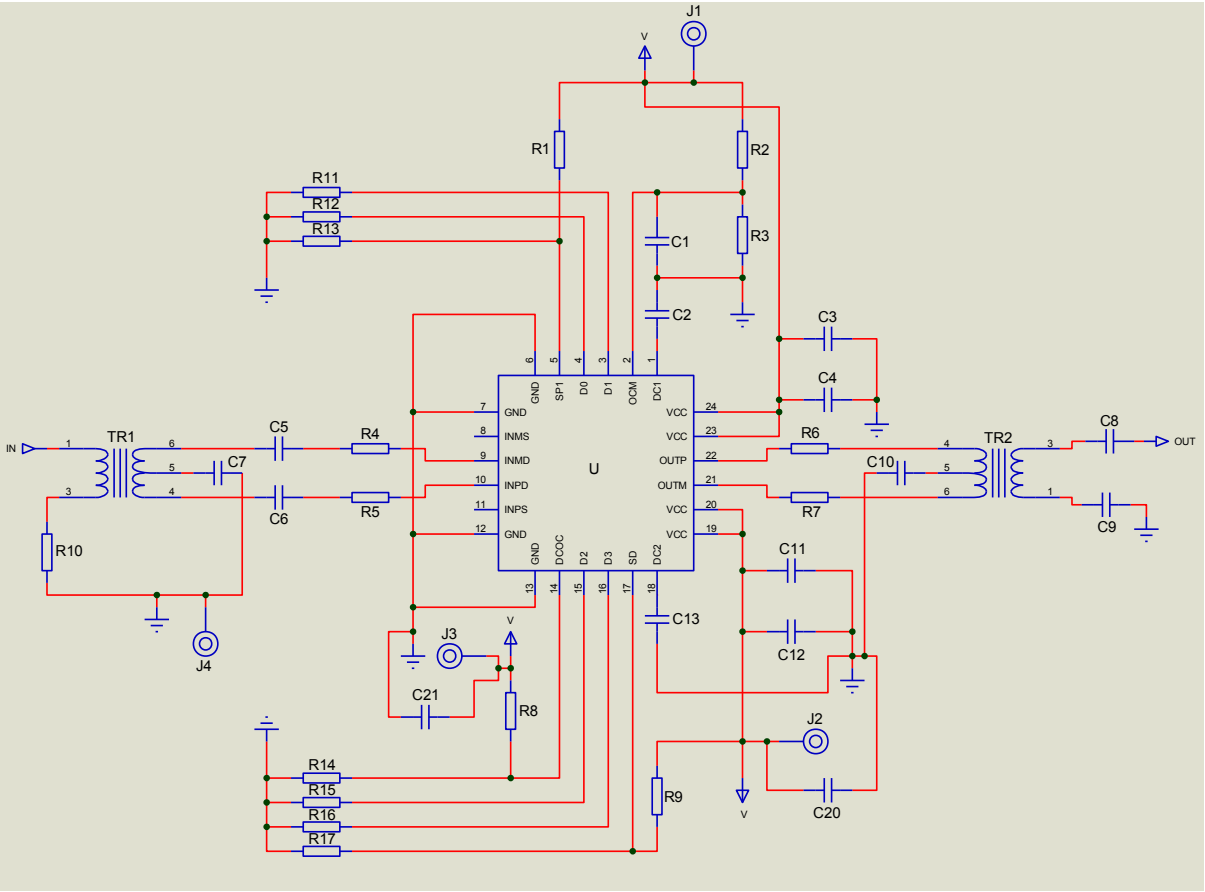

Figure 5.11: Schematic diagram of the LMH6881 amplifier with single ended output interface

The layout for fabrication was designed by maintaining PCB design rules [13-14] while designing conductor's width, thickness, spacing and turn shapes. All the components were placed on the top layer of the board. The bottom layer was mainly used as ground. A conductor line was also used at the bottom layer to connect the power supply pins together. C20 – C23 capacitors were used to maintain the ground continuity on either sides of this line. The amplifiers were prototyped on a 0.8mm thick FR4 substrate with 35-micron thick copper. The track widths of the input and output transmission lines are calculated using microstrip design formulas [19]. The ratio of the track width and board thickness, (W/d), was found using the formula (5.4) considering the characteristic impedance is equal to 50Ω and the dielectric constant of the FR4 substrate is 4.3.

$$\frac{W}{d} = \frac{8e^{A}}{e^{2A} - 2} \qquad \text{for W/d} < 2 \qquad (5.4)$$

Where,

$$A = \frac{Z_0}{60}\sqrt{\frac{\epsilon_r + 1}{2}} + \frac{\epsilon_r - 1}{\epsilon_r + 1}\left(0.23 + \frac{0.11}{\epsilon_r}\right) \qquad (5.5)$$

W = Width of the microstrip line

d = Thickness of the substrate

Z_0 = Characteristic Impedance

ε_r = Relative dielectric constant of the substrate

The track width W was calculated as 1.556 mm. The desired characteristic line impedance (Z_0) has to be 50Ω to be matched with the 50Ω measurement standards. The value of Z_0 was double-checked using the obtained calculated track width value in equation (5.6) and (5.7). The effective dielectric constant of a microstrip line is given approximately by

$$\epsilon_{eff} = \frac{\epsilon_r + 1}{2} + \frac{\epsilon_r - 1}{2}\frac{1}{\sqrt{1 + 12d/W}} \qquad (5.6)$$

and as W/d ratio is less than 1, the characteristic impedance can be calculated as

$$Z_0 = \frac{120\pi}{\sqrt{\epsilon_{eff}}[W/d + 1.393 + 0.667\ln(W/d + 1.444)]} \qquad (5.7)$$

The effective dielectric constant and then the characteristic impedance were calculated as 3.2662 and 50.224Ω respectively using W = 1.556 mm. Figure 5.12 represents the layout design of both amplifiers. The chip LMH6881 RFIC was mounted using reflow oven and soldering of all other surface mount components were carefully carried out by hand. The constructed prototypes on 0.8mm thick FR4 substrate are shown in Figure 5.13.

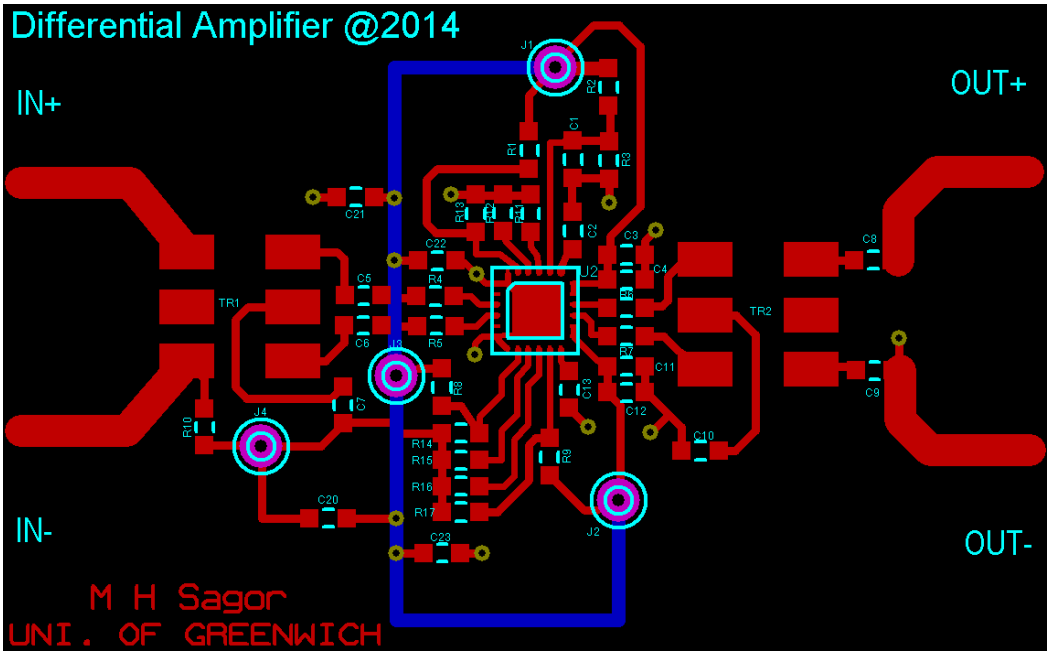

(a) LMH differential amplifier with single ended output configuration

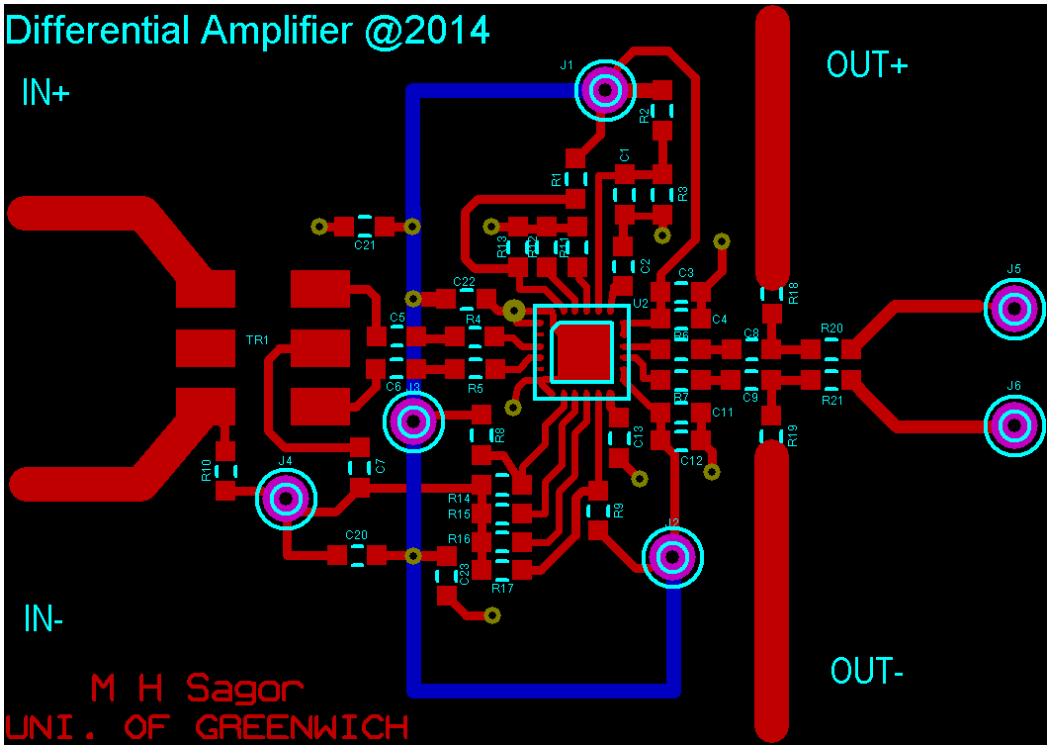

(b) LMH differential amplifier with differential output configuration

Figure 5.12: Design layouts of the LMH6881 differential amplifiers

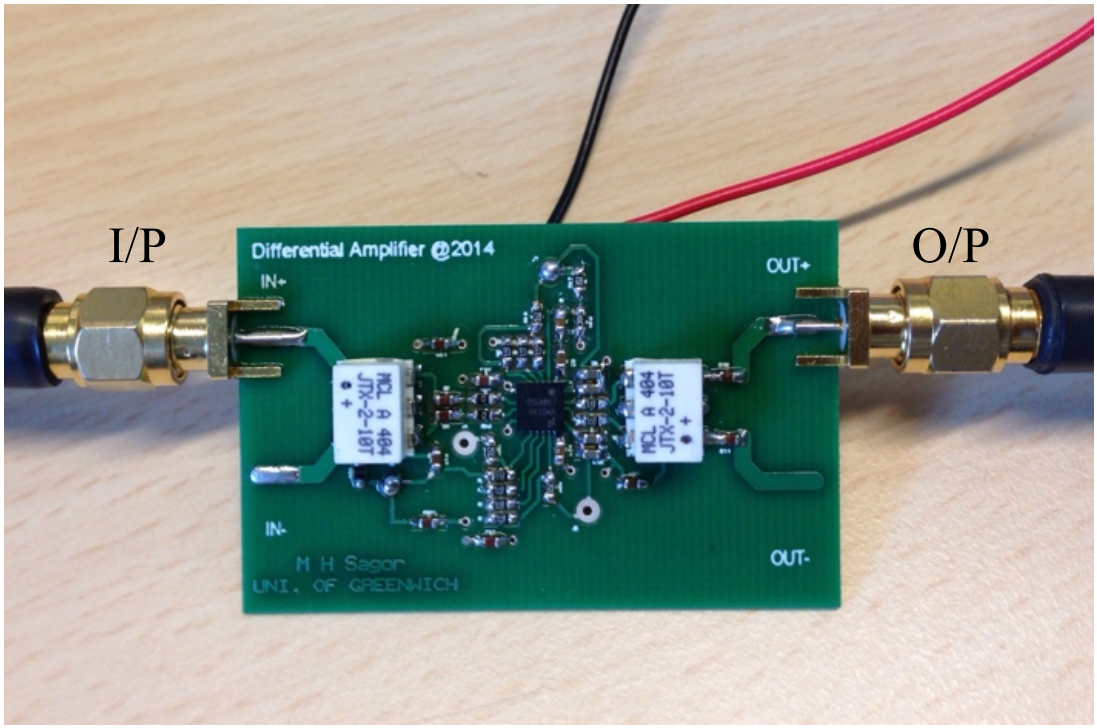

(a) LMH differential amplifier with single ended output configuration

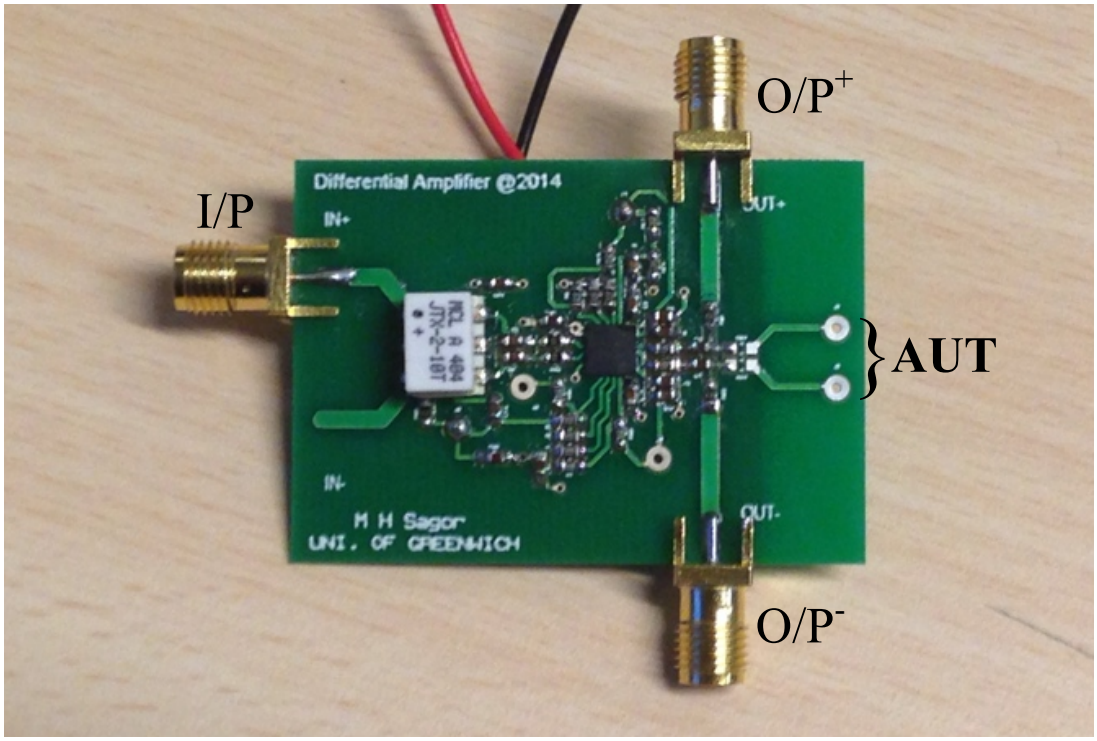

(b) LMH differential amplifier with differential output configuration

Figure 5.13: Prototypes of the LMH6881 differential amplifiers

5.8 Measurement of Differential Signals at RF Frequency

5.8.1 Conventionally Measured Frequency Response of LMH6881

The return loss and gain of the LMH6881 prototypes was initially measured using Agilent N5230A 2-port network analyser. While measuring the amplifier with differential output, measurement was carried out on one output port while the other output port was terminated with a 50Ω load. The frequency responses of these measurements are presented in Figure 5.14. Theoretically, the differential gain of the amplifier (with balun in this case) should be double (3dB higher) compared to the gain at each port of the differential amplifier. But we can see that the gain is less than 2dB higher compared to the gain at each port till around 1GHz. So more than 1 dB gain is lost because of the balun effect. Moreover, the gain rolls off after 1GHz, as this balun is restricted to work till 1GHz. It can be observed that the balun is affecting the bandwidth.

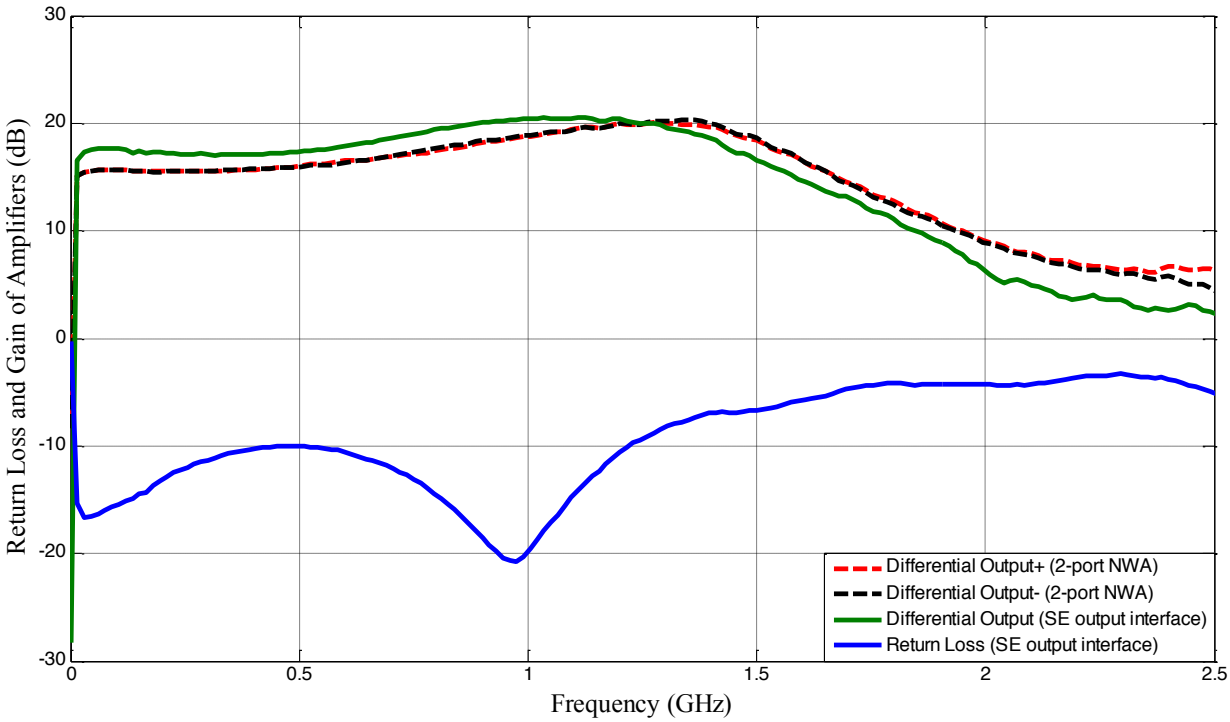

Figure 5.14: Return Loss (S11) and Gain (S21 & S31) of differential amplifiers measured by 2-port network analyser.

5.8.2 Differentially Measured Frequency Response of LMH6881

A differential device should be measured differentially in order to appropriately characterize the performance. A 4-port Agilent N5230A PNA-L network analyser was used to measure the amplifier fully differentially. The network analyser was properly calibrated for 4 ports using the provided calibration kit. As the input is single ended and the output is balanced, SE-BAL topology was chosen. The single input port was considered as the input logical port and two output ports were considered as output logical port. The response of this true differential measurement is illustrated in Figure 5.15. It can be observed that the differential gain (Sds21) of the amplifier is giving double gain (~3dB higher) compared to the gain at each port throughout the frequency range. Gains of the two ports are also more stable at higher frequency. So it can be established that just by using true differential interface, it is possible to achieve higher and more stable gain from same device using same components. It can also be confirmed that a differential device must be measured in a differential way.

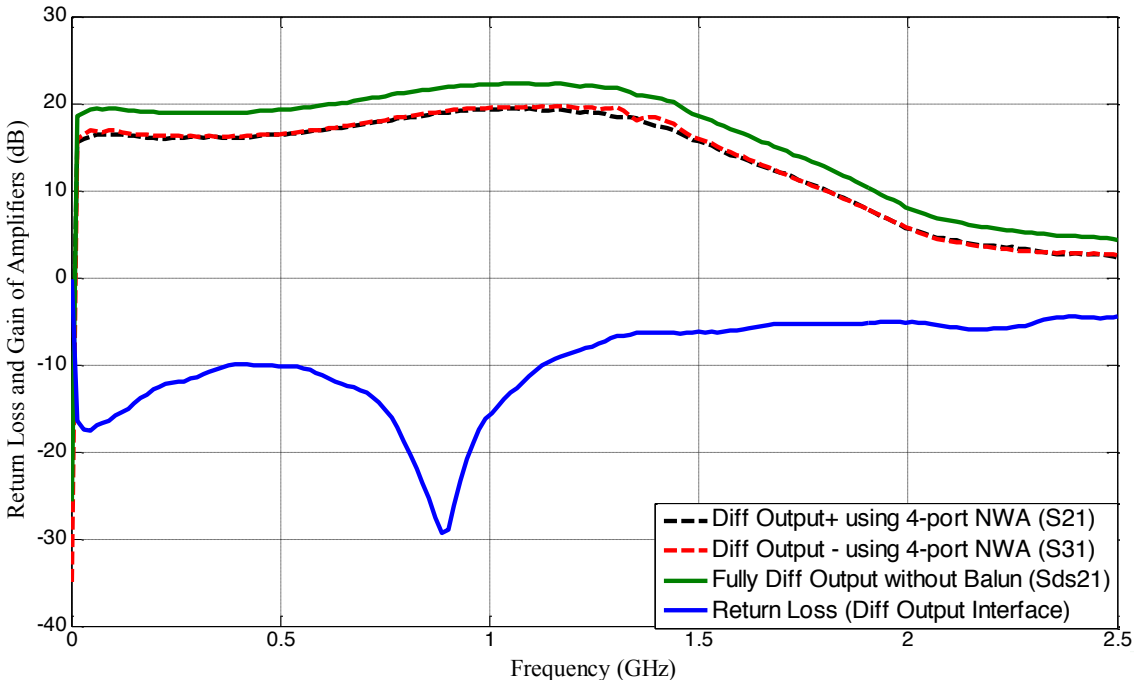

Figure 5.15: Measured return Loss (S11) and Gain (S21, S31 & Sds21) of differential amplifiers measured by 4-port network analyser

5.9 Phase Response of LMH6881 Differential Amplifier Design

It is well known that the output signal of a balanced circuit comprises two signals with the same magnitude but 180-degree out of phase. It can be seen from Figure 5.15 that the fully

differential amplifier comprises almost similar magnitudes (Red & Black) in its two output ports. Figure 5.16 shows that the ports were also maintaining around 178-180 degree phase difference throughout this measurement range.

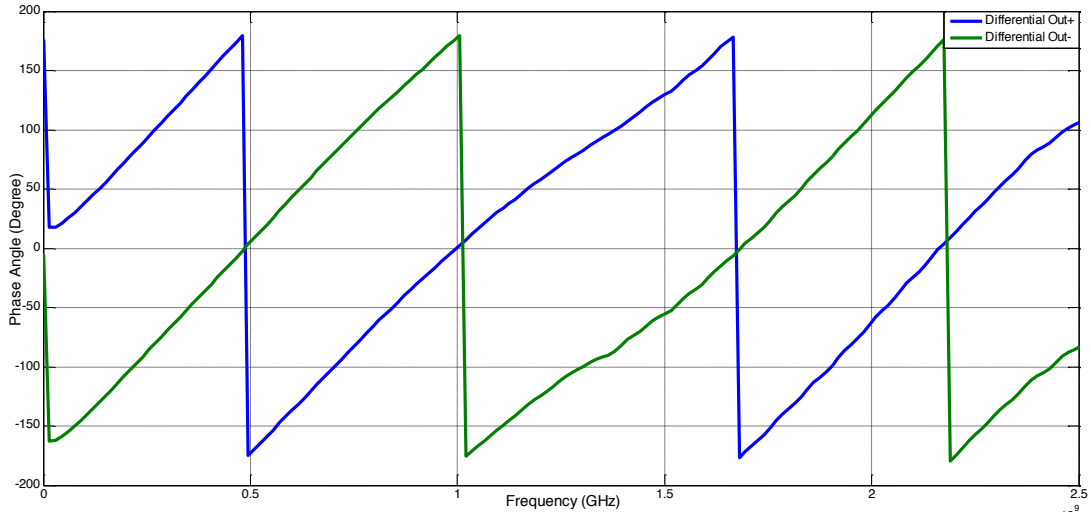

Figure 5.16: Phase difference of the LMH6881 differential amplifier.

5.10 Gain Compression and Linearity of Differential Amplifier

Linearity is one of the primary concerns in power amplifiers. An amplifier is called linear when the output power increases linearly with the input power and the resultant transfer curve appears as a straight line with a slope of unity. But a practical amplifier is not perfectly linear. The nonlinearity of practical amplifiers sets a realistic power range, or dynamic range, over which the amplifier will perform as desired [19]. If the output power is plotted against the input power and the input power is continuously increased, it will reach at a stage where the output power does not increase with the input power. A typical amplifier P_{in} vs P_{out} response is explained in Figure 5.17.

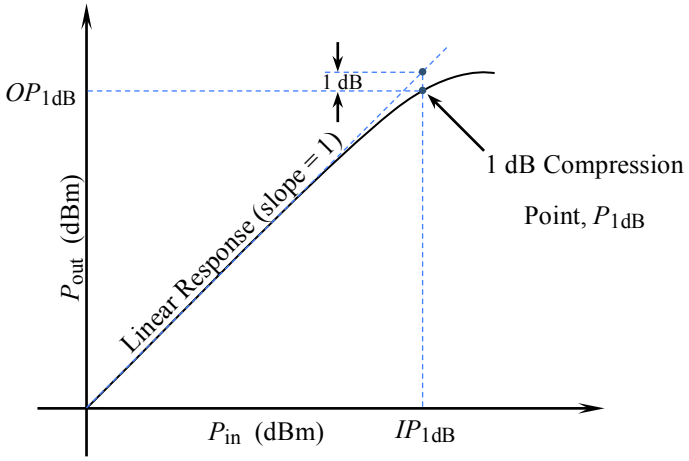

Figure 5.17: 1 dB Compression point for a nonlinear amplifier (Reproduced from [19]).

As the output power begins to saturate, it deviates from the ideal linear characteristics. At one point the actual output power is 1dB less than the ideal power level and this point is known as 1dB compression point of that amplifier. This power level is usually denoted by P_{1dB}, and can be stated in terms of either input power (IP_{1dB}) or output power (OP_{1dB}) [19]. When the amplifier is set to operate at a higher power than P_{1dB}, it will result in distorted performance or even may cause damage to the device itself.

The LMH6881 amplifiers with single ended output and with differential output configurations were measured for P_{in} vs P_{out} and the measurement results are plotted in Figure 5.17. Both amplifiers were measured using a 4-port network analyzer and only the single ended output amplifier was measured using a synthesizer at 900 MHz. A sudden small increase in the gain can be seen on the measurements using VNA, just before the amplifiers go into saturation. This might be because of the swept response of power sweep is not being able to capture the output power from both ports simultaneously. But the effect is completely gone when the output power was captured from a spectrum analyzer and the input power was increased manually from a synthesizer. The key point to notice here is that the differentially measured LMH6881 is providing about 1.5dBm more power, eventually more linearity, compared to the same amplifier with single ended output configuration. The output referred compression point (OP_{1dB}) is 5.9dB for the SE configuration and 7.55dB for fully differential output configuration.

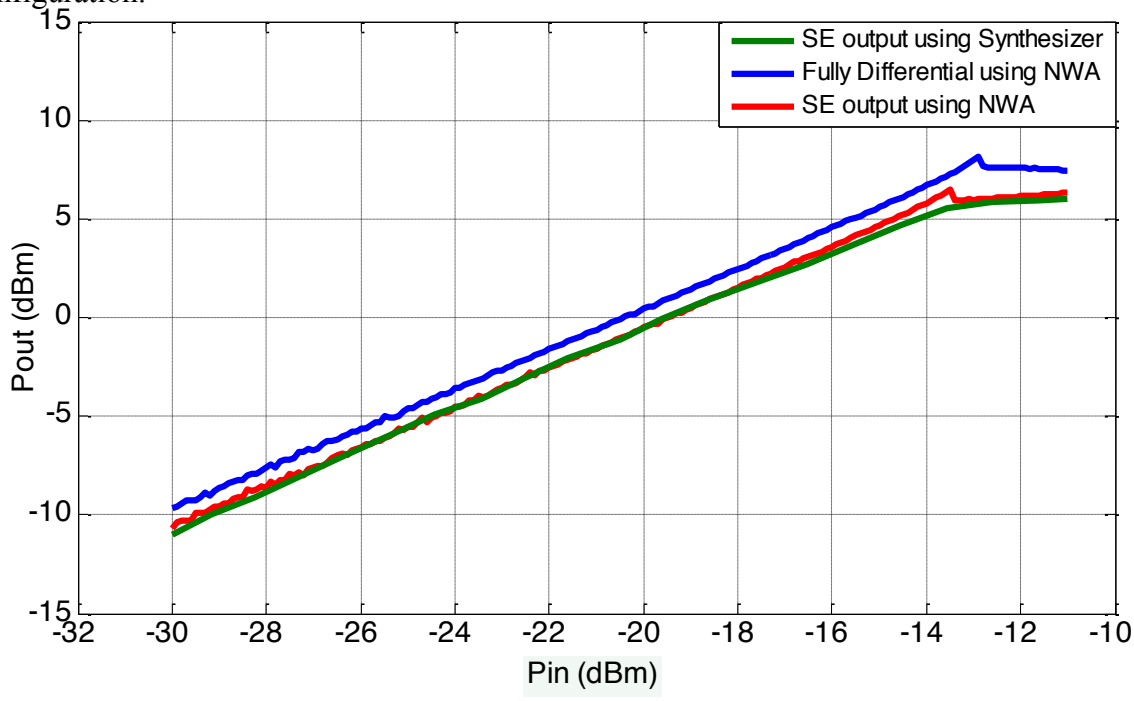

Figure 5.18: P_{in} vs P_{out} curves of LMH6881 differential amplifiers

5.11 Common Mode Rejection Ratio of the LMH6881 Amplifier

Another important figure of merit of a differential amplifier is the common mode rejection ratio (CMRR). When same voltage is applied in the inputs of a differential amplifier, the amplifier is considered to be operating in a common mode configuration. Many disturbance and noise signals appear as a common input signal to both the input terminals, which should be rejected by the differential amplifier. The ability of a differential amplifier to reject these common mode signals is called common mode rejection ratio (CMRR). CMRR is the ratio between the differential gain and the common mode gain. The ideal common-mode gain of a differential input amplifier is zero; hence the ideal CMRR value is infinite [20]. However, in practical circuit there will be a common-mode gain due to the asymmetry in the circuit and due to the effects of resistance mismatches [21]. The value of CMRR is usually expressed in dB and described as CMR,

$$CMR\ (dB) = 20log_{10}\left|\frac{A_{dm}}{A_{cm}}\right| \tag{5.4}$$

A high value indicates more rejection of common mode, which is desirable in all devices. At lower frequency CMR values are usually very high but it deteriorates at higher frequency [22]. The CMR of the LMH6881 differential amplifier was measured using fully differential measurement technique. Figure 5.19 shows the measurement result where it can be noticed that the amplifier is showing almost 30dB CMR at a frequency as high as 1GHz. The CMR is almost stable in different input powers until the amplifier goes to saturation.

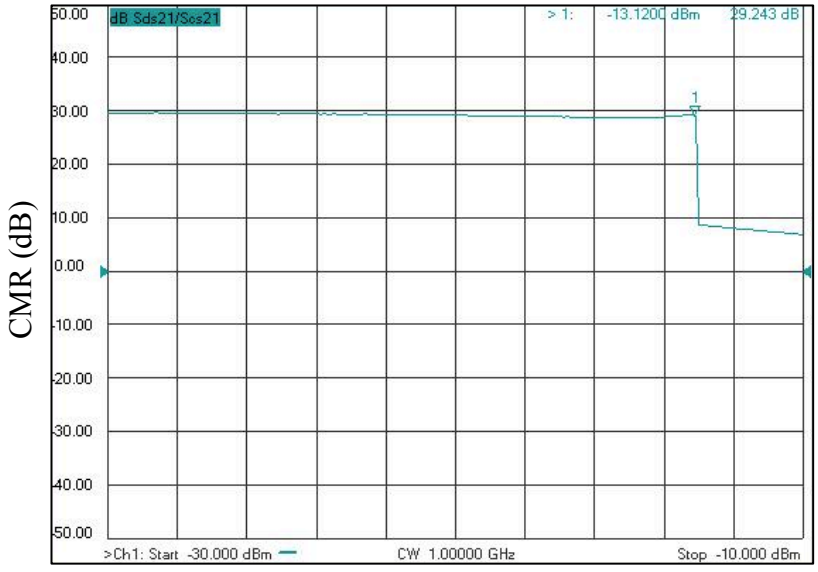

Figure 5.19: Common Mode Rejection Ratio of the LMH6881 differential amplifier.

5.12 Summary

The design and characterization of a differential amplifier has been the main focus in this chapter. Small signal and RF single ended and differential amplifiers were assembled using BJT technologies. Amplifier design steps were followed to design and simulate and then measure the real fabricated amplifiers. Simulated results verified the theory of superior performance of differential amplifier over its single ended counterpart. Then it was comprehended that constructing a RF differential amplifier to operate at higher frequency is not as easy as designing a single ended form. The current mirror technique was also demonstrated and was implemented is a circuit construction using a transistor array.

Afterwards, LMH6881 RFIC from Texas Instruments was adopted to develop a broadband differential amplifier. Careful process of design and fabrication delivered a high gain broadband differential amplifier with single ended output formation as well as one with fully differential output configuration. The measured frequency response, phase response, compression point and common mode rejection ratio confirmed high performance and broadband differential amplifier realization. The comparison of performance between two equivalent amplifiers has suggested that the fully differential output arrangement provides higher and more stable gain without compromising the operating bandwidth and delivers higher linearity compared to the design with single ended output configurations.

References

[1] John L. B. Walker (2011), *Handbook of RF and Microwave Power Amplifiers*, Cambridge: Cambridge University Press, Chapter 1.

[2] Thomas H. Lee (2004), *The Design of CMOS Radio-Frequency Integrated Circuits*. 2nd ed. Cambridge: Cambridge University Press. Chapter 11.

[3] Datta, S.; Saha, H.; , "A 950-MHz fully differential class-E power amplifier in 0.18µm CMOS for wireless communications," *Emerging Trends in Electronic and Photonic Devices & Systems, 2009. International Conference on* , vol., no., pp.88-91, 22-24 Dec. 2009.

[4] Dehghani, R (2013), *Design of CMOS Operational Amplifiers,* Norwood: Artech House. Chapter 5.

[5] James Karki (2002), *Fully-Differential Amplifiers,* Application Report, Texas Instrument.

[6] C. Park, Y. Kim, H. Kim, and S. Hong, "A 1.9-GHz Triple Mode Class-E Power Amplifier for a Polar Transmitter," IEEE Microw. and Wireless Components Lett., vol. 17, no. 2, pp. 148-150, Feb. 2007.

[7] Staric, P., Margan, E. (2006), *Wideband Amplifiers*, Netherlands: Springer Publications, Chapter 3.

[8] U.A.Bakshi, A.P.Godse (2009), *Basic Electronics Engineering*, Pune: Technical Publication, Chapter 1.

[9] Albert Malvino, David Bates (2006), *Electronic Principles*, McGraw-Hill Higher Education. Chapter 7.

[10] ON Semiconductors, "Small Signal Switching Transistor" 2N2222A, November, 2013; Available at: http://www.onsemi.com/pub/Collateral/2N2222A-D.pdf

[11] R. L. Boylestad, L. Nashelsky (2007), *Electronic Devices and Circuit Theory*. 9th ed. Ohio: Prentice Hall. Chapter 4.

[12] Siemens, "Low Noise Silicon Bipolar RF Transistor" BFP520, 23rd April, 2013; Available at: http://www.alldatasheet.com/datasheet-pdf/pdf/44571/SIEMENS/BFP520.html.

[13] Brian C. Wadell (1991), *Transmission Line Design Handbook*, Boston: Artech House Microwave Library, Chapter 9.

[14] R. S. Khandpur (2006), *Printed circuit boards,* McGraw-Hill, New York, Chapter 3.

[15] Sedra, A.S.; Smith, K.C (2010), *Microelectronic Circuits*, 6th ed. Oxford: Oxford University Press, Chapter 6.

[16] Intersil, "Ultra High Frequency Transistor Arrays" HFA3046, Aug 8, 2013; Available at: http://www.intersil.com/content/dam/Intersil/documents/hfa3/hfa3046-3096-3127-3128.pdf

[17] Texas Instruments, "LMH6881 DC - 2.4GHz, High Linearity, Programmable Differential Amplifier", March 2013; Available at: http://www.ti.com/lit/ds/symlink/lmh6881.pdf

[18] Mini-Circuits, "Surface Mount RF Transformer" JTX-2-10T; Available at: www.minicircuits.com/pdfs/JTX-2-10T.pdf

[19] David M. Pozar (2012), *Microwave Engineering*, 4th ed. USA: John Wiley & Sons, Inc. Chapter 3.

[20] Bakshi, U. A., Godse, A. P. (2009), *Linear Integrated Circuits*, 4th ed. India: Technical Publications. Chapter 2.

[21] Franco, Sergio. (2002), *Design with operational amplifiers and analog integrated circuits*, 3rd ed., McGraw-Hill, New York, Chapter 2.

[22] Hunk Zumbahlen (2009), *Linear Circuit Design Handbook*, 1st edition., Elsevier, Oxford, Chapter 1.

Chapter 6

Characterizing Effective Radiated Power and Distortion From Differentially Fed Narrow Band Antennas

6.1 Introduction

RF power amplifiers play an important role in modern telecommunication systems. Telephone, internet, email, radio broadcast, gaming, online television all are merged together in a same device in contemporary communication devices. The design of such multitasking single mobile device requires a high level of integration with low power consumption and low production cost, which demands more linear amplifiers. Designing linear and efficient RF power amplifier presents one of the most challenging aspects in the RF industry. Careful optimization must be performed to obtain the required gain, efficiency and linearity. One solution to meet this demand is to use linearization techniques without compensating gain and bandwidth. Recently a great deal of attention has been directed towards the design of amplifiers employing special distortion correction methods. Researchers have proposed several linearization techniques recently [1-3] but most of them were accomplished by considering complex design techniques or by adding extra components in the circuit.

In this chapter, the nonlinear distortion characteristics of the LMH6881 will be analysed. Techniques to achieve higher gain and linearity from same device by changing output impedance will also be investigated. Following that an experimental proof is presented confirming that differential feeding configuration can provide higher gain and greater linearity compared to its single ended counterpart. The adjacent channel leakage ratio (ACLR) of both active antennas will be presented to compare the distortion characteristics of differential and single ended interface. The chapter concludes with a proposal of the best approach for achieving higher gain and greater linearity for present communication system.

6.2 Methods to Quantify Distortion

An ideal perfect linear amplifier is a completely linear device regardless of the input power level. It is just a theoretical concept that does not exist in reality. All practical components possess a small amount of loss and nonlinearities. Devices become nonlinear at a certain power level while operating out of its dynamic range. This nonlinear characteristics lead to undesirable noise and distortion and generates spurious frequency components. As a result, the amplifier experiences increased loss and possible interference with other radio channels. These possible effects of nonlinearity in RF circuits can be quantified by some distortion measures mainly by 1dB compression points, harmonic generation, intermodulation distortion and spectral regrowth [4]. Evaluating these figures of merit plays a vital role on the correct specification of power amplifiers. The 1dB compression points or gain compression has already been discussed in the previous chapter and the harmonic distortion topic will be reviewed in the next chapter. In this chapter, the intermodulation distortion and spectral regrowth or adjacent channel leakage ratio will be considered as an approach to demonstrate the distortion characteristics of the LMH6881 differential amplifiers.

6.2.1 Intermodulation Distortion (IMD)

When the input signal interacting in a non-linear device consists of two closely spaced frequencies, additional spurious components will be generated at the sum and difference of integer multiples of the original frequencies [5]. These unwanted signals are known as intermodulation products of the device. If the input signal comprises of two fundamental frequencies f_1 and f_2, distortion products will occur at frequencies $af_1 \pm bf_2$, where a and b are integers ≥ 1. Only the odd order mixing products creates distortion close to the main signals. Specially, the third order intermodulation products ($2f_1$-f_2 & $2f_2$-f_1) remain very close to the fundamental frequencies and cannot be easily filtered out [6]. The even orders do not affect the transmitting signal as much as the odd order harmonics as they can be easily filtered out because they are generated at a greater distance from the original signal. The two-tone stimulus is a better representation signal distortions than the pure sinusoid one-tone test such as gain compression.

Two-tone test was carried out on the LMH6881 differential amplifier to compare the IMD level with a true single ended amplifier. A commercially available high gain broadband single ended amplifier ZFL-2500+ [7], as shown in Figure 6.2(a), was acquired and measured along

with the differential amplifier. Synthesizer and network analyser were used as two signal sources of frequencies 900 MHz and 905 MHz. The signals were then summed into a power combiner and then fed into the amplifier. An attenuator was also used between the DUT and the spectrum analyser. Though attenuator is optional in two-tone measurement process, it gives some flexibility in changing the input power levels of both the signal generators simultaneously. It can also be used in testing whether the instruments themselves are creating some spurious signal or not. The measurement setup is shown in Figure 6.1.

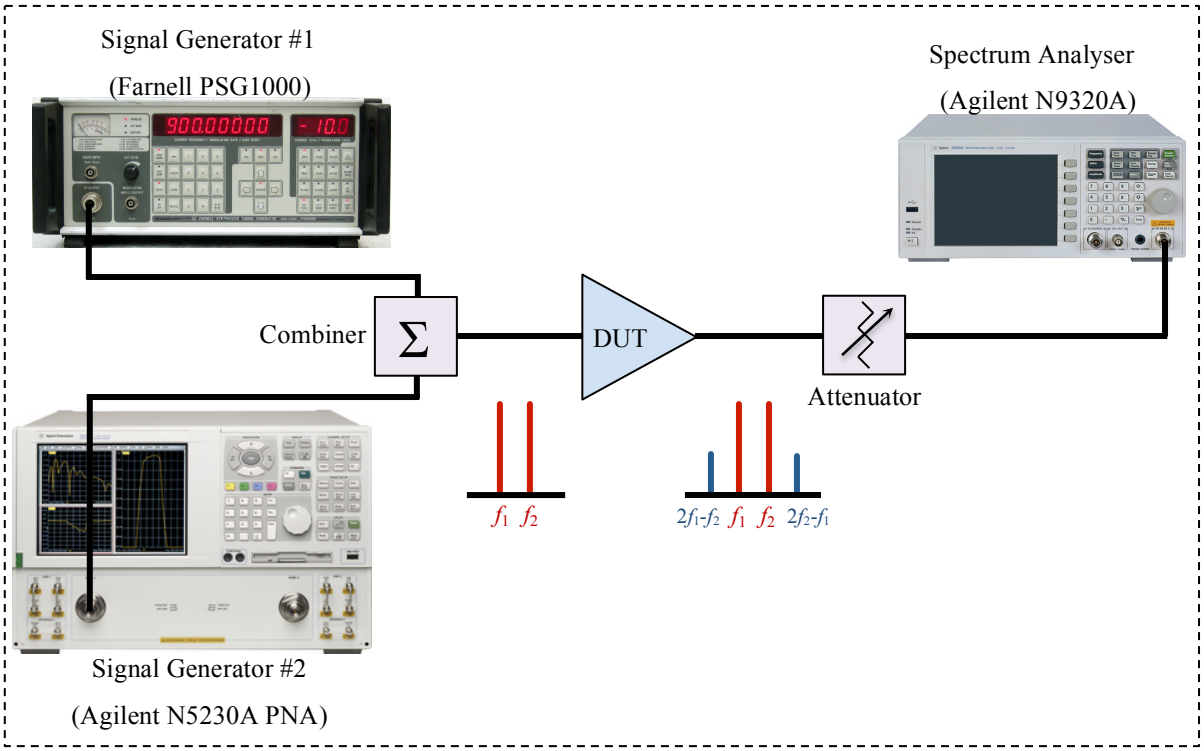

Figure 6.1: Block diagram of the measurement setup on the bench.

The measurement result of two-tone intermodulation test of the single ended and differential amplifier for -15dBm input power is presented in Figure 6.2. The fundamental signal magnitude of the single ended amplifier was normalised to the level of the differential one by changing the degree of attenuation. It can be observed that with a similar fundamental power the differential amplifier has almost 10.5 dBc lower third order intermodulation distortion product (IMD3).

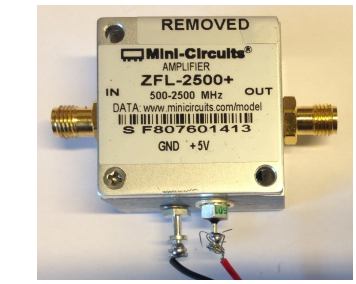

ZFL Single Ended

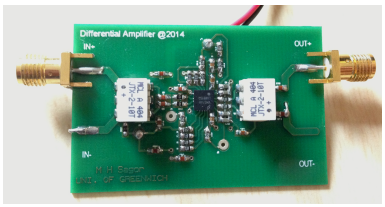

LMH Differential

(a)

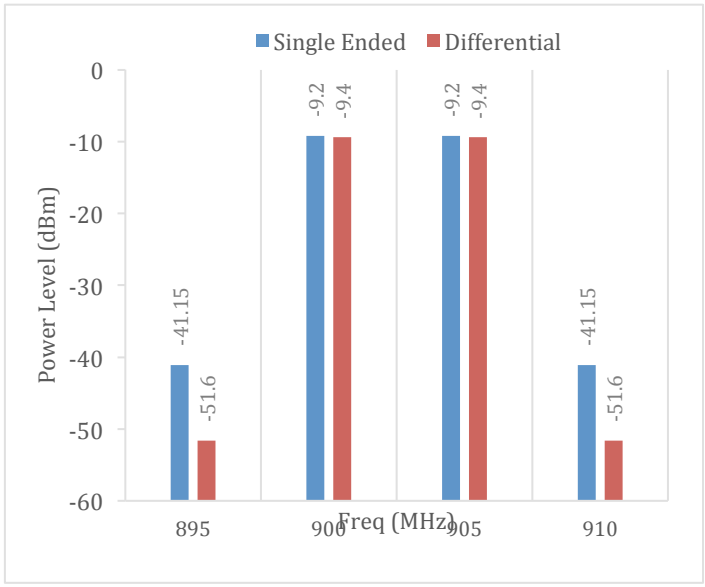

(b)

Figure 6.2: (a) Single Ended and Differential Configurations for IMD test (b) Two-tone IM test of ZFL single ended and LMH differential amplifiers.

Another significant figure of merit for characterizing the IMD in nonlinear devices is the third order intercept point or IP3. IP3 is a fictitious point that is obtained when the extrapolated 1-dB/dB slope line of the output fundamental power intersects the extrapolated 3-dB/dB slope line of the IMD power [8]. In practical case both fundamental and third order IM product go under compression, but if the lines are extended for the idealized response, the hypothetical intersect point is then measured as IP3. It can be expressed either with respect to input power (IIP3) or with respect to output power (OIP3). The concept of IP3 is explained in Figure 6.3.

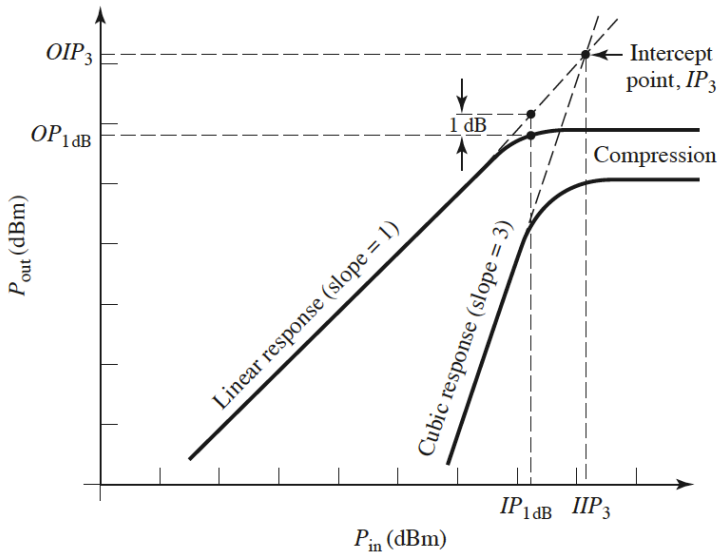

Figure 6.3: Third-order intercept diagram for a nonlinear component [9].

IMD3 and IP3 measurement tools are widely used by researchers to measure the linearity of RF amplifiers. The IP3 measurement results for both test amplifiers are shown in Figure 6.4, which illustrates that the IIP3 of the ZFL single ended amplifier is about 2dBm and the IIP3 of the differential amplifier is around 12dBm. So, the differential one is providing ~10dBm IIP3 improvement at similar power consumption. It should be noted here that this measurement is not with same differential amplifier with different output configurations. Rather, one is a true single ended amplifier and another is a differential amplifier with single ended output configurations. The response of the single ended amplifier was normalized to the fundamental of the differential one to plot on the same graph for IIP3 measurements. From these measurement results it is evident that differential amplifier demonstrates higher linearity compared to the single ended amplifier.

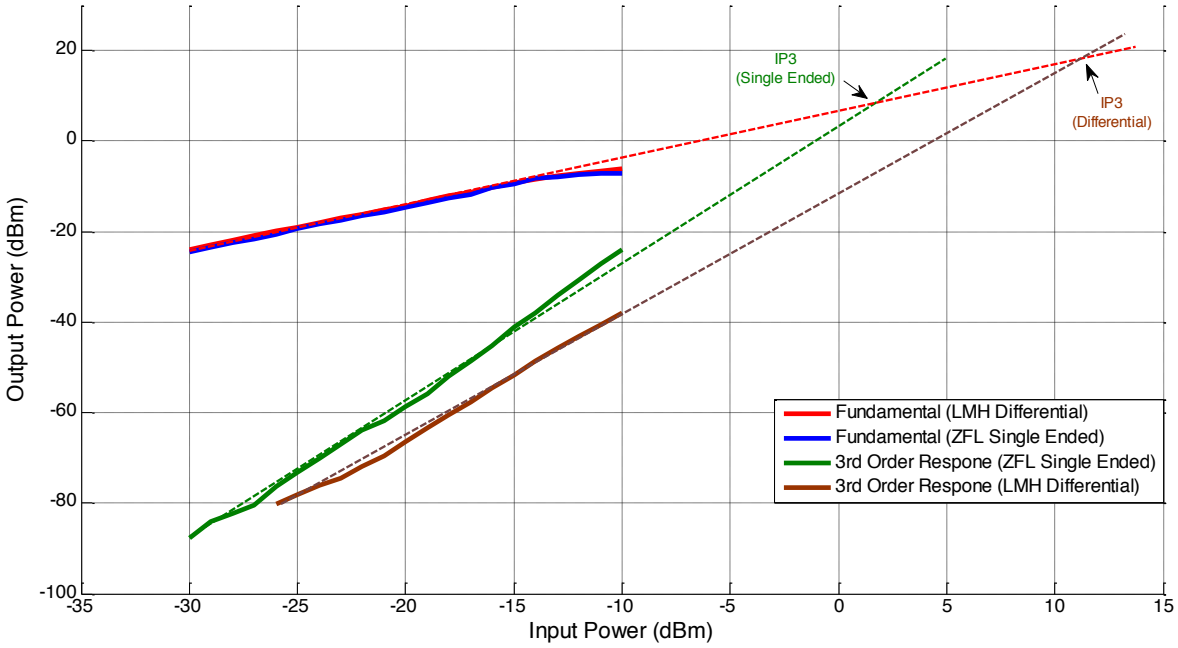

Figure 6.4: IP3 measurement of single ended and differential amplifier (measured frequency is around 900 MHz)

6.2.2 Adjacent Channel Leakage Ratio (ACLR)

With the increasing expansion of digital economy, the second generation cellular technology which supports voice call, SMS, and a slower data rate can no longer satisfy mobile users' demand. Users these days want access to high speed data, video, images and other multimedia information in a single portable unit. To satisfy these demands the third and fourth generation

communications technology have been developed, which use digital modulated signals. At present, the Wideband Code Division Multiple Access (W-CDMA), Long Term Evolution (LTE) and Evolved Universal Terrestrial Radio Access (E-UTRA) or Advanced LTE are the most commonly used 3G and 4G communication networks. These technologies need to satisfy stringent performance requirements as large dynamic range, low noise, high sensitivity and particularly high linearity [10]. When the linearity behaviour of an amplifier has to be evaluated, the two-tone third order intercept point (IP3) is usually used as a standard. But as the modulation becomes more complex, the standard two-tone distortion measurement does not really capture the complete distortion characters of a device. Therefore, the transmission standard requires more accurate analysis of nonlinear effects on complex modulation techniques such as Adjacent Channel Leakage Ratio (ACLR). ACLR is usually defined as the ratio of the average power in the adjacent frequency channel to the average power in the transmitted frequency channel as shown in equation (6.1) [11]. ACPR gives the indication on how a signal may interfere with a neighbouring channel in a wideband communication application. It characterizes the spectral re-growth of the modulated signal caused mainly by non-linearity.

$$ACLR = 10\,log_{10}\left(\frac{power_{adj\_channel}}{power_{main\_channel}}\right) \tag{6.1}$$

ACLR measurements are done in the relative power at ± 5 MHz and ± 10 MHz frequency offsets with a reference channel bandwidth. These different frequency offsets specify the distance from the centre frequency of the main channel to the centre frequency of the neighbouring channels. The measurement with ± 5 MHz frequency offset are referred to as the upper and lower adjacent channels and with ± 10 MHz offsets are referred to as the upper and lower alternate channels [12]. Different criteria exist for adjacent channel power measurements depending on the technology standard to be measured. For example, (W-CDMA) wireless standard requires transmissions to fit within a 3.84 MHz measurement bandwidth for 5MHz offset bandwidth, but 4G Advanced LTE (E-UTRA) requires to occupy different measurement bandwidth in its six different channel bandwidth ranging from ±1.4 MHz to ±20 MHz, specifically 4.515 MHz for a 5 MHz offset [13]. Table 6.1 below represents the measurement carrier bandwidth of E-UTRA for all six LTE channel bandwidth.

Table 6.1: Channel measurement bandwidth of E-UTRA for different LTE channels.

Channel BW/Offset	1.4 MHz	3 MHz	5 MHz	10 MHz	15 MHz	20 MHz
Channel Meas. BW	1.08 MHz	2.7 MHz	4.5 MHz	9.0 MHz	13.5 MHz	18 MHz

The ACLR concept is illustrated in the Figure 6.5 below which is a response from LMH6881 amplifier with an E-UTRA (4G) digital modulated signal generated from Agilent M9381A PXIe Vector Signal Generator.

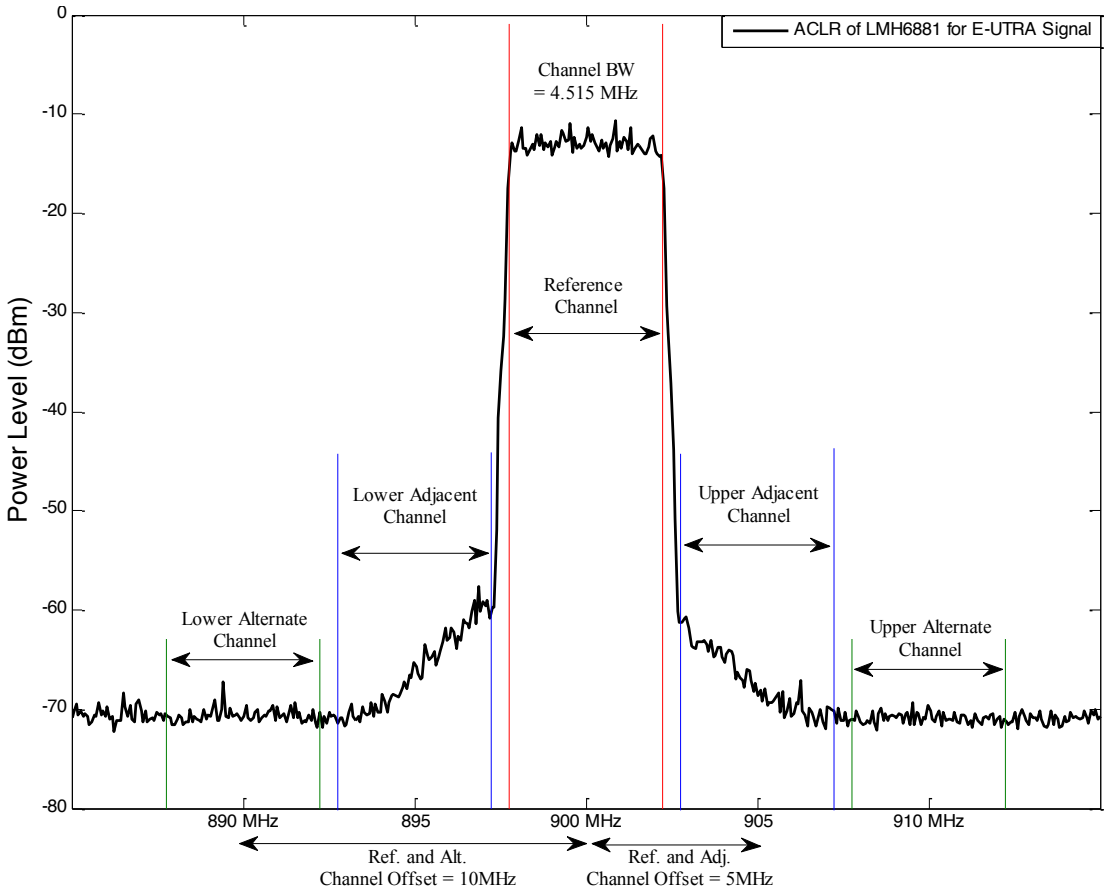

Figure 6.5: Illustration of Adjacent Channel Leakage Ratio

Various ACLR requirements are set for different devices used in base station equipment and user equipment (UE). The acceptance levels are also diverse for different signal standards. For example, the ACLR of W-CDMA should not exceed -33dB and -43dB at ±5 MHz and ±10 MHz respectively [12]. But these requirements will not be scrutinised in depth in this thesis because the main intention is to compare the level of ACLR of a same LHM6881

amplifier in similar operating condition with different output interfaces. The ACLR measurement should be carried out close to the maximum output capability of the amplifier. Therefore, all measurements were carried out at a power level before the amplifier goes into its saturation region. The ACLR in this region are usually very high so even a small improvement with fully differential output interface is crucial.

To measure the level of ACLR, the LMH6881 amplifier with single ended output was fed with a 4G Advanced LTE (E-UTRA) test signal from the vector signal generator. The measurement was carried out considering the centre frequency at 900 MHz. As (E-UTRA) has a channel measurement bandwidth of 4.5 MHz for 5 MHz offset, the main channel and adjacent channels were allocated as shown in Table 6.2.

Table 6.2: Allocation of main and adjacent channels for ACLR measurement with 4.5 MHz channel measurement bandwidth and 5 MHz offset.

Channel Name	Channel Measurement BW	Frequency Range
Main Channel	(900±2.25) MHZ	897.75 MHz to 902.25 MHz
Lower Adjacent Channel	(895±2.25) MHz	892.75 MHz to 897.25 MHz
Upper Adjacent Channel	(905±2.25) MHz	902.75 MHz to 907.25 MHz
Lower Alternate Channel	(890±2.25) MHz	887.75 MHz to 892.25 MHz
Upper Alternate Channel	(910±2.25) MHz	907.75 MHz to 912.25 MHz

This measurement and calculation setup will be maintained in all of the ACLR measurements presented in this thesis. Figure 6.6 shows the modulation spectrum of LMH6881 amplifier and Table 6.3 represents the calculated ACLR values. It can be seen that at lower input power level, the ACLR is showing quite good performance. As the amplifier moves towards the saturation level, power leakage increases. Here, the ACLR of only one amplifier is presented. Comparisons of both configurations in different measurement conditions will be shown in following sections and chapter.

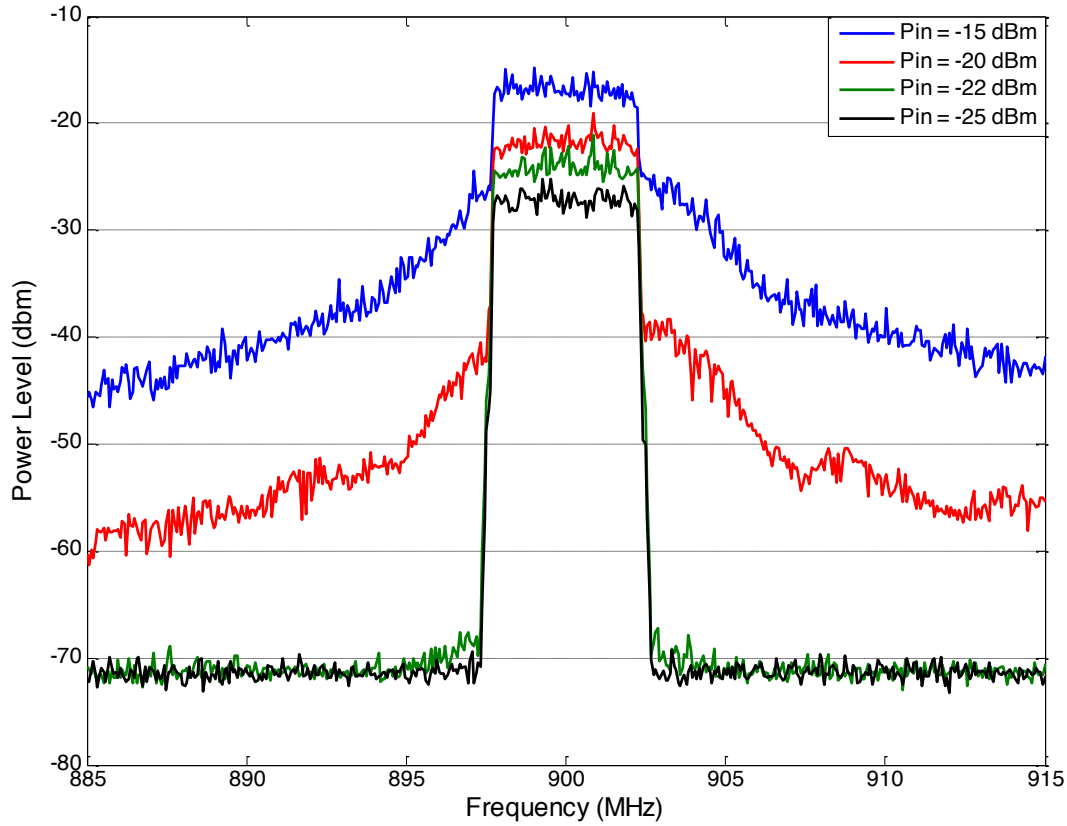

Figure 6.6: Spectral plot of LMH6881 amplifier for different input power level.

Table 6.3: Measured and calculated ACLR for LMH6881 differential amplifier.

Channels	-25dBm	-22dBm	-20dBm	-15dBm
Main Channel	-21.6	-18.7	-16.1	-11.4
Lower Adjacent Channel (dBm)	-71.2	-68.9	-43.7	-27.4
Upper Adjacent Channel (dBm)	-71.4	-69.9	-40.1	-25.6
Lower Alternate Channel (dBm)	-71.4	-71.6	-50.1	-35.1
Upper Alternate Channel (dBm)	-71.5	-71.5	-48.2	-33.9
ACLR (5 MHz Offset) (dBc)	**-49.7**	**-50.7**	**-25.8**	**-15.1**
ACLR (10 MHz Offset) (dBc)	-49.8	-52.8	-33.1	-23.1

6.3 Effects of Changing Load Impedance of Differential Amplifier

A power amplifier generally forms the final stage of an RF front-end. It demands stringent requirements compared to those of small signal low profile amplifiers. Power amplifiers must deliver a considerable amount of power while avoiding distortion products in the output signal at the same time [14]. To obtain the maximum power from a BJT or FET, the input and output impedances of the device should be conjugate matched, which means the resistive parts must be the same and the imaginary parts must be of same magnitude with opposite polarity [15]. Similarly, matching is also needed to efficiently drive an antenna by the amplifier.

The purpose of the impedance matching network is to convert the load impedance into the impedance required to produce the desired output power at a specified voltage and operating frequency [16]. Typically the conjugate matching does not really produce the possible maximum output. Instead, the load is designed such that the amplifier has the correct voltage and current to deliver the required power, which is often the maximum power [17]. To illustrate this concept, a generator with an internal resistance R_S feeding a resistive load is shown in Figure 6.7. This internal resistance tends to dissipate some of the power as heat when a load R_L is connected to its output terminals. So the full power fed into the amplifier can't be drawn out of it as some power is wasted in R_S.

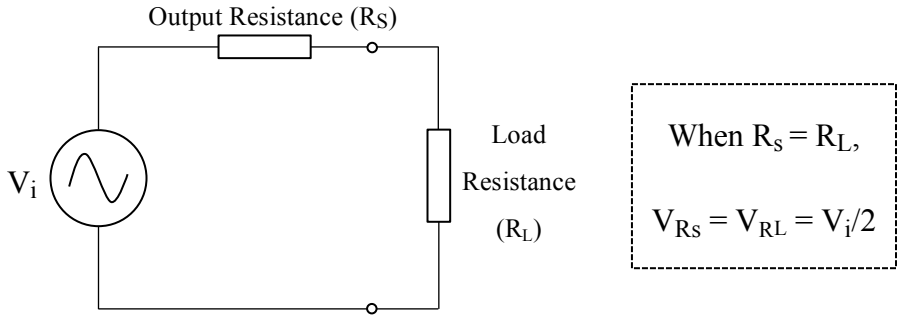

Figure 6.7: A generator with internal resistance R_S and load resistance R_L.

The amount of power in the load reaches a peak when the load resistance matches the output resistance. But at the same time the actual power being dissipated in the amplifiers internal resistance is identical to the power reaching the load. That means only half of the power produced by the generator is delivered to the load (the other half is lost in R_S) for a transmission efficiency of 50%. This efficiency can only be improved by making R_S as small as possible [9]. For similar reason in terms of voltage transfer, R_S and R_L acts as a voltage divider across the generators so that only half of the output voltage appears across the load, causing a 6dB loss. It is well known that if an output voltage is a sinusoid with the peak voltage value V_{CC}, and a load resistance R_L, the load power is determined as [14,18],

$$P = \frac{{V_{CC}}^2}{2R_L} \tag{6.2}$$

It can be seen from the equation that the power increases as the load resistance R_L decreases. The load impedance R_L is often considered as 50Ω because of the conventional load or coaxial cable impedance being 50Ω. So it would be investigated whether we can get higher power by changing that R_L value to the smallest amount possible. It has already been stated in this thesis that the conventional 50Ω approach for all kind of devices may not be ideal, especially when using differential amplifier. Therefore, the effect of changing load impedance of LMH6881 differential amplifier has been explored. The output resistors were changed to provide differential output of 0Ω, 100Ω (2*50Ω) and 300Ω (2*150Ω). These values have been chosen to provide different impedances for different antennas used in subsequent sections. The frequency response, power sweep and ACLR were measured for all these different configurations. However, this was not an ideal measurement technique as the amplifier with different output impedances were measured using conventional 50Ω terminated equipment. Still those were investigated ignoring that small loss caused by unmatched impedance. In later part of this chapter, these configurations will be examined with antenna with different output impedances and different load impedances.

6.3.1 Frequency Response for Different Output Impedance

The gain (S_{21}) and return loss (S_{11}) of LMH6881 amplifier was measured with 3 configurations having different output impedances. It can be observed from Figure 6.8 that arrangement with the lowest value of resistors (0Ω) has the highest gain, as expected according to theory [18]. In this configuration the circuit output only has the internal RFIC resistance of 0.4Ω. When the output resistors (R6 and R7 in Figure 5.11) were replaced by higher values of 50Ω and then 100Ω resistors, the gain decreased. This proves that by making the output impedance as small as possible, higher gain can be realised. The increment of gain is not equal throughout the measured bandwidth. It maintains almost stable increment till around 1GHz and after that it has uneven changes in gain. This might be because of the balun effects after 1GHz as this balun is rated to provide better performance until 1GHz.

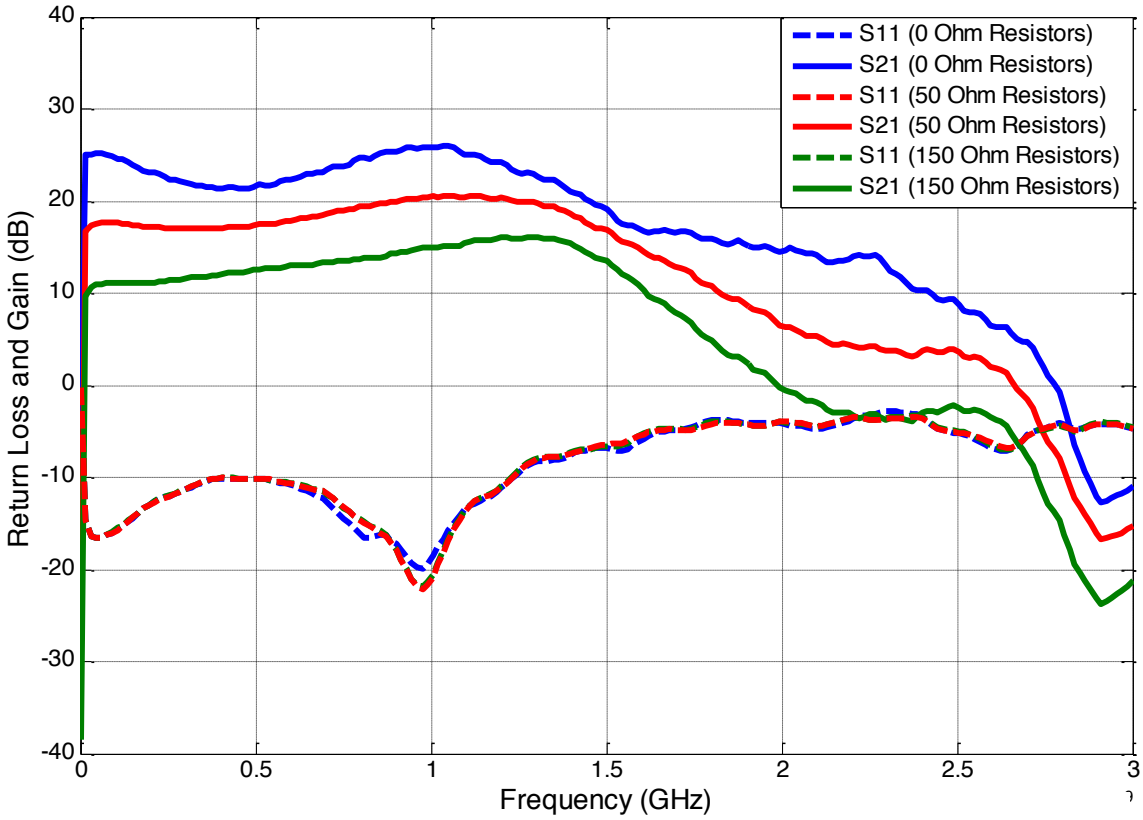

Figure 6.8: Return Loss (S_{11}) and Gain (S_{21}) of the LMH6881 single ended output configuration with different resistor values at the output.

6.3.2 Power Sweep for Different Output Impedance

The Pin vs Pout measurements were carried out with different output resistances at 900 MHz. The measurement approach has been shown in a simplified circuit level model in Figure 6.9 to define the setup more clearly. Here the internal resistance of LMH6881 differential amplifier R_i is fixed as 0.4Ω, which is very low and negligible. The load resistance RL is also fixed to 50Ω. The output resistance R_S was changed with 0Ω, 50Ω and 150Ω resistors. The change in power according to Ohm's Law ($P = V^2/R$) for these different resistors is illustrated in Table 6.4.

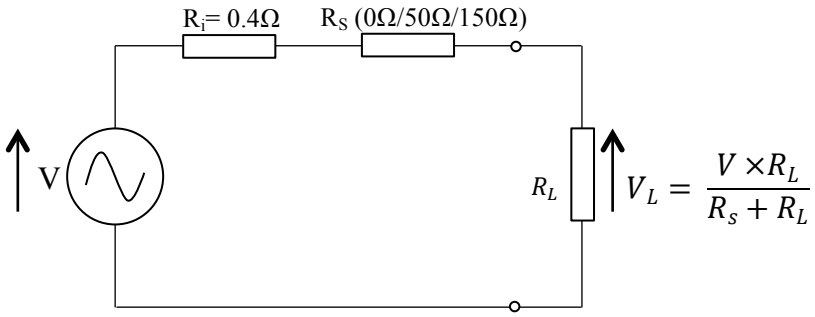

Figure 6.9: Circuit level model of LMH6881 with different output resistances.

Table 6.4: Change of load voltage (V_L) and power (P) for different output resistance.

$R_s\ (\Omega)$	$R_L(\Omega)$	$V_L = \frac{V \times R_L}{R_s + R_L}$	$P = \frac{{V_L}^2}{R_L}$
50	50	$\frac{V}{2}$	$\frac{V^2}{4R_L}$
150	50	$\frac{V}{4}$	$\frac{V^2}{16R_L}$
0 + 0.4	50	0.992V = ~V	$\frac{V^2}{R_L}$

Now if we take R_S = 50Ω as the standard we get

$$P_0 = 4P_{50} = +6dB$$

$$P_{150} = ¼\ P_{50} = -6dB$$

The real measurement result is illustrated in Figure 6.10. The simple solid line shows the response of the amplifier, which is matched to the 50Ω load impedance of coaxial cable. The solid line with square boxes and circles represent the responses with very low impedance and high impedance, respectively. A significant improvement in OP_{1dB}, hence, linearity can be observed for smaller output impedance which is 0.4 Ω in this particular instance. It can also be seen that the measured output power is about 6dBm more and less for 0Ω and 150Ω resistors respectively, which is coordinated with the theory explained above. Though the output resistance wasn't matched to the load resistance in the case of 0Ω resistors, this still gives us an important indication. We can expect substantial improvement in linearity and power by using same differential amplifier with very low output impedance and by matching that with a similar low impedance antenna. But again, this is not an easy task. As amplifier goes into saturation, the reactive effects get stronger for the impedance with very low resistive part and as a result the 6dB power difference is not maintained after the saturation point. If it is connected to an amplifier with high reactance the effects can be more significant. This active antenna approach for different impedance value will also be demonstrated in a later section of this chapter.

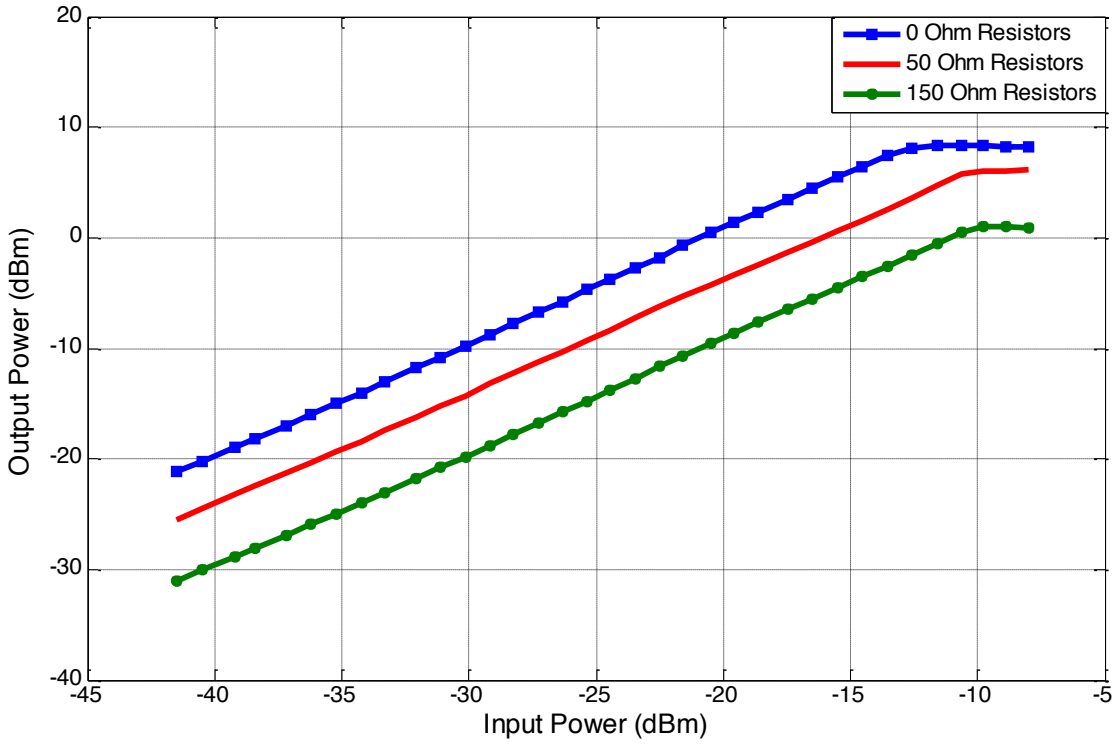

Figure 6.10: Pin vs Pout measurement of LMH6881 differential amplifier with different output impedance.

6.3.3 ACLR for Different Output Impedance

The generated spectral plot of LMH6881 for different resistor values at the output is shown in Figure 6.11 and the ACLR results obtained from this is presented in Table 6.5. It can be seen that unlike the gain and power sweep measurements discussed above, changing output impedance hasn't really caused any significant difference in ACLR. Though the power level of main channel has increased for smaller impedance but the ACLR ratio is almost similar. This indicates that for generated advanced LTE signal, lower output impedance increases the main channel power level as well as the IMD products in adjacent channels. The measurement was carried out at various input power level and the results for only -20dB input power are presented here.

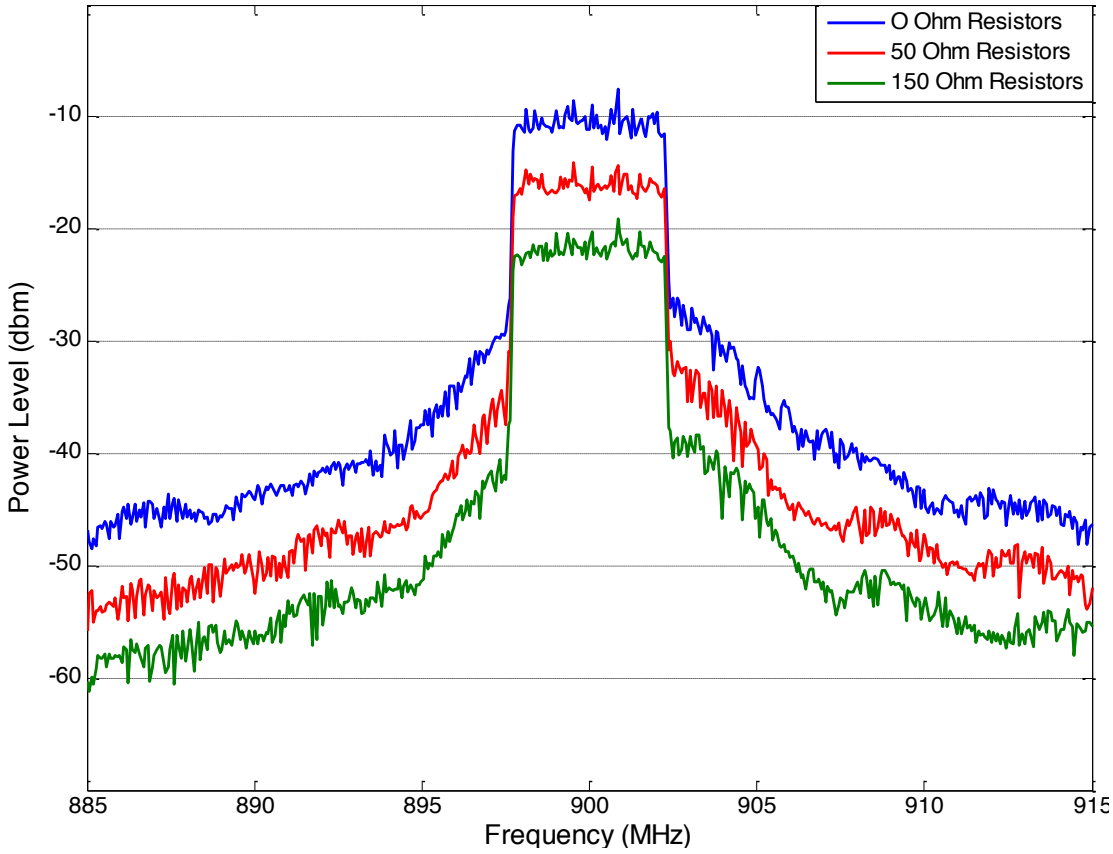

Figure 6.11: Spectral plot of LMH6881 differential amplifier with different output impedance.

Table 6.5: ACLR measurement of LMH6881 amplifier with different output impedance.

Channels	0 Ω	50 Ω	150 Ω
Main Channel	-10.6	-16.1	-21.9
Lower Adjacent Channel (dBm)	-37.6	-43.7	-49.2
Upper Adjacent Channel (dBm)	-34.7	-40.1	-45.3
Lower Alternate Channel (dBm)	-43.9	-50.1	-55.6
Upper Alternate Channel (dBm)	-43.1	-48.2	-53.6
ACLR (5 MHz Offset) (dBc)	**-25.6**	**-25.8**	**-25.4**
ACLR (10 MHz Offset) (dBc)	-32.9	-32.9	-32.7

6.4 Radiated Power Measurement of Active Antennas

Feeding a balanced antenna with a balanced amplifier can imply numerous benefits for 4G mobile applications, which has already been discussed in Chapter 2. Despite these benefits, this area has not been thoroughly explored, mainly due to the eccentricity of the approach and complex measurement techniques. Researchers have tried several approaches, which have been) reported in Chapter 2, but a balanced transmit antenna fed by the true differential amplifier hasn't been demonstrated yet. In this section, the benefits of differential feeding technique are presented. The radiated power of the LMH6881 with balun was measured and compared with the bench test results. The same amplifier was then investigated using a true balanced feed arrangement with no balun at the output terminal. It is shown experimentally that this technique provides higher power & efficiency using the same component and power supply. Therefore, there is motivation to apply this balanced technique and develop antennas for future mobile devices applications.

The antennas used for this experiment are the simplest form of wire monopole and dipole operating in the frequency range of 855MHz-945MHz. The PCB versions of these antennas, as shown in Chapter 3, are also used for same experiment. As they provided almost identical

results, measurement results with printed antennas will be presented here. It is well known that the impedance of a monopole (~37Ω) is half that of the corresponding dipole (~73Ω) which conveniently provides matching to the corresponding amplifier (the differential amplifier also having double the impedance). The λ/4 printed monopole was mounted on a metal ground plane, which is a few wavelengths in size around the monopole to keep the impedance of the antenna minimally affected. Two identical conductive elements were selected to construct the dipole form. These simplest forms were chosen to keep the measurement simple and make sure nothing else is affecting the measurement.

Following this, the radiated test was done inside the anechoic chamber. The minimum distance between the two antennas were calculated by Fraunhofer and Rayleigh formula, where the minimum distance, $R > 2D^2/\lambda$, where D is the largest dimension of either antenna [19]. In this case, D is the height of the Rx dual polarized horn antenna (ets-3164-03). The amplifier with single ended output was connected to the monopole antenna using a 50Ω coaxial cable whilst dipole was soldered directly to the differential output terminals. These active antennas were placed 2.5m away from the receive horn antenna inside the chamber, which is connected to a spectrum analyzer to observe the output signal. A signal generator, generating 900 MHz signal, was connected to the input port of the amplifier. Figure 6.12 shows the measurement setup of both active antennas.

Figure 6.12: Measurement setup of conventionally fed monopole antenna (left) and differentially fed dipole antenna (right)

A cross-polar radiation pattern was obtained for both antennas to compare the radiated gain towards the direction of the receive antenna and to adjust the effective antenna gain to the actual output power from the amplifier. It is difficult to make direct comparison for balanced and unbalanced antennas. Although unbalanced monopole and balanced dipole antennas are 'complementary', but in practice patterns can be significantly different. In case of monopole with a ground plane, the energy tends to radiate into one direction so we get 3dB more peak power compared to same dipole configuration. Figure 4 shows the radiation pattern of the monopole and dipole and the direction of AUT towards the receive antenna during radiated power measurement setup (as Figure 6.12). It can be observed that the dipole radiated 1.4dB more gain during the P_{in} vs P_{out} measurement (at 90 degree on Figure 6.13), which must be taken into consideration while calculating the actual radiated power. The dipole radiation pattern is not ideal as it wasn't measured in a balanced way and due to this the cable is slightly affecting the radiation pattern.

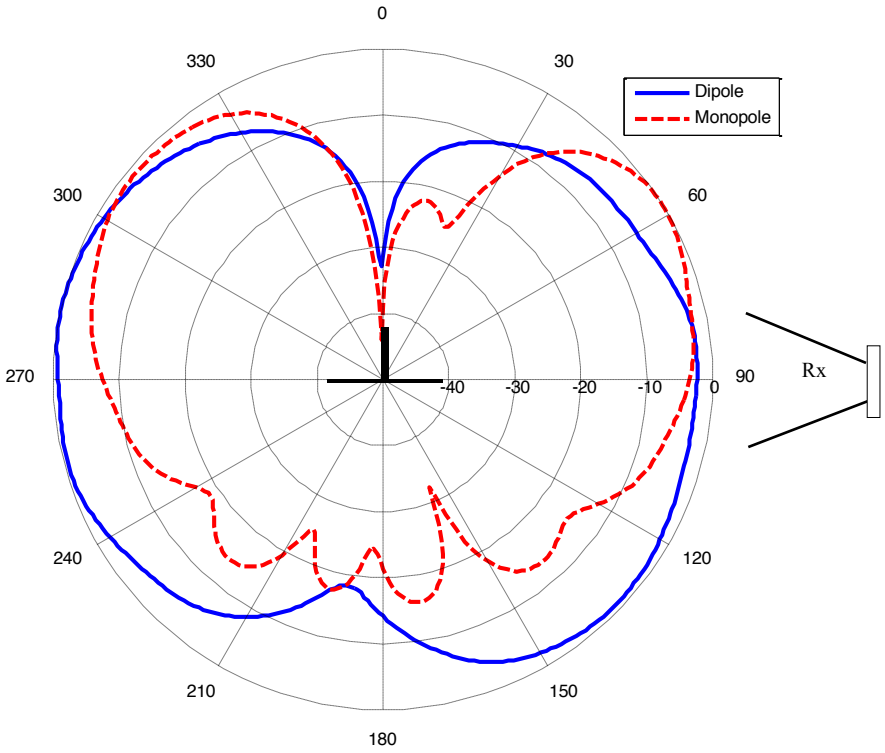

Figure 6.13: Radiation pattern of the simple monopole and dipole antenna and antenna direction during P_{in} vs P_{out} measurement in principle plane.

To measure the P_{in} vs P_{out}, the power level of the input signal was varied from -40dBm to the saturation of the amplifier. Figure 6.14 shows the results of the bench and radiated power test.

The actual radiated output power was calculated by adding the free space path loss (FSPL) and adjusting the antenna gain and cable loss, according to Friis transmission equation [19,20]. The received power level was estimated using this Friis formula as below:

$$P_r = G_t G_r \left(\frac{\lambda}{4\pi R}\right)^2 P_t \tag{6.3}$$

Where,

Pr and *Pt* are the received to transmitted power respectively,

Gr and *Gt* are the respective power gains of the two antennas,

R is the distance between two antennas (m) and

λ is the wavelength.

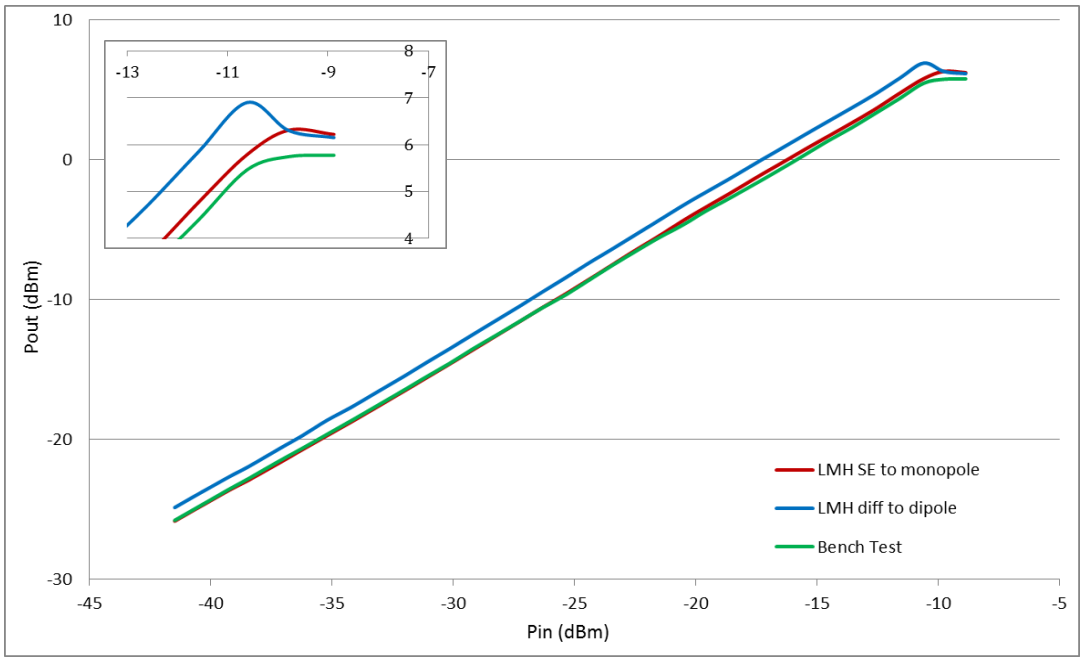

Figure 6.14: P_{in} vs P_{out} results of the conventionally fed and differentially fed active antennas.

Good agreement is observed between the bench test result and the radiated one for the amplifier with single ended output and this verifies the accuracy of this measurement method. More than 1dB higher gain throughout the entire range and higher output power from the differentially fed active antenna can be realized due to eliminating the balun loss. A dip can

be observed near the saturation region of the balanced active antenna, which might have been caused by the impedance change as it goes into saturation.

6.5 AIA Radiated Power Measurement for Different Antenna and Impedance

The radiated power test of LMH6881 differential amplifier for different output impedance was carried out inside the anechoic chamber. For each impedance varieties, one antenna will be a matched load having similar impedance. The idea is to investigate the received output power with standard 50Ω impedance (100Ω differential), then with almost 0Ω and then with 300Ω differential output impedance feeding a standard half wavelength dipole antenna, then a very low impedance loop antenna and a folded dipole antenna with higher impedance of almost 300Ω. But the small loop antenna possesses a very low resistance and a high reactance resulting in very low efficiency. They are therefore poor radiators and normally are used only in the receiving mode [21].

To provide a 300Ω differential output impedance, a folded dipole antenna was designed and fabricated. The folded dipole antenna consists of a standard half wavelength dipole with an added transmission line connecting the two ends together to make a complete loop. The feed-point impedance is four times as large as for an unfolded dipole of the same length [21]. These antennas are usually fed by using a 300 Ω twin-lead transmission line. The two active antennas used in this radiated test are shown in Figure 6.15.

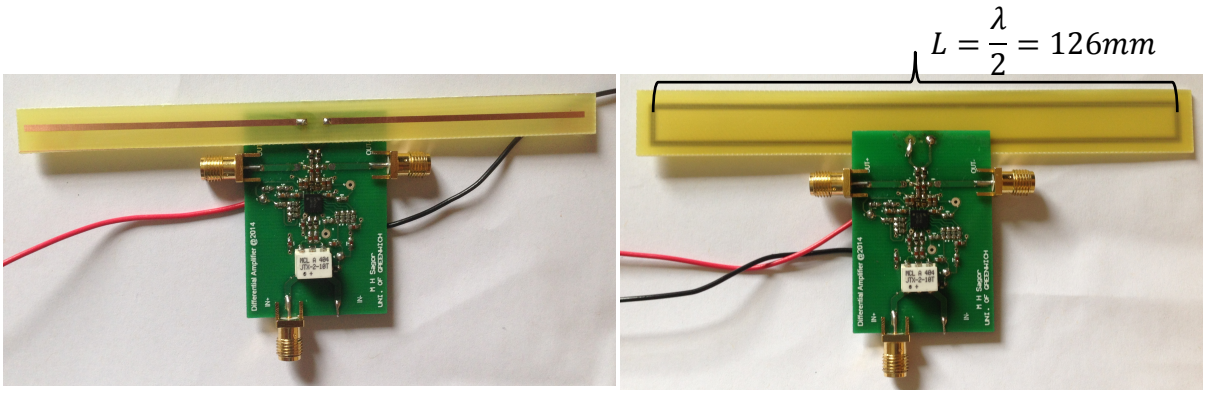

Figure 6.15: AIA configurations of half wavelength dipole and folded dipole

It has already been illustrated in bench tests (section 6.3.2) that amplifier with lower output impedance provides higher output power and greater linearity. But those measurements were

carried out using 50Ω coaxial cable. In this section, those measurements have been done using active antennas by radiated measurements. Besides verifying the bench test results, this experiment indicated that the amplifier delivers the maximum power and gain when the output impedance is matched to the load impedance, which is the input impedance of antennas for an active antenna. As we can see from Figure 6.16, curves with very low impedance have higher gain but as the output impedances and the load impedances are not matched, they are not stable near the saturation region. The LMH6881 differential amplifier feeding a standard dipole antenna provides higher gain with 100Ω differential output resistors compared to the folded dipole antenna with ~300Ω impedance. And the folded dipole antenna is performing best when fed by a differential amplifier with 300Ω differential output impedance. The outcome suggests that a differential amplifier with very low impedance feeding a matched low impedance antenna can deliver substantial improvement in output power and linearity. Attempts were taken to design a low impedance resonant loop antenna by compensating its high reactance by using lumped elements. But because of time constraints, it couldn't be investigated any further.

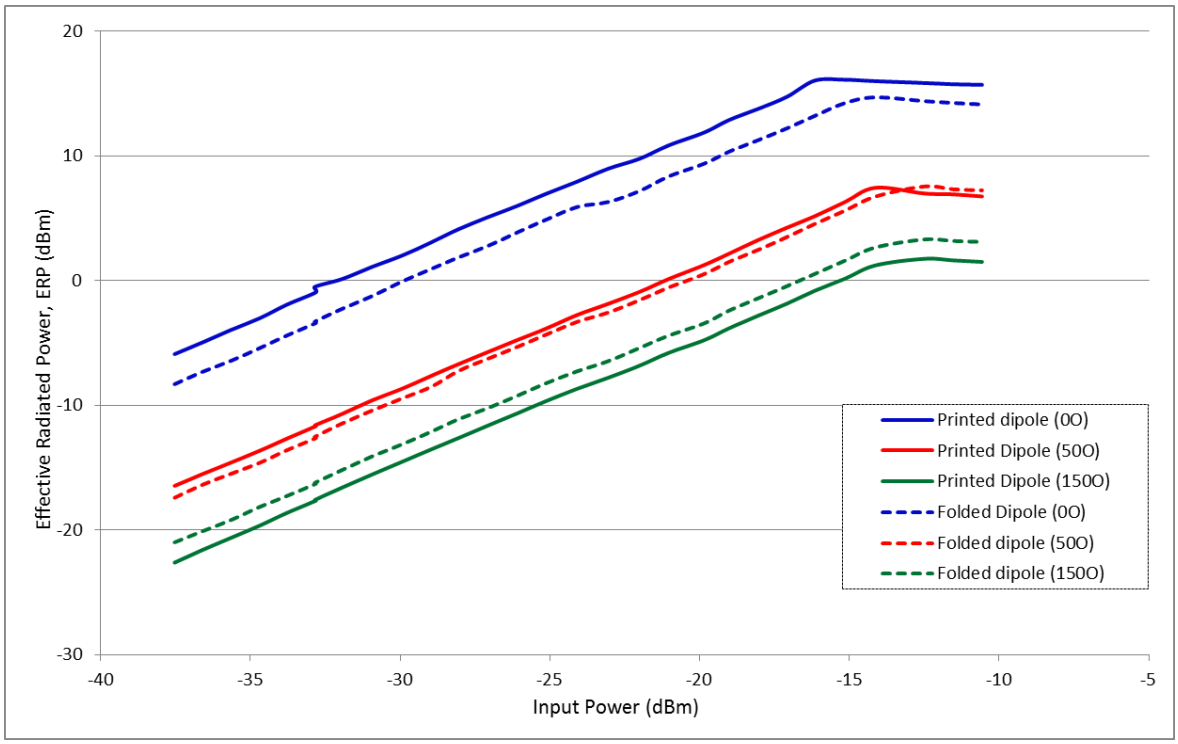

Figure 6.16: Radiated Pin vs ERP measurement of LMH6881 differential amplifier with different output impedance.

6.6 ACLR Comparison of Active Integrated Antennas

The radiated measurement for ACLR was carried out for active unbalanced/monopole antenna and differentially fed balanced/dipole antenna. The spectral plot of both active antennas for -15dBm and -18dBm is shown in Figure 6.17 and the ACLR results obtained from that is shown in Table 6.6. It can be observed that the differentially fed dipole has provided ~1.35dB higher ACLR compared to the unbalanced active antenna with simple monopole. It might not be a significant improvement but more than 1.3 dB increase in ACLR for the same device with different interface is worth reporting.

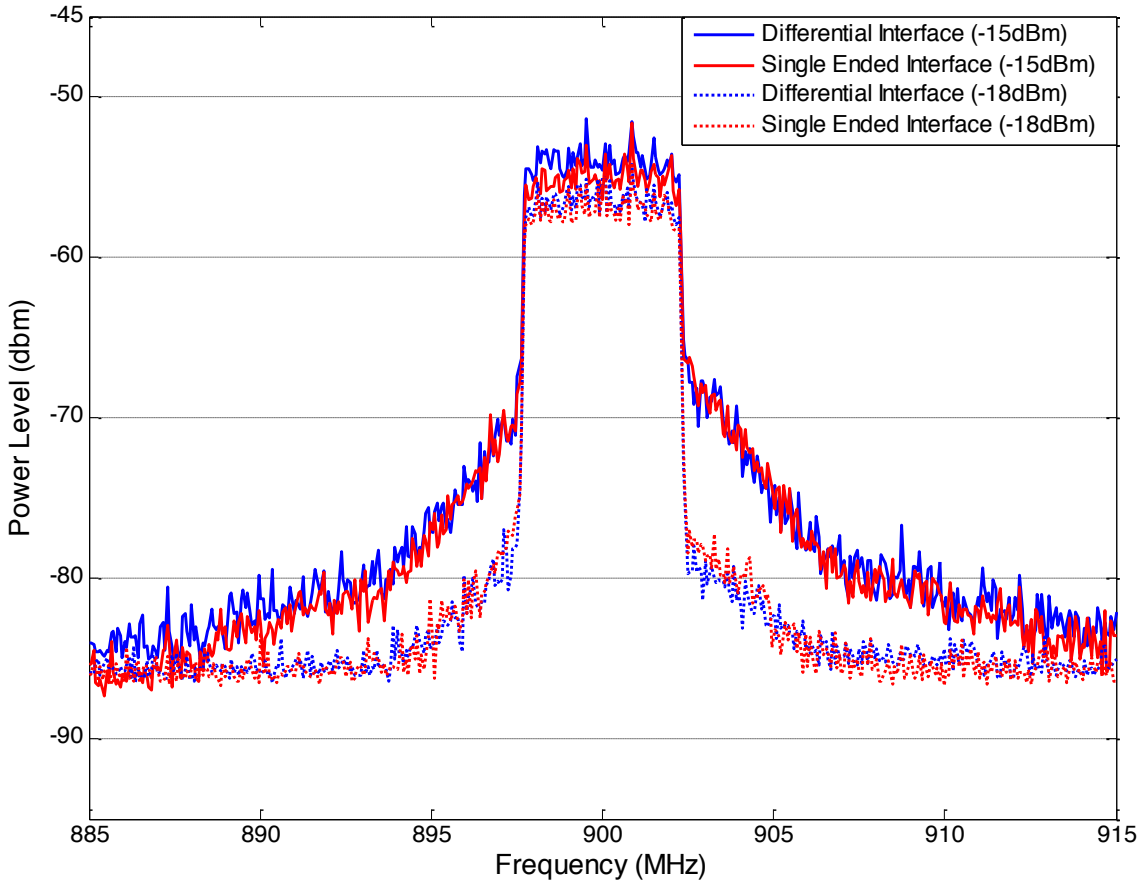

Figure 6.17: Spectral plot of monopole active antenna with single ended interface and dipole antenna with fully differential output interface.

Table 6.6: ACLR of AIA with single ended interface and differential output interface.

Channels	Single Ended -18dBm	Differential -18 dBm		Single Ended -15 dBm	Differential -15 dBm
Main Channel	-57.1	-56.3		-55.1	-53.5
Lower Adjacent Channel (dBm)	-83.1	-83.4		-77.1	-76.5
Upper Adjacent Channel (dBm)	-82.1	-82.6		-74.3	-74.3
Lower Alternate Channel (dBm)	-85.8	-85.5		-83.1	-81.6
Upper Alternate Channel (dBm)	-85.6	-85.1		-81.4	-80.3
ACLR (5 MHz Offset) (dBc)	**-25.5**	**-26.7**		**-20.6**	**-21.9**
ACLR (10 MHz Offset) (dBc)	-28.6	-28.0		-27.2	-27.4

6.7 Summary

A thorough analysis of the third order distortion behaviour of the nonlinear LMH6881 differential amplifier by investigating two-tone and multi-tone spectrum has been presented. The effect of different output impedance in the gain, linearity and distortion behaviour has been comprehensively investigated. Techniques to feed a balanced antenna by differential amplifier has been discussed and it has been demonstrated experimentally that higher gain and output power is achievable using the same RFIC and same power supply by interfacing balanced antenna with a differential RF amplifier. The antenna doesn't always need to be matched to 50Ω to be fed differentially. It has also been suggested that a substantial improvement in linearity can be realized by feeding a low impedance antenna with a differential amplifier comprising low output impedance. The most accepted test parameter for characterizing distortion of amplifier, the ACLR test, confirms that in addition to provide higher gain and linearity the balanced interface also keeps the distortion level lower. Moreover, by eliminating balun its physical size on small devices and costs can also be avoided. It is believed that this approach can become the key in developing more power efficient devices offering higher linearity and eventually greater battery life for modern wireless communication systems.

References

[1] Zhiwen Zhu; Xinping Huang; Caron, M.; Leung, H., "A Blind AM/PM Estimation Method for Power Amplifier Linearization," *Signal Processing Letters, IEEE* , vol.20, no.11, pp.1042,1045, Nov. 2013.

[2] Sangsu Jin; Byungjoon Park; Kyunghoon Moon; Myeongju Kwon; Bumman Kim, "Linearization of CMOS Cascode Power Amplifiers Through Adaptive Bias Control," *Microwave Theory and Techniques, IEEE Transactions on* , vol.61, no.12, pp.4534,4543, Dec. 2013.

[3] Ali, M.T.; Ruiheng Wu; Callaghan, P.; Rapajic, P., "Design of a highly linear high frequency amplifier using Volterra model," *Microwave, Antenna, Propagation, and EMC Technologies for Wireless Communications (MAPE), 2011 IEEE 4th International Symposium on* , vol., no., pp.355,358, 1-3 Nov. 2011.

[4] S. A. Maas (2003), *Nonlinear Microwave and RF Circuits*, 2nd ed., Norwood: Artech House, Chapter 1.

[5] F. M. Ghannouchi, M. S. Hashmi (2013), *Load-Pull Techniques with Applications to Power Amplifier Design*, New York: Springer, Chapter 1.

[6] Reinaldo Perez (1998), *Wireless Communications Design Handbook*, 3rd ed. San Diego, CA: Academic Press, Chapter 3.

[7] Mini-circuits, “Coaxial Amplifier” ZFL-2500+, Available at: http://www.minicircuits.com/pdfs/ZFL-2500+.pdf

[8] J. C. Pedro, N. B. Carvalho (2003), *Intermodulation Distortion in Microwave and Wireless Circuits*, Boston: Artech House microwave library, Chapter 2.

[9] David M. Pozar (2012), *Microwave Engineering*, 4th ed. New York: John Wiley & Sons, Inc., Chapter 2.

[10] J. I. Agbinya, M. C. Aguayo-Torres (2013), *4G Wireless Communication Networks*, Denmark: River Publishers, Chapter 1.

[11] L. Leyssenne, E. Kerhervé, Y. Deval (2011), *Reconfigurable RF Power Amplifiers on Silicon for Wireless Handsets*, Springer Science & Business Media, Chapter 1.

[12] H. Holma, A. Toskala (2010), *WCDMA for UMTS: HSPA Evolution and LTE*, 5th ed. UK: John Wiley & Sons, Chapter 20.

[13] Muray Rumney (Agilent Technologies) (2013), *LTE and the Evolution to 4G Wireless: Design and Measurement Challenges*, 2nd ed. UK: John Wiley & Sons, Ltd., Chapter 2.

[14] M.H. Rashid (2011), *Microelectronic Circuits*, 2nd ed. Stamford, USA: Cengage Learning Inc., Chapter 11.

[15] C. J. Kikkert (2013), *RF Electronics: Design and Simulation*, James Cook University Publishers, Australia, Chapter 9.

[16] Marian K. Kazimierczuk (2008), *RF Power Amplifiers*, UK: John Wiley & Sons, Inc., Chapter 5.

[17] John W.M. Rogers (2010), *Radio Frequency Integrated Circuit Design*, 2nd ed. Boston: Artech House Microwave Library, Chapter 11.

[18] Sedra, A.S.; Smith, K.C (2010), *Microelectronic Circuits*, 6th ed. Oxford: Oxford University Press, Chapter 14.

[19] Balanis. C (2005), *Antenna Theory: Analysis and Design*, 3rd ed. Hoboken, NJ: John Wiley & Sons, Inc., Chapter 2.

[20] John L. Volakis (2007), *Antenna Engineering Handbook*, 4th ed., Maidenhead: McGraw-Hill. Chapter 28.

[21] Balanis. C (2008). *Modern Antenna Handbook*. New Jersey: John Wiley & Sons, Inc.. Chapter 2.

Chapter 7

Measurement of Radiated Harmonic using Broadband Active Balanced Antenna

7.1 Introduction

The extensive implementation of latest digital wireless services has confronted researchers and designers with more restricted linearity specifications. In an ideal situation, an amplified output signal is completely linear or scaled replica of the input signal. But the unpleasant truth is that almost all physical devices exhibit some form of nonlinear behavior. Any nonlinearity in the amplitude and phase of an output signal must be minimized to preserve the shape and spectrum of the signal. To measure nonlinear effects on various signals, few methods have been devised such as harmonic distortion, gain compression, intermodulation distortion, adjacent channel interference and so on [1]. The 1dB compression point of LMH6881 has been investigated in Chapter 5 and the intermodulation distortion and ACLR have been explored in Chapter 6.

This chapter treats the characterization and measurement of harmonic distortion of the LMH6881 differential amplifier. The concentration will be on measuring the harmonic distortion of single ended amplifier, differential amplifier with single ended output and differential amplifier with fully differential output configurations. Measurement results for both bench tests and radiated harmonic tests will be assessed and finally results will be compared to recommend the best approach for lower level of harmonic distortions. The design requirement of balanced broadband antenna elements for radiated harmonic tests will also be presented.

7.2 Reduced Even Order Harmonic from Differential Amplifier

Distortion on a device can either alter the amplitude and phase or can create spurious frequencies that are not present in the main signal. Harmonic distortion is one form of the latter types of distortion. Harmonics are unwanted frequencies generated by system nonlinearities. They are multiples of the fundamental test frequency and generally the higher the multiple, the less the amplitude of the harmonic. The second and third harmonics possess the largest amplitude and hence these are the harmonics that are considered in the analysis of nonlinear distortion [2].

If a single-frequency sinusoid input $v_i = V_0 \cos \omega_0 t$ is applied to a general nonlinear network, the output response can be expressed as a Taylor series in terms of the input signal voltage as [3],

$$v_o = a_0 + a_1 V_0 cos\omega_0 t + a_2 {V_0}^2 cos^2\omega_0 t + a_3 {V_0}^3 cos^3\omega_0 t + \ldots\ldots\ldots\ldots$$
$$= \left(a_0 + \frac{1}{2} a_2 {V_0}^2\right) + \left(a_1 V_0 + \frac{3}{4} a_3 {V_0}^3\right) cos\omega_0 t + \frac{1}{2} a_2 {V_0}^2 cos2\omega_0 t + \frac{1}{4} a_3 {V_0}^3 cos3\omega_0 t + \cdots \quad (7.1)$$

Here, the DC Component = $\frac{1}{2} a_2$

Fundamental Component at $\omega_0 = a_1 V_0 + \frac{3}{4} a_3 {V_0}^3$

2nd Harmonic Component at $2\omega_0 = \frac{1}{2} a_2 {V_0}^2$

3rd Harmonic Component at $3\omega_0 = \frac{1}{4} a_3 {V_0}^3$

By taking Taylor Series expansion for both outputs (v_{o+} & v_{o-}) of a nonlinear differential device with respect to its inputs, we get the simplified differential output ($v_{od} = v_{o+} - v_{o-}$) equation as,

$$v_{od} = a_1 cos\omega_0 t + a_3 cos3\omega_0 t + a_5 cos5\omega_0 t + \cdots \quad (7.2)$$

This is because in the series expansion ofv_{o-}, the odd-order output terms retain their polarity, while the even-order terms are always positive. So, the input-output relationship is an odd

function of the input difference voltage v_{id} and thus only odd terms appears in the Taylor series expansion of v_{od} in terms of v_{id} [4]. This suggests that in an ideal fully differential circuit, the even order harmonics get cancelled. But this is not that perfect case for real-life circuits. However, differential topology significantly reduces even order harmonics and thus improves linearity performance. This will be verified experimentally in subsequent sections. Also radiated harmonics will be measured and compared using a single ended amplifier and same differential amplifier with single ended output and differential output interface. Radiated harmonic measurement comparison of this kind hasn't been reported in literature until now.

7.3 Choice of Antenna Element for Radiated Harmonic Measurements

One of the key factors to measure the radiated harmonic distortions is the requirement of a broadband antenna that has a stable radiation pattern at least from the fundamental frequency to the frequency of third harmonic. Also, balanced antenna is essential for the true differential feeding. To fulfil these demands, this measurement requires a broadband dipole/balanced antenna configuration. The antenna should have a minimum bandwidth of 900 MHz to 2.7 GHz in order to respond to at least the 3rd harmonic. A dipole-type element is sought to provide an omni-directional pattern in the x-z plane. Out of many kinds of dipole structures, the bow-tie element offers the desired omni-directionality but has a limited bandwidth [5,6]. On the other hand, a disc-pole element offers good matching but can suffer from pattern distortions at higher frequencies [7]. These two dipoles were designed and analyzed for 900MHz to investigate the theory. The structures are presented in Figure 7.1 and the simulated results are shown in Figure 7.2. It can be seen that the printed bow-tie antenna has an excellent omnidirectional pattern but possesses a very narrow bandwidth of about 100MHz. In contrast, the circular dipole is showing a very wide bandwidth but has very poor radiation pattern just after 2.7 GHz.

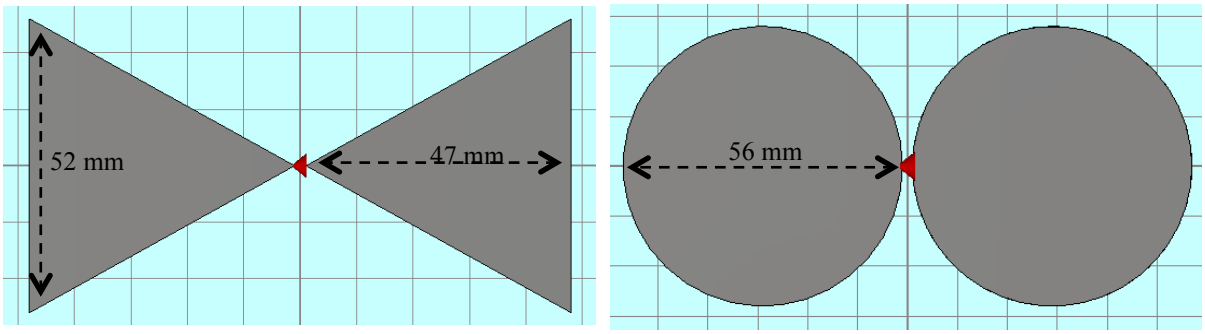

Figure 7.1: Bow-tie antenna (left) and circular dipole antenna (right) software model

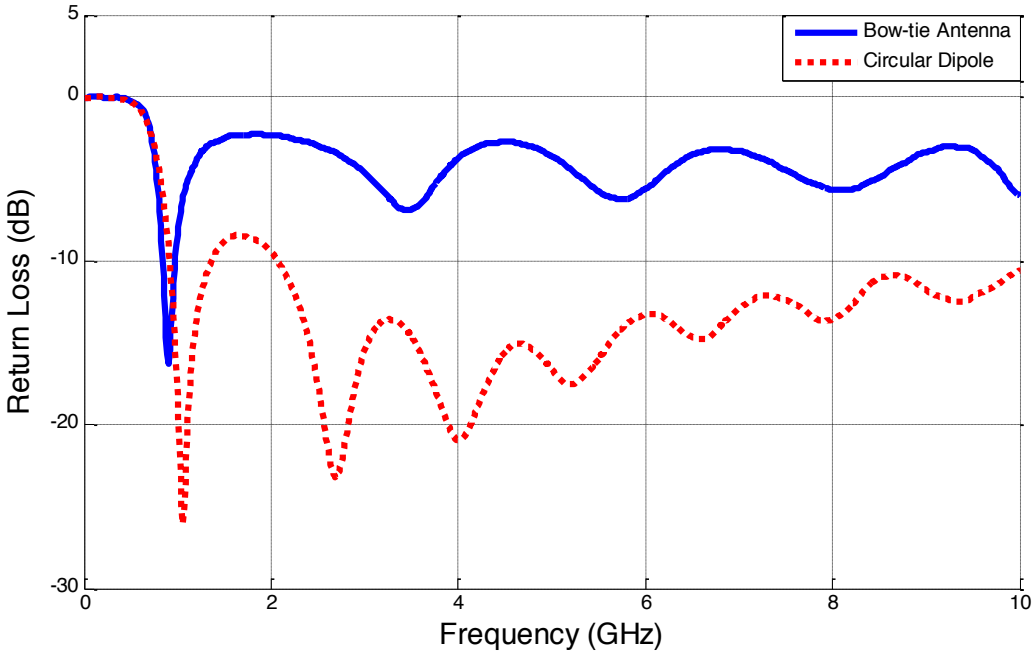

Return loss of both antennas

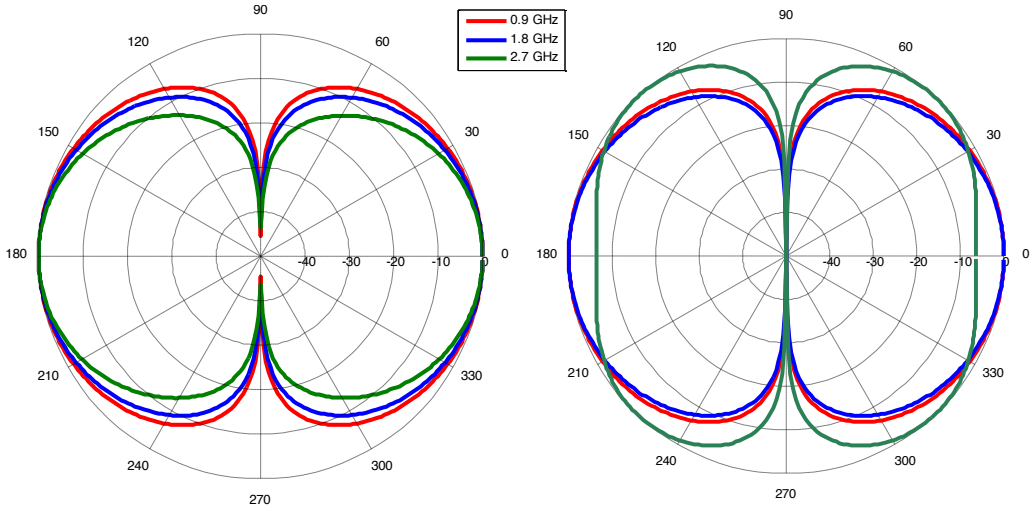

Bow-tie Antenna

Circular dipole Antenna

Figure 7.2: Simulated return loss and radiation pattern of bow-tie antenna and circular dipole antenna

Thus, for the radiated harmonic experiment a Modified Bow-Tie (MBT) element was considered as it offers a reasonable compromise between impedance and radiation pattern. Therefore, a compromised shape of both bow-tie antenna and disc dipole was designed. Each arm of the MBT dipole is half of an ellipse. The antenna was fabricated on 0.8mm thick FR4 substrate. The designed and fabricated model of the balanced MBT antenna is shown in Figure 7.3.

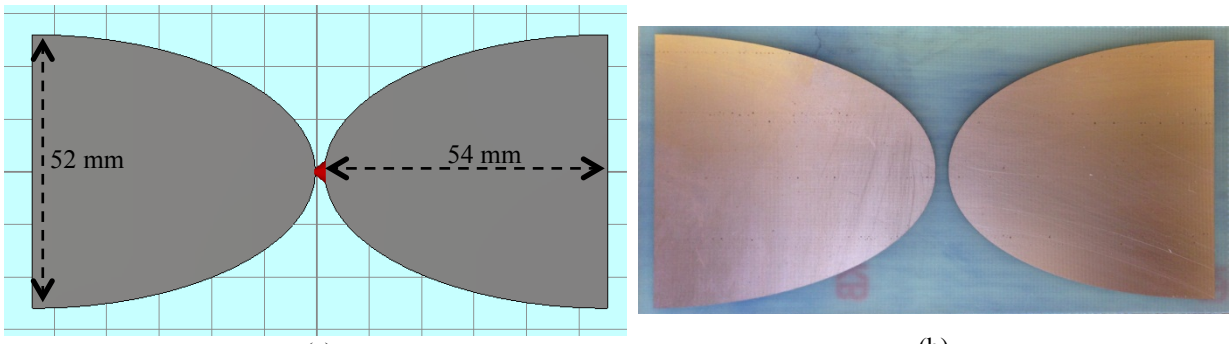

(a) (b)

Figure 7.3: (a) Design model of the MBT antenna and (b) Fabricated MBT antenna

A monopole counterpart was also designed by putting one arm of the dipole on a large metal ground plane. The simulated and measured return loss (S_{11}) and impedance on smith chart for both antennas are shown in Figure 7.4.

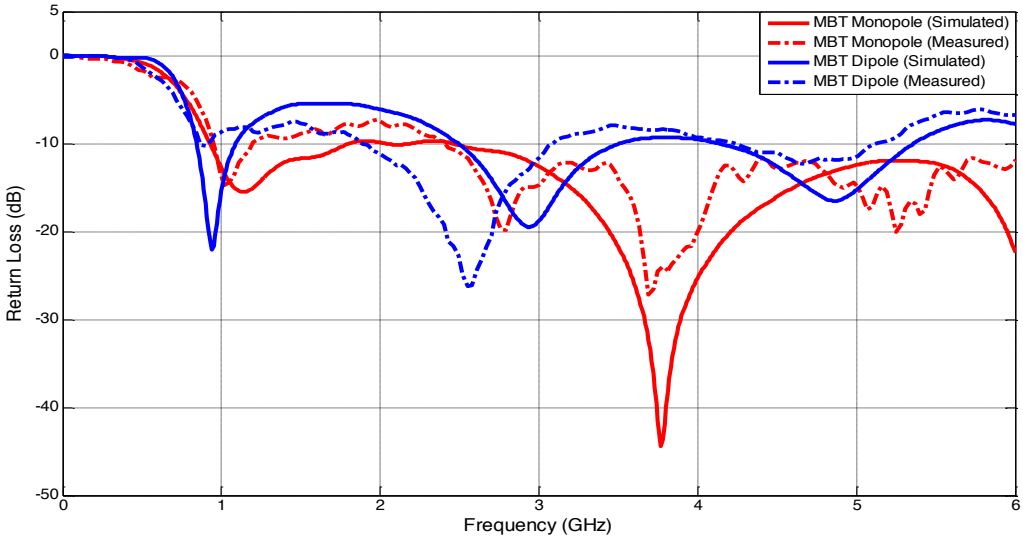

(a) Simulated and measured S11of MBT

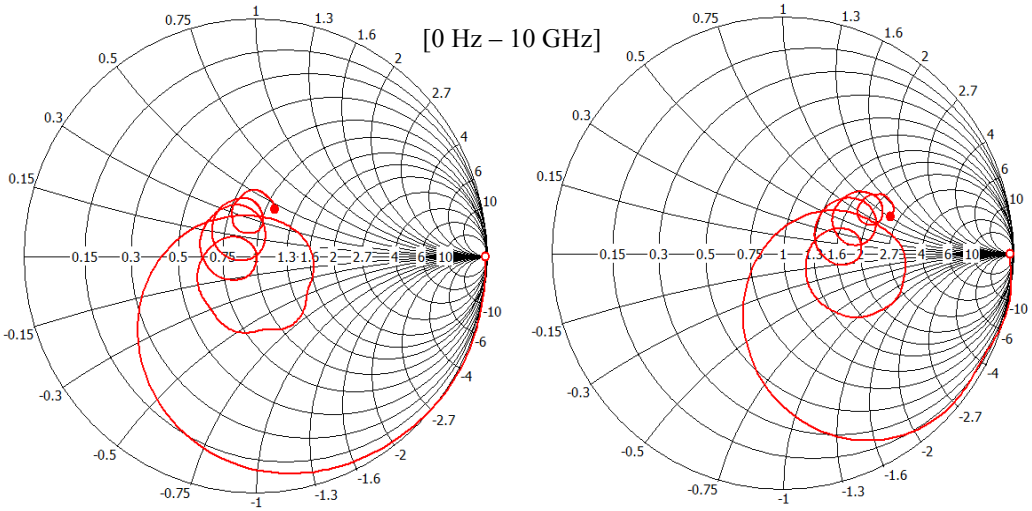

(a) Simulated impedance view of MBT monopole (left) and dipole (right)

Figure 7.4: Simulated and measured return loss and simulated smith chart of MBT antennas

It can be noticed that the MBT monopole and dipole antennas show an acceptable return loss from around 900 MHz up to high frequency. Smith charts show that the impedance of the MBT dipole is shifted around ~100Ω from ~50Ω impedance of the monopole MBT, as expected according to theory discussed in Section 3.5. The radiation pattern of MBT dipole is presented in Figure 7.5, which shows an omnidirectional pattern at 0.9GHz, 1.8GHz and 2.7GHz.

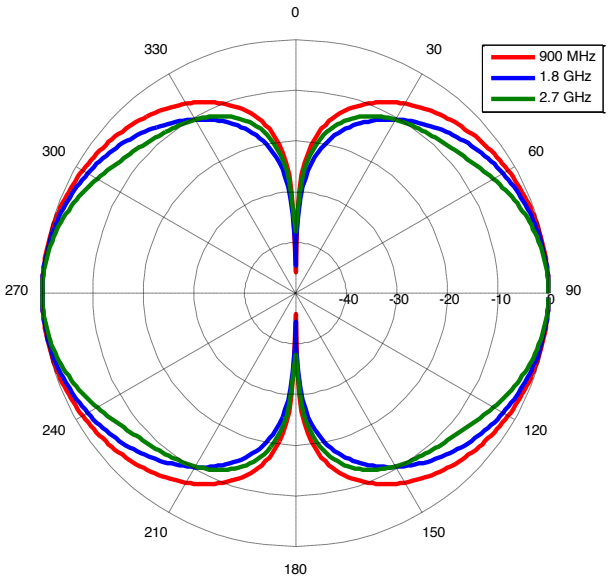

Figure 7.5: Simulated radiation pattern of MBT dipole antenna at different frequencies.

7.4 Harmonic Measurement for Single Ended and Differential Amplifiers

The single ended ZFL-2500+ amplifier and the LMH6881 differential amplifier with single ended output (similar to Figure 6.2 (a)) was measured in the bench using synthesizer and spectrum analyser. A 900 MHz signal was generated and the input power level was increased gradually from a low level till the amplifier went into saturation. The amplitude of the output fundamental signal along with 2^{nd} and 3^{rd} harmonics was captured from the spectrum analyser.

The Figure 7.6 shows the obtained results from this test. It can be noticed that the ZFL single ended amplifier generates –36.7 dBc (decibels relative to carrier) 2^{nd} harmonic while the LMH differential amplifier is showing –53.35 dBc 2^{nd} harmonic for an input power level of -25 dBm. But these 2^{nd} and 3^{rd} harmonics captured for LMH6881 differential amplifier were almost similar to the harmonics generated by the Signal Generator itself until the saturation point. Also it is well known, as shown in equation (7.1), the amplitude of 2^{nd} and 3^{rd} harmonics increase by 2dB and 3dB respectively for 1dB increase in fundamental power.

Harmonics of ZFL single ended amplifier shown in Figure 7.6(a) in almost maintaining the trend as they are harmonics actually generated from the amplifier. But for the differential amplifier, the harmonics are not increasing according to what is expected. The measurement of harmonics generated from signal generator shows that those plots are actually harmonics generated by the signal generator and the real harmonics generated by differential amplifier are even lower. Even with these results, it can be seen that LMH differential amplifier possesses better 2nd order harmonic distortion characteristics. In the next section, the harmonic distortion level of LMH6881 amplifier with fully differential output configuration will be compared along with these two amplifiers.

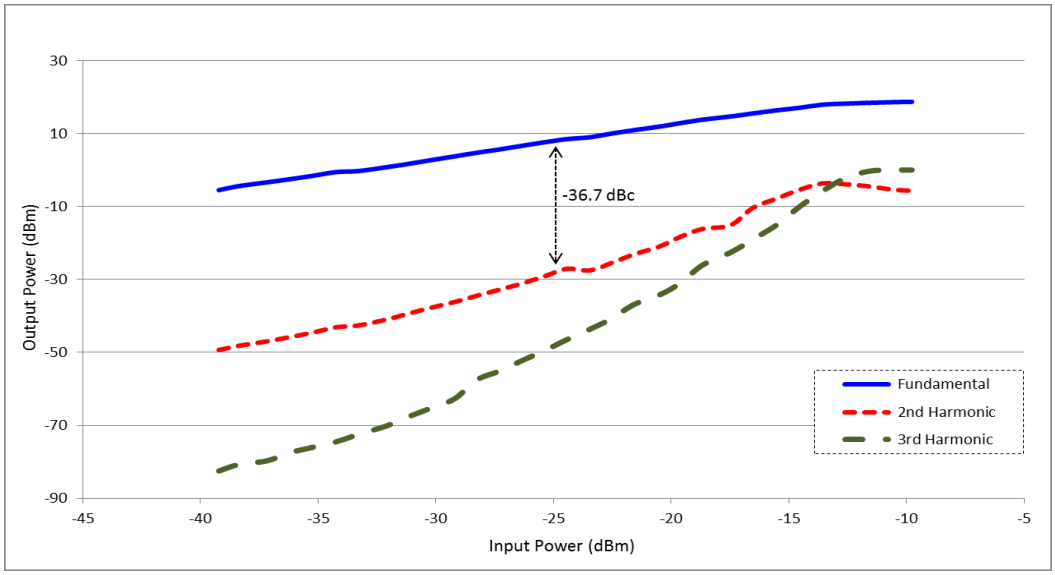

(a) Harmonic distortion of ZFL-2500+ single ended amplifier

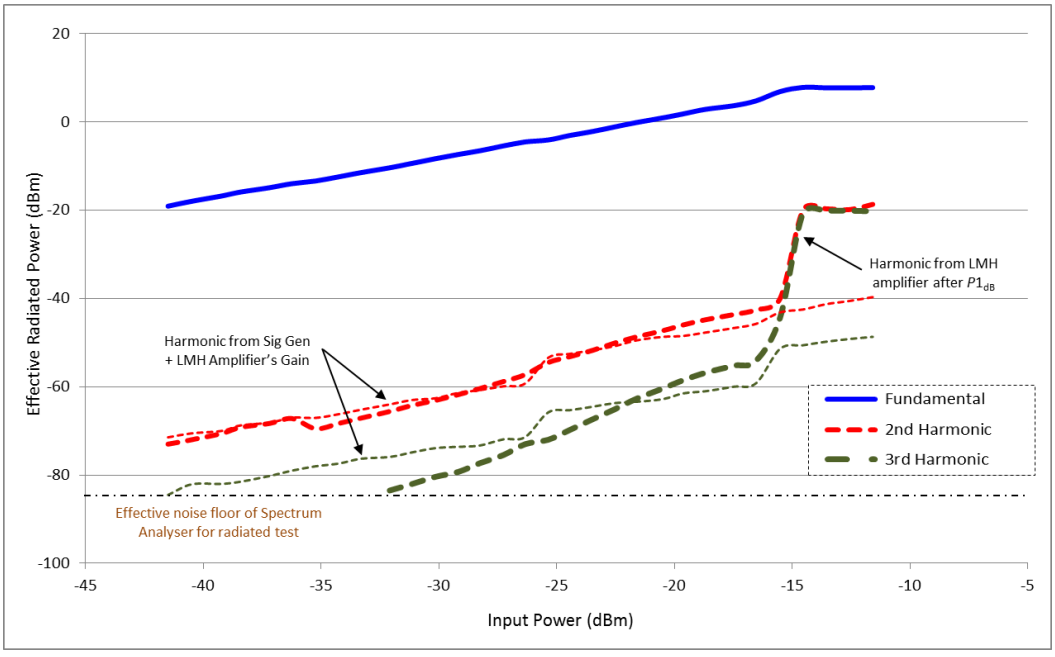

(b) Harmonic distortion of LMH6881 differential amplifier (SE output interface)

Figure 7.6: Harmonic distortions for single ended and differential amplifier in the bench

7.5 Radiated Harmonic Measurement of Single Ended and Differential Amplifier

In an audio or RF system, amplifiers are usually the major source of harmonic generation. However, to measure the full system distortion, it is preferable to measure harmonics of amplifiers while connected with antenna by the radiated harmonic measurement technique. In order to measure at least the third radiated harmonic, the antenna and the spectrum analyser both should have a minimum bandwidth from fundamental frequency to the frequency of third harmonic. The broadband Modified Bow-Tie (MBT) antenna was designed to fulfil this demand.

In this section, the radiated harmonics of the ZFL-2550+ single ended amplifier, LMH6881 differential amplifier with single ended output and the same LMH6881 amplifier with differential output interface were measured. Amplifiers with single ended interfaces (ZFL and LMH with balun) were connected to MBT monopole antenna and amplifier with fully differential output interface (as shown in Figure 5.18(b)) was connected to MBT dipole antenna. The dipole was placed right after the output resistors of the differential amplifier to eliminate any transmission effect. Figure 7.7 presents the complete broadband active balanced antenna configuration.

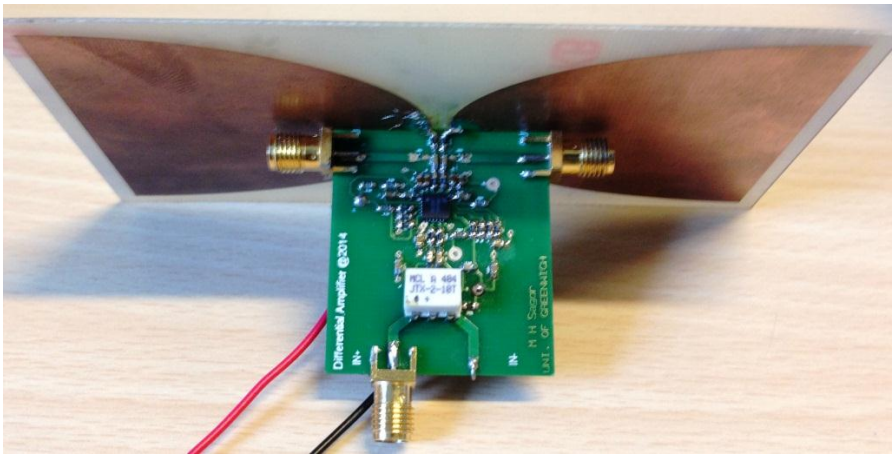

Figure 7.7: Broadband active antenna with balanced MBT antenna differentially fed by LMH6881 amplifier.

The radiated power measurement was carried using the same procedure described in Section 6.4. Active antennas were placed 2.5m away from the receive horn antenna inside the chamber, which is connected to a spectrum analyzer to observe the output signal. The output

power levels for the fundamental frequency (900 MHz) and for the harmonic frequencies (1.8 GHz & 2.7 GHz) were captured from the spectrum analyzer. Figure 7.8 shows the measurement setup of active antennas, with an inset on each showing the feeding technique.

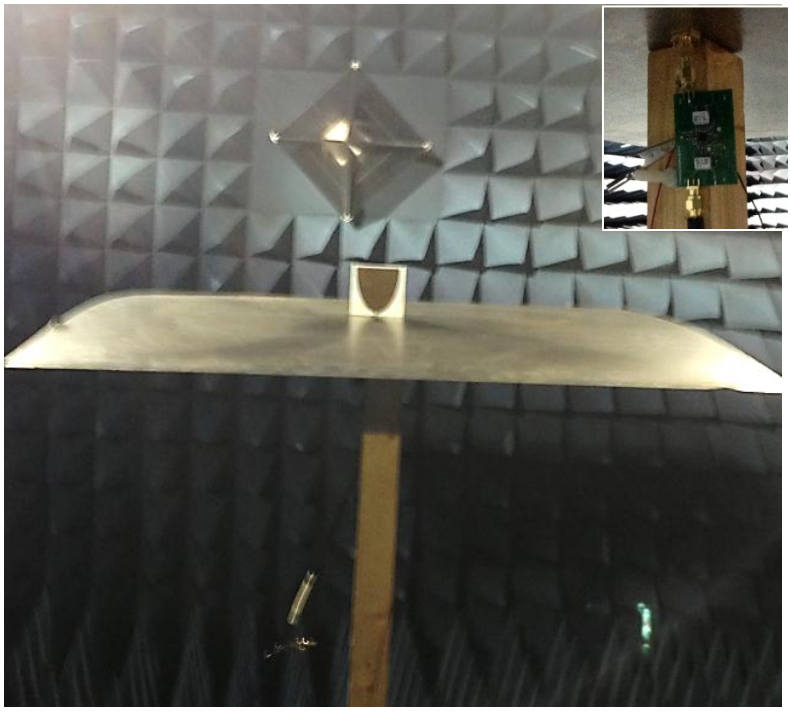

(a) Differential amplifier (with balun) feeding monopole antenna (inset: feeding point)

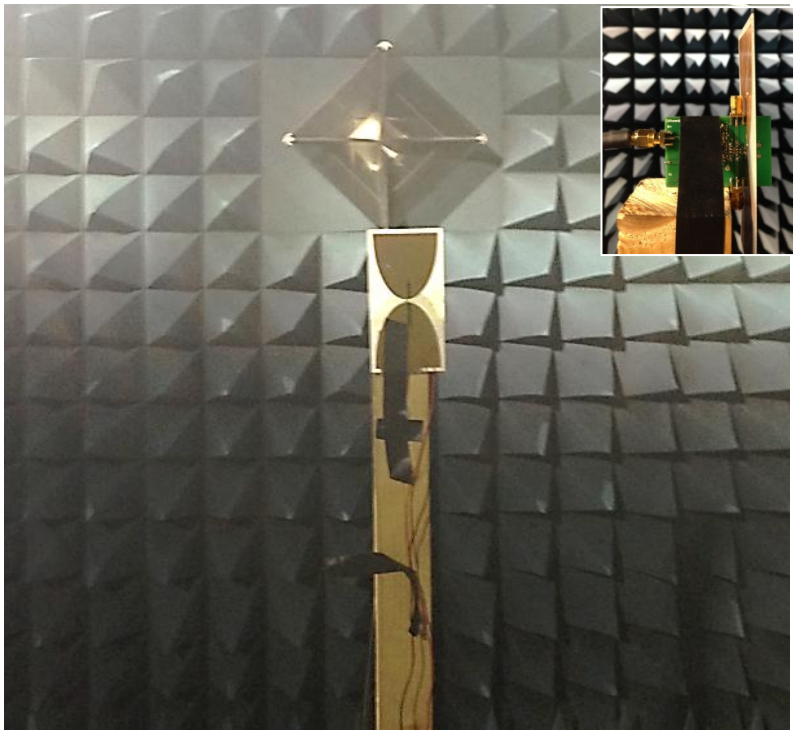

(b) Differential amplifier feeding balanced antenna differentially (inset: feeding point)

Figure 7.8: Measurement setup of radiated harmonics using broadband (a) MBT monopole & (b) MBT dipole antenna.

Radiation pattern of both MBT antennas were measured to adjust the effective antenna gain to the actual output power from the amplifier. Figure 7.9 shows the radiation pattern of the MBT monopole and dipole and the direction of AUT towards the receive antenna during radiated power measurement setup.

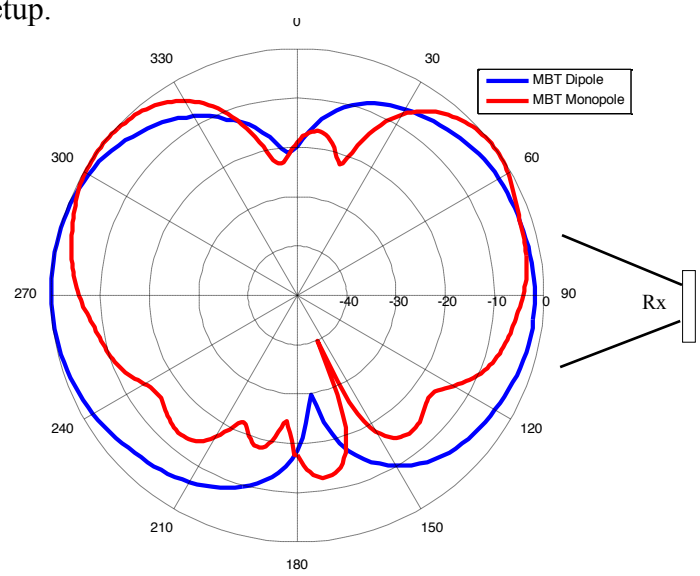

Figure 7.9: Radiation pattern of the MBT monopole and dipole antenna in principle plane

The effective radiated power was calculated for each frequency using the Friis transmission equation. The FSPL for 0.9GHz, 1.8GHz and 2.7GHz were calculated as 39.49dB, 45.51dB and 49.03dB respectively. The harmonic distortions (HD) were measured by the difference between fundamental and harmonics power levels. Figure 7.10 presents the fundamental and radiated harmonic distortion power level for all three different active antenna configurations.

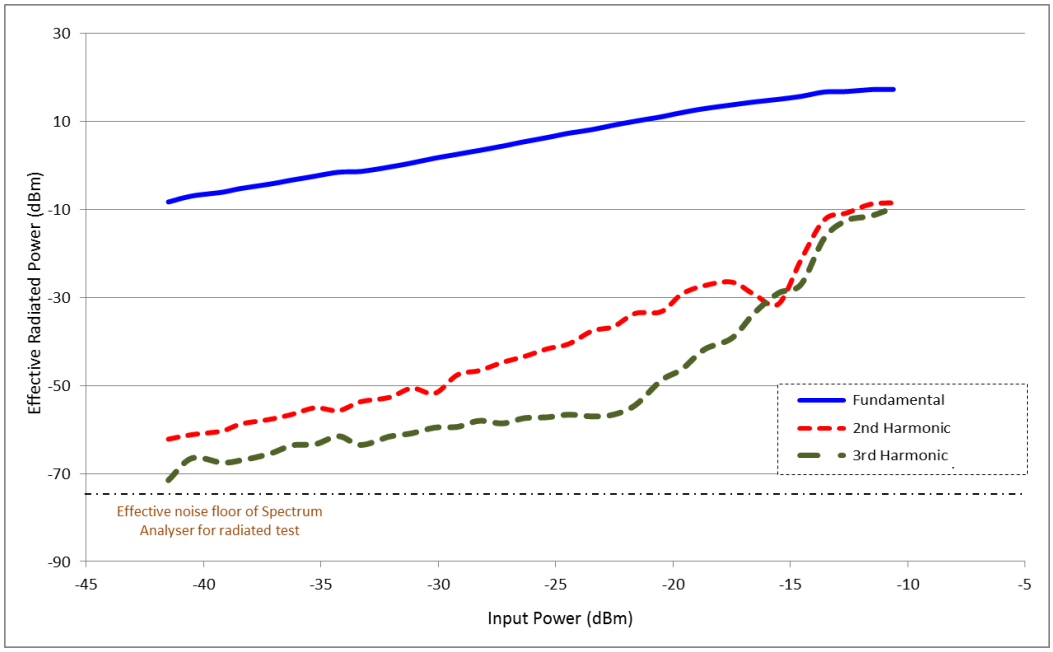

(a) Radiated HD of ZFL-2500+ single ended amplifier feeding MBT monopole

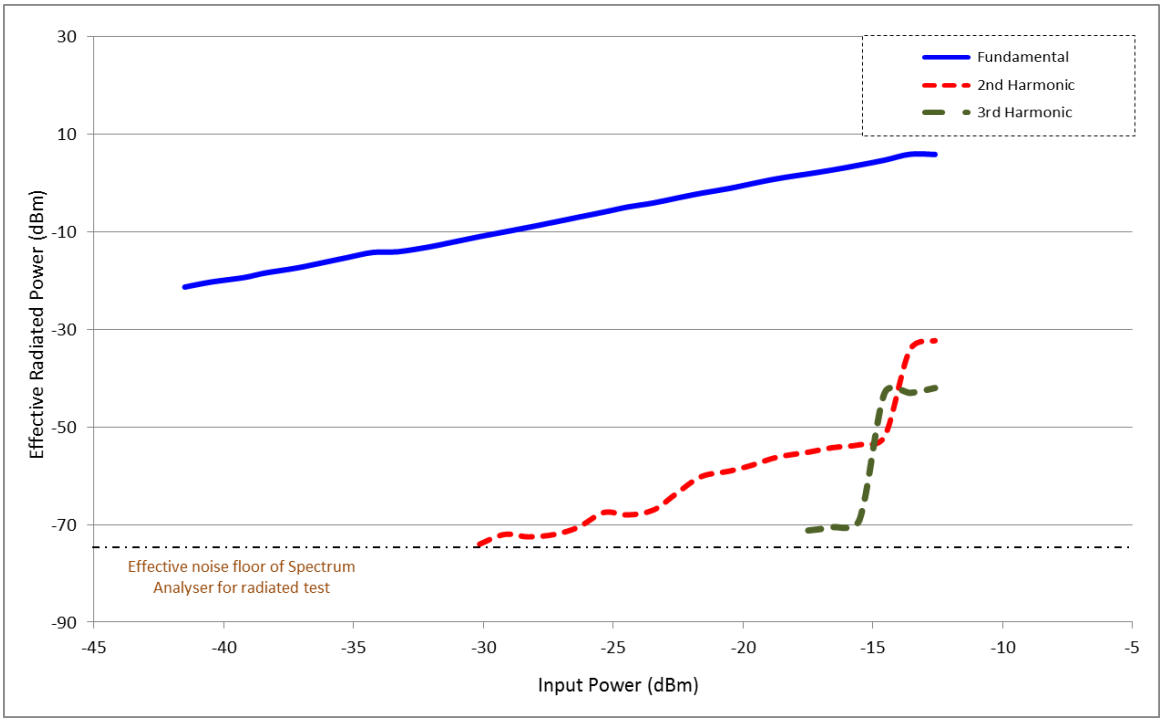

(b) Radiated HD of LMH6881 with single ended output interface feeding MBT monopole

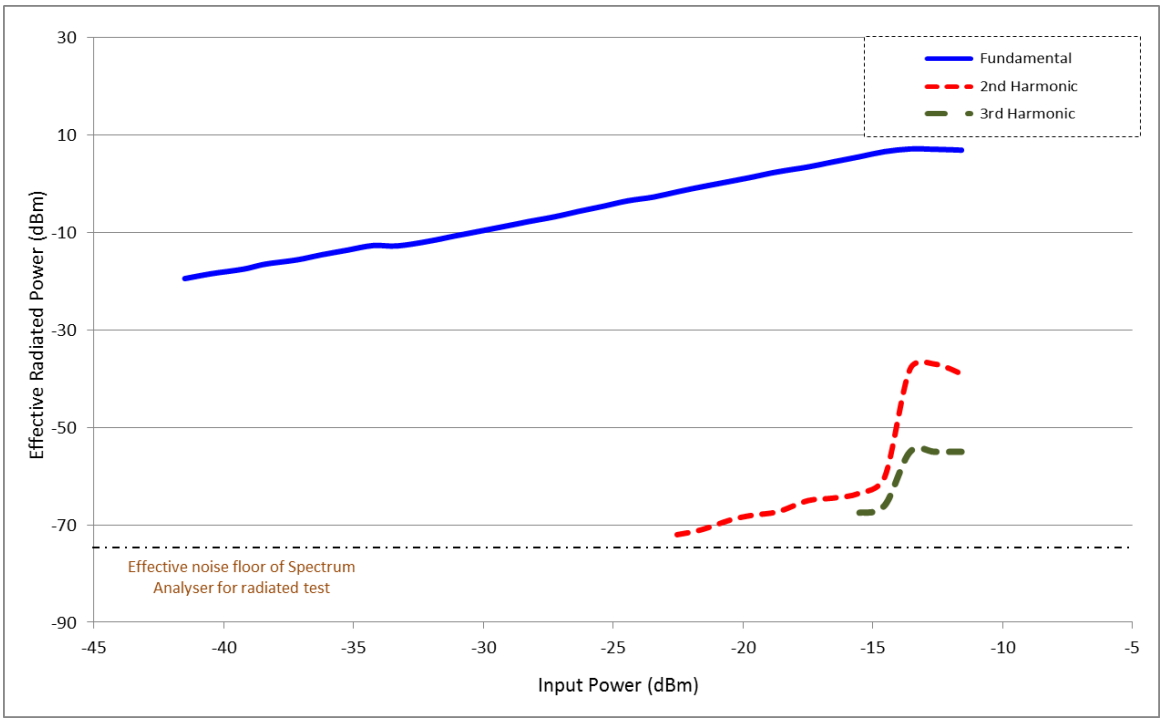

(c) Radiated HD of LMH6881 with fully differential output interface feeding MBT dipole

Figure 7.10: Radiated harmonic distortion measurements of single ended and differential amplifier feeding unbalanced and balanced antennas.

7.6 Does Differential Approach Reduce Even Order Harmonics?

From the measurement results presented in Figure 7.10, it can clearly be seen that the harmonic distortion level of LMH6881 feeding an unbalanced antenna was lower than the single ended ZFL amplifier feeding the same unbalanced antenna. This radiated harmonic measurement matches with the bench test illustrated in Section 7.4. Theoretically, it is also anticipated that differential amplifier would have lower second harmonics but the interesting part of this radiated measurement is that when the same LMH6881 differential amplifier fed a broadband dipole antenna differentially, the distortion was even lower. The 3rd radiated harmonic before 1dB compression point ($P1_{db}$) was below noise floor of the spectrum analyzer. In the same time, the gain of the fundamental signal was about 2 dB higher. Another fact to be noticed here is that the sudden dip occurred near the saturation point in the radiated power test with narrowband antenna in Chapter 6 (Figure 6.14) is not present in this measurement with broadband antenna. Thus, it is evident that harmonic distortions in a system can be significantly reduced by using fully differential interface. Figure 7.11 illustrates the 2nd harmonic components in dBc for these different active antenna configurations. The figure is clearly demonstrating lower 2nd harmonic for amplifier with differential interface.

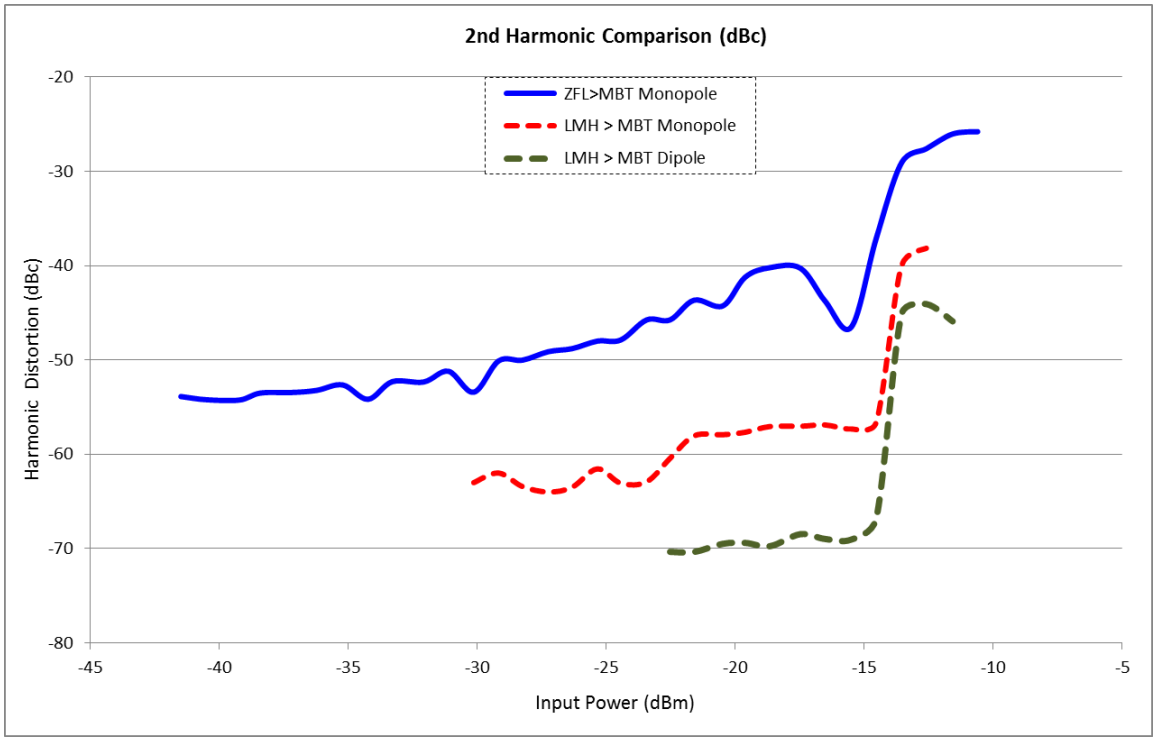

Figure 7.11: Radiated harmonic distortion comparison of single ended and differential amplifiers feeding unbalanced and balanced antennas.

7.7 ACLR of Amplifiers Using Broadband MBT Antennas

The ACLR experiment was also conducted with the broadband MBT antennas. The radiated measurement for ACLR was carried out for active unbalanced/monopole antenna and differentially fed balanced/dipole antenna. The spectral plot of both active antennas for -15dBm and -18dBm is shown in Figure 7.12 and the ACLR results obtained from that is shown in Table 7.1. It can be observed that the ACLR with broadband antennas are providing slight better performance than that with narrowband antennas with same amplifier and configurations. LMH amplifier with fully differential output feeding MBT dipole antenna is giving ~1.8dB higher ACLR compared to the LMH amplifier with single ended output interface feeding a monopole MBT antenna.

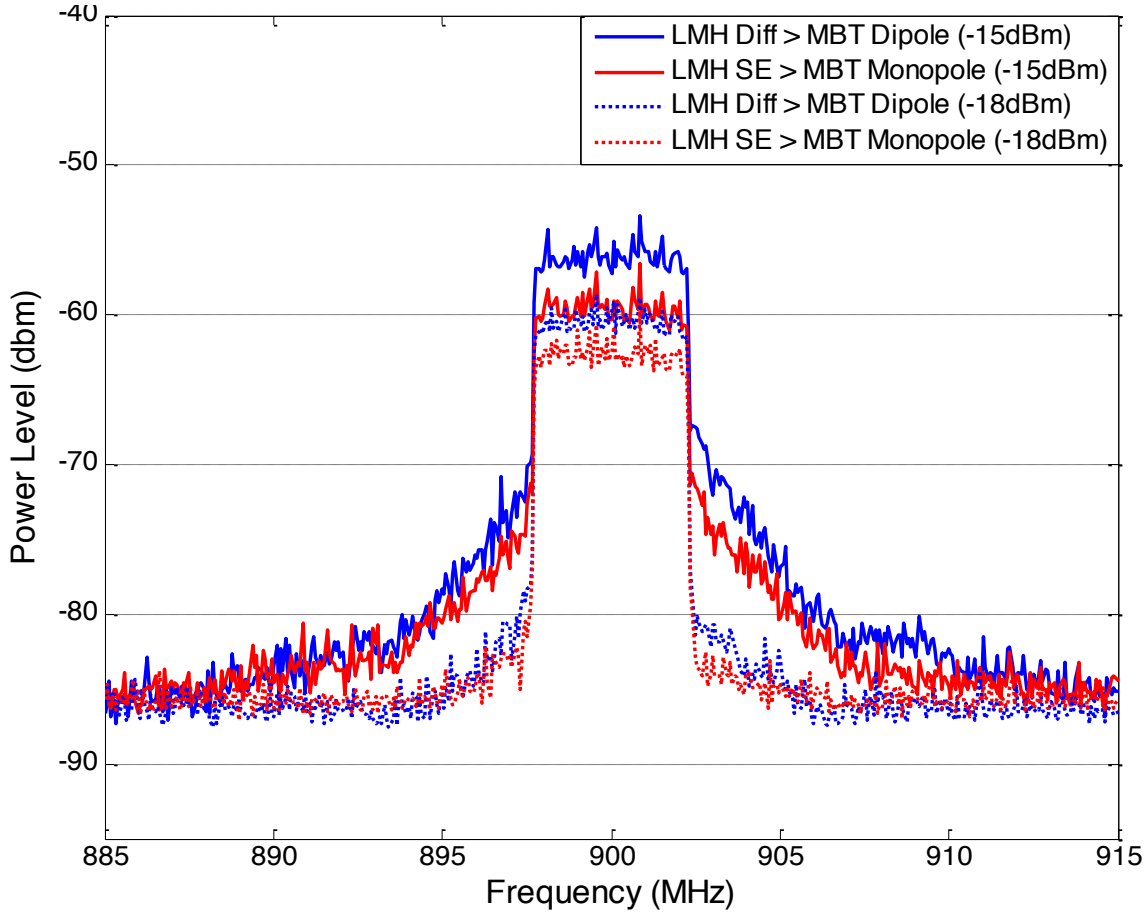

Figure 7.12: Spectral plot LMH6881 amplifiers with broadband MBT antennas, for single ended interface and differential output interface.

Table 7.1: ACLR of Broadband AIA for different output interface.

Channels	Single Ended -18dBm	Differential -18 dBm		Single Ended -15 dBm	Differential -15 dBm
Main Channel	-62.7	-60.6		-59.7	-56.4
Lower Adjacent Channel (dBm)	-84.9	-84.8		-79.9	-78.4
Upper Adjacent Channel (dBm)	-85.0	-84.4		-78.9	-76.5
Lower Alternate Channel (dBm)	-85.7	-86.2		-84.0	-83.9
Upper Alternate Channel (dBm)	-85.7	-86.1		-84.3	-82.8
ACLR (5 MHz Offset) (dBc)	**-22.2**	**-24.0**		**-19.7**	**-21.4**
ACLR (10 MHz Offset) (dBc)	-23.0	-25.6		-24.5	-27.3

7.8 Summary

In previous chapter, characterization of in band distortion of amplifier was considered using narrowband antennas. In this chapter, the harmonic distortion characteristics of LMH6881 amplifiers feeding broadband antennas have been explored. A broadband balanced antenna was designed with stable impedance and radiation pattern to satisfy the requirement of measuring radiated harmonic distortion. Harmonics of the single ended amplifier and differential amplifier with single ended output were measured in the bench. Then, these two configurations and the differential amplifier with fully differential output interface were measured with radiated measurement techniques. It has been experimentally proven that a differential amplifier generates lower harmonic distortions compared to a single ended amplifier. It has also been demonstrated that harmonic of same differential amplifier was reduced just by using differential interface, rather than single ended interface with a balun. The measurement results presented in this chapter have confirmed that differential amplifier feeding a balanced antenna differentially can significantly reduce harmonic distortion of a system.

References

[1] M. Golio, J. Golio (2008), *RF and Microwave Circuits, Measurements, and Modeling*; 2nd ed. New York: CRC Press, Chapter 6.

[2] U.A.Bakshi, A.P.Godse (2008), *Electronic Devices And Circuits – II*, 4th ed. Pune: Technical Publications, Chapter 3.

[3] David M. Pozar (2012), *Microwave Engineering*, 4th ed. New York: John Wiley & Sons, Inc., Chapter 10.

[4] Dehghani, R (2013), *Design of CMOS Operational Amplifiers,* Norwood: Artech House. Chapter 5.

[5] Warren L. Stutzman, Gary A. Thiele (2012). *Antenna Theory and Design*. 3rd ed. New York: John Wiley & Sons Inc.. Chapter 7.

[6] Balanis. C (2005), *Antenna Theory: Analysis and Design*, 3rd ed. Hoboken, NJ: John Wiley & Sons, Inc., Chapter 9.

[7] I. Oppermann, M. Hämäläinen, J. Iinatti (2004). *UWB: Theory and Applications*. West Sussex: John Wiley & Sons, Inc.. Chapter 6.

Chapter 8

Conclusion and Future Works

The research outline was set to explore the benefits of differentially fed active balanced antenna and the potential of this approach in future communication system. The study began with a comprehensive literature review into active antennas. To underpin the study of active antennas, an investigation into practical antennas for wireless applications resulted in a novel method of compensating ground plane effects followed by a novel approach of antenna measurement technique. Broadband differential amplifiers were then reviewed with a view to feed balanced and unbalanced antennas for demonstrating the potential of differential feeding technique over the conventional one. A detailed summary of the contributions of this research study is presented in Section 8.1. The discussion is concluded with some remarks in Section 8.2. Besides the key contributions, this study has also identified several interesting areas for future work, which is explained in Section 8.3.

8.1 Key Contributions of This Thesis

Empirical study of differential amplifiers and antennas has answered the fundamental research questions arose in the process of this research. Those questions will be reviewed in this section, summarising the answers provided by this thesis. These answers are the reflection of the key contributions of this research work.

(i) Why does differentially fed balanced antenna approach need to be explored?

A comprehensive literature review on active integrated antenna has been presented in Chapter 2. It can be noticed that researchers and circuit designers have always been giving efforts to minimise losses from microwave circuits. Their efforts in early 1960s projected that integrating active elements directly into the antenna significantly compensates transmission

losses and substrate losses while providing better antenna bandwidth [1-2]. Due to their compactness and better performance active antennas are extensively used in communication industry. In 1965, Kurokawa reported balanced amplifier with various advantages [3]. The improved linearity and distortion characteristics made balanced amplifier a prominent research topic amongst researchers and the technology advanced in a distinct surge. This technology has now reached in a stage where differential circuits are the preferred choice for CMOS RFIC designs [4] due to their relatively lower loss and excellent noise immunity. In the other sector of RF industry, antenna researchers have demonstrated superiority of balanced antenna over its unbalanced counterpart. It has been proven by plenty of experiments that balanced antenna reduces the unintended user effects when users hold the handset adjacent to their body [5-7]. It also offers higher efficiency and stable radiation pattern in the vicinity of human head or hand [8].

After this review, it is evident that an active balanced antenna fed by differential amplifier would offer considerably better performance in RF circuit design. Despite all these advantages, recent published works [9-11] show that researchers still tend to avoid balanced circuits and antennas. Although the RFIC industry widely uses differential interface, but they use single ended PAs and LNAs for the feeding part because the antenna industry still wants to stick to the idea of conventional 50Ω interface. Several research works have been conducted in recent years [12-14] on this topic but almost all of them were either not with a true differential feed or included balun. The benefits of using a true differential amplifier fed by a balanced antenna as a receiver have been demonstrated recently [15]. Thus this promising research area of differentially fed balanced transmit antennas needs to be explored.

(ii) Does ground plane of an antenna have any effect on its performance and can it be compensated?

The modern wireless devices demand smaller and compact antennas, where the metallic body of the device usually acts as a ground plane. Conventional design approach is therefore for an ‘unbalanced’ antenna with a finite ground plane. An ideal ground plane is perfectly conducting and infinite in extent. But real ground planes are finite in size and can be responsible for distorted radiation pattern [16]. In Chapter 3, the ground plane effects on a planar and reduced height monopole antenna have been studied. Simulation and measurement results suggested that antenna radiation pattern could be significantly influenced due to the

current flow on its ground plane. At the beginning of the experiment, a substantial change was observed just by reducing the height of the ground plane of a designed planar antenna. It was then demonstrated that ground plane effects can be compensated by introducing slot cut to limit the flow of current on the ground plane. A truncated slot line in the ground plane at quarter wavelength distance from the antenna triggered some alteration in the radiation pattern and impedance matching of the antenna. After that a 'choke-slot' was introduced and that completely eliminated the null and degradation the antenna had with a solid ground plane structure. This provides evidence that antenna ground plane can affect the radiation performance of an antenna. Therefore, design of antennas for small portable devices needs to encompass the whole structure – and cannot simply introduce a 'radiating' element avoiding ground plane structure. However, it has been proposed in this thesis that the antenna designers can apply techniques to control the ground plane current and limit any degradation.

(iii) Is it possible to measure wireless devices 'wirelessly' in modern anechoic chamber?

Modern antenna test methods inside the anechoic chamber require a cable to be attached to the device under test (DUT). But attaching a cable to a small device containing an integrated antenna can lead to erroneous results. To avoid these unwanted effects the antenna should be measured in a 'wireless' condition. In Chapter 4, a novel antenna measurement method has been demonstrated overcoming the need to connect a cable to the DUT. Radiation pattern of a simple 2.4 GHz dipole antenna was measured using the proposed injection locking technique. To provide a locking signal from the VNA, a directive horn antenna was placed facing towards the DUT. A local oscillator on the device under test was synchronized to the injected signal. The test setup was arranged in such a way that the injected signal remains locked throughout the whole radiation pattern measurement. The radiation pattern of the DUT was measured conventionally by attaching a cable and then by using proposed injection-locking technique without any cable attached. The measured radiation pattern for a low power injected signal was seen to be close, or even better, compared to the conventional measurement. This result indicates that it is possible to measure a battery operated wireless device in anechoic chamber without any cable connection by using this alternative novel method for antenna radiation pattern measurement.

(iv) Can higher power and linearity be achieved by adopting differential feeding technique?

A differential amplifier, LMH6881, used in active antenna investigations was characterized in Chapter 5. Two different output interfaces were developed using the same commercially available RFIC and biasing components. The single ended output interface consisted a balun to transform differential signals into single-ended signal to carry out measurements using standard measurement equipment. Another LMH6881 amplifier was designed with fully differential output interface without balun at its output port. The frequency response and power of these two amplifiers were measured and compared. Amplifier with single ended output was measured with 2-port VNA and same amplifier with differential output interface was measured with 4-port VNA. The frequency response showed that the 2-port measurement does not possess a stable differential gain, introduces loss and the gain rolls of after 1GHz (Figure 5.19). In contrast, the fully differentially measured amplifier provided double gain (~3dB higher) compared to the gain at each port throughout the measured bandwidth up to 2.5 GHz (Figure 5.20). In the case of power sweep measurement, differentially measured amplifier also demonstrated ~1.5dB higher output power and higher linearity (Figure 5.23). The amplifiers showed similar performance in the radiated power measurement in Chapter 6 (Figure 6.14). Differential amplifier feeding balanced antenna showed higher gain, output power and greater linearity. These measurements were carried out to relate the performance of a same amplifier having single ended and differential output interfaces. Empirical analysis has demonstrated that higher power and linearity can be achieved using same components by adopting differential feeding technique.

(v) Is it possible to achieve further improvement in power & linearity by lowering the load impedance?

After some promising results from differential output interface, an investigation was carried out to find whether further increase in linearity is achievable by this promising technique. The Ohm's law was implemented and the output resistance was changed. Measurement was carried out in the bench and as well as in the anechoic chamber with different antennas

integrated to LMH amplifiers. A significant improvement in $OP1_{dB}$, hence, linearity was observed for smaller output impedance (Figure 6.10). In the radiated measurement, it was noticed that the amplifier delivers the maximum power and gain when the output impedance is matched to the load impedance (Figure 6.16). The outcome suggests that a differential amplifier with low output impedance feeding a low impedance transmit antenna can deliver substantial improvement in output power and linearity of the system.

(vi) Does active balanced antenna produce less distortion than its unbalanced counterpart?

The excellent distortion characteristics of LMH6881 with differential output are another reason to look into the potentiality that differential interface can offer. The distortion level of LMH differential amplifier with single ended output and differential output was explored in Chapter 6 and Chapter 7. The IMD test of amplifier with single ended output was performed in the bench and the result was compared with a commercial single ended ZFL-2500+ amplifier. More than 10dB decrease in IMD_3 product was realised for the differential amplifier (Figure 6.2). The input third order intersect point was also excellent for the differential one.

In Chapter 7, the radiated harmonic distortion measurement was performed using three different amplifiers; ZFL true single ended, LMH differential with single ended output and LMH differential with differential output interface. The LMH differential with single ended output showed lower harmonic distortion compared to ZFL single ended one, which is expected from a differential amplifier. But the exciting part of this radiated measurement was that when the same LMH6881 differential amplifier fed a broadband dipole antenna differentially, the harmonic distortion was even lower. Thus, it can be assured that differentially fed active balanced antenna can be the best choice for applications demanding lower harmonic distortions.

(vii) Does this differentially fed balanced antenna approach possess any benefit for future mobile communication system?

To satisfy the ever increasing demand of mobile consumers, RF components have to maintain incredibly high performance with minimal distortions. In 4G technology such as LTE or WCDMA, the modulation becomes more complex and the nonlinear effects have to be measured by Adjacent Channel Leakage Ratio. The ACLR of the LMH amplifier with both output configurations were measured and analysed. In Chapter 6 the measurement was carried out inside the anechoic chamber while the amplifiers were attached to narrowband antennas. The differentially fed active antenna provided ~1.3dB better ACLR in that measurement (Table 6.6). In Chapter 7, the ACLR measurement was done with broadband antennas and the differential interface illustrated about 1.8dB improvement (Table 7.1). It might not be a substantial improvement but about 2dB increase in ACLR for the same device with different interface is noteworthy.

8.2 Conclusion

The research work has been conducted to ascertain the benefits of differentially fed active antennas over the conventional feeding techniques. Empirical study has demonstrated the superiority of differential feeding in every aspects of performance characterizations. But the RF industry is still stuck at the 'bottleneck' of a 50Ω, unbalanced interface. After analyzing all the measurements on differential interface carried out in this thesis, it can be concluded that is it time to re-evaluate the industry standard interface of antennas and RF circuitry.

8.3 Suggestions for Future Work

This thesis has consolidated an extensive amount of measurement data and provided adequate evidence of better performance of differential amplifier with fully differential interface. Throughout the course of this research few areas of further research work were identified.

- In Chapter 3, ground plane effect of a mobile antenna with finite ground plane was investigated. It was realised in the measurement that even after compensation the measured radiation pattern was a little distorted as the essential balanced antenna (Figure 3.15 (a)) was fed by conventional coaxial cable. Ideally if that antenna could be measured with a differential amplifier feeding, that distortion could be eliminated. The slotted ground plane antenna was initially designed to work at PCS 1.9 GHz frequency and the LMH6881 amplifier adopted in active antenna work had a poor impedance matching and gain at that frequency. Therefore, the measurement was discarded. Further investigation could be pursued by designing an antenna with finite ground plane matched within the frequency bandwidth of the differential amplifier and the ground plane effect of a fully differentially fed mobile antenna can be investigated.

- In Section 6.5, a significant improvement in linearity was perceived for an amplifier with low output impedance (Figure 6.16). The outcome suggested that a differential amplifier with low output impedance feeding a matched low impedance transmit antenna can deliver significantly improved linearity and higher power. Attempts were taken to design a low impedance resonant loop antenna by compensating its high reactance by using lumped elements. But because of time constraints, it couldn't be investigated any further. This can be an excellent direction of future work.

- A limitation of this work is that it has been mostly a measurement based research work. To compare the measured data with simulations, the amplifier can be modelled in Agilent Advanced Design System (ADS) software or AWR Microwave Office. Then by importing the antenna data from CST Microwave Studio the integration can be realised in ideal software environment. This will validate the measured data more strongly.

- It was noticed that in the harmonic measurements conducted in Section 7.4, the harmonics generated by the differential amplifier were almost similar or even lower compared to the harmonics generated by the signal generator itself (Figure 7.6). Thus the real harmonics generated by the amplifier was not possible to measure. This can be overcome by designing a RF filter for those harmonic frequencies and then using that to filter out harmonics generated by the signal generator.

- A commercially available voltage controlled oscillator (VCO) was used to measure device wirelessly in Chapter 4. The Z-communications SMV2490L oscillator has a buffer amplifier, which might have caused a poor locking bandwidth. A VCO can be designed in order to achieve a better locking bandwidth to gain greater flexibility in cable less radiation pattern measurement. Also a VCO with differential output can be constructed to measure balanced antenna and differential circuit by this novel measurement technique.

References

[1] Frost, A, "Parametric amplifier antenna," Antennas and Propagation, IEEE Transactions on , vol.12, no.2, pp.234,235, Mar 1964.

[2] Fujimoto, K., "Active antennas: Tunnel-diode-loaded dipoles," *Proceedings of the IEEE* , vol.53, no.5, pp.556,556, May 1965.

[3] K. Kurokawa, "Design Theory of Balanced Transistor Amplifiers," Bell System Tech. J., vol. 44, pp. 1675-1698, Oct. 196511.

[4] Carlos Calvo. (2010), *The differential-signal advantage for communications system design*, Available: http://www.eetimes.com/document.asp?doc_id=1276467&. Last accessed 31st October, 2014.

[5] Morishita, H.; Furuuchi, H.; Fujimoto, K., "Performance of balance-fed antenna system for handsets in the vicinity of a human head or hand," *Microwaves, Antennas and Propagation, IEE Proceedings* , vol.149, no.2, pp.85,91, Apr 2002.

[6] Arenas, J.J., Anguera, J., Puente, C.: 'Balanced and single-ended handset antennas: free space and human loading comparison', Microw. Opt. Technol. Lett., 2009, 51, (9), pp. 2248–2254.

[7] Morishita, H., Hayashida, S., Ito, J., Fujimoto, K.: 'Analysis of built-in antenna for handset using human (head, hand, finger) model', Electron. Commun. Jpn., 2003 Part 1, 86, (9), pp. 35–45.

[8] Collins, B.S., Kingsley, S.P., Ide, J.M., Saario, S.A., Schlub, R.W., O'Keefe, S.G.: 'A multi-band hybrid balanced antenna'. IEEE 2006 Int. Workshop on Antenna Technology: Small Antennas; Novel Metamaterials, White Plains, New York, 6–8 March 2006, pp. 100–103.

[9] Sanchez-Montero, R.; Rigelsford, J.M.; Lopez-Espi, P.L.; Alpuente-Hermosilla, J., "An active multiband antenna for future wireless communications," *Antennas and Propagation (EuCAP), 2014 8th European Conference on* , vol., no., pp.2989,2991, 6-11 April 2014.

[10] Jui-Han Lu; Jia-Ling Guo, "Small-Size Octaband Monopole Antenna in an LTE/WWAN Mobile Phone," Antennas and Wireless Propagation Letters, IEEE , vol.13, no., pp.548,551, 2014.

[11] Shao-li Zuo; Zhi-ya Zhang; Jia-Wei Yang, "Planar Meander Monopole Antenna With Parasitic Strips and Sleeve Feed for DVBH/ LTE/GSM850/900 Operation in the Mobile Phone," Antennas and Wireless Propagation Letters, IEEE , vol.12, no., pp.27,30, 2013.

[12] Chan, K.M.; Lee, E.; Gardner, P.; Hall, P.S., "A differentially fed electrically small antenna," *Antennas and Propagation Society International Symposium, 2007 IEEE* , vol., no., pp.2447,2450, 9-15 June 2007.

[13] Lee, E.; Chan, K.M.; Gardner, P.; Dodgson, T.E., "Active Integrated Antenna Design Using a Contact-Less, Proximity Coupled, Differentially Fed Technique," *Antennas and Propagation, IEEE Transactions on* , vol.55, no.2, pp.267,276, Feb. 2007.

[14] Zubir, F.; Gardner, P., "Differentially fed multilayer antennas with harmonic filtering for push-pull Class B Power Amplifier integration," Microwave Conference (EuMC), 2013 European , vol., no., pp.96,99, 6-10 Oct. 2013 .

[15] García-Pérez, O.; Segovia-Vargas, D.; García-Muñoz, L.E.; Jiménez-Martín, J.L.; González-Posadas, V.; , "Broadband Differential Low-Noise Amplifier for Active Differential Arrays," *Microwave Theory and Techniques, IEEE Transactions on* , vol.59, no.1, pp.108-115, Jan. 2011.

[16] Huang, J.: 'The finite ground plane effect on the microstrip antenna radiation patterns', IEEE Transaction on Antennas and Propagation, 1983, 31, (4) pp. 649–655.